STUDIES ON GAIT CONTROL USING A PORTABLE PNEUMATICALLY POWERED ANKLE-FOOT ORTHOSIS (PPAFO) DURING HUMAN WALKING

BY

MAZHARUL ISLAM

DISSERTATION

Submitted in partial fulfilment of the requirements
for the degree of Doctor of Philosophy in Mechanical Engineering
in the Graduate College of the
University of Illinois at Urbana-Champaign, 2016

Urbana, Illinois

Doctoral Committee:

Professor Elizabeth T. Hsiao-Wecksler, Chair
Associate Professor Prashant Mehta
Associate Professor Srinivasa Salapaka
Associate Professor Ramavarapu S. Sreenivas

ABSTRACT

A powered ankle-foot orthosis (AFO) can be very useful for people with neuromuscular injury. Control of powered AFOs will be more efficient to provide assistance to individuals with lower limb muscle impairments if we can identify different gait events during walking. A walking or gait cycle can be divided into multiple phases and sub-phases by proper gait event detection, and these phases/sub-phases are associated with one of the three main functional tasks during the gait cycle: loading response, forward propulsion, and limb advancement. The gait cycle of one limb can also be characterized by examining the limb's behavior over one stride, which can be quantified as 0% to 100% of a gait cycle (GC). One easy approach to identify gait events is by checking whether sensor signals go above/below a predetermined threshold. By estimation of a walker's instantaneous state, as represented by a specific percentage of the gait cycle (from states *0* to *100,* which correlate with 0% to 100% GC), we can efficiently detect the various gait events more accurately. Our Human Dynamics and Controls Laboratory previously developed the portable pneumatically powered ankle-foot orthosis (PPAFO), which was capable of providing torque in both plantarflexion and dorsiflexion directions at the ankle. There were three types of sensor attached with the PPAFO (two force sensitive resistors and an angle sensor). In this dissertation, three aspects of effective control strategies for the PPAFO have been proposed. In the first study, two improved and reliable state estimators (Modified Fractional Time (MFT) and Artificial Neural Network (ANN)) were proposed for identifying when the limb with the PPAFO was at a certain percentage of the gait cycle. A correct estimation of percentage of gait cycle will assist with detecting specific gait events more accurately. The performance of new estimators was compared to a previously developed Fractional Time state estimation technique. To control a powered AFO using these estimators, however, detection of proper actuation timing is necessary. In the second study, a supervised learning algorithm to classify the appropriate start timing for plantarflexor actuation was proposed. Proper actuation timing has only been addressed in the literature in terms of functional efficiency or metabolic

cost during walking. In this study, we will explore identifying the plantarflexor actuation timing in terms of biomechanics outcomes of human walking using a machine learning based algorithm. The third study investigated the recognition of different gait modes encountered during walking. The actuation scheme plays a significant role in walking on level ground, stair descent or stair ascent modes. The wrong actuation scheme for a given mode can cause falls or trips. A gait mode recognition technique was developed for detecting these different modes by attaching an inertial measurement unit and using a classifier based on artificial neural networks. This new algorithm improves upon the current one step delay limitation found as a drawback of a previously developed technique. Overall, this dissertation focused on addressing some important issues related to control of powered AFO that ultimately will help to assist people wearing the device in daily life situations during walking. The proposed approaches and algorithms introduced in this dissertation showed very promising results that proved that these methods can successfully improve the control system of powered AFOs.

To my Father and Mother

ACKNOWLEDGMENTS

I am grateful to numerous numbers of people for continuously supporting me throughout my long Ph.D. journey. Their motivation, encouragement and advices make my graduate life a memorable one and it might not be possible for me to complete my dissertation without them.

First and the foremost, I am heartily thankful to my supervisor Prof Elizabeth T. Hsiao-Wecksler, whose guidance, support and encouragement from the initial to the final level enabled me to develop an understanding of the subject and without which this work would have not been possible. She taught me how not only to approach a problem in a systematic way, but also to solve the problem in an effective way. Every time when I felt in a situation where I could not find the solution, her valuable advice makes me overcome difficulties. She also help me to develop my presentation skills as well as public speaking skills in front of large number of audiences. Moreover, her advices helped me to improve my technical writing skills. I am forever grateful for her patience and support throughout my studies in University of Illinois at Urbana-Champaign. I also owe my deepest gratitude to other members of my doctoral committee, Prof Ramavarapu S. Sreenivas, Prof Srinivasa Salapaka and Prof Prashant Mehta for their unconditional help while developing the ideas for my dissertation.

I am also indebted to many of my colleagues to support me for understanding the Biomechanics and Controls. I would like to thank Matt Petrucci and Louis A DiBerardino III for helping me formulate new ideas and also giving me reading materials for improving my knowledge. I would also like to show my gratitude to Yifan Li and Morgan Boes who helped me a lot to finalize the experimental setup. Moreover, I also specially thank to Deen S Farooq, Alan Gaglio and Carrie Liang for continuously helping me testing the experimental setup and collecting data. I am also thankful to Chenzhang Xiao, David Lin and Souransu Nandi for assisting me making the electronic circuits. Furthermore, I acknowledge the support of other colleagues (Ziming Wang, Michael J. Angelini, Michael J. Wineman, Mei Kuen Hsu, Richard Kesler) of HDCL Lab.

I would like to thank my friends who constantly supported me during my PhD life. I am specially thankful to Zubaer Hossain, Kallol Das, Wasim Akram, Reaz Mohiuddin, Ahmed Khurshid and many other friends who continuously advised me throughout this time.

Finally, I would like to express my earnest gratitude to my family members. My wife, Tanjila Alam, was always with me throughout this time of my graduate life and has supported me in every way possible. I followed the steps of my father (Nurul Islam) to become a mechanical engineer and later my dream for pursuing for higher education also came from my father's encouragement. I am extremely grateful to my mother (Nurun Nahar Islam), a professor of mathematics, who helped me to build up my knowledge in mathematics from my childhood. I believe that it is her blessing that help me to finish my PhD works. I am also very thankful to my sister (Normin Islam) and brother (Nahid Islam) for their unconditional love and support during my PhD journey.

This work is supported by the NSF Engineering Research Center for Compact and Efficient Fluid Power # 0540834.

Table of Contents

CHAPTER 1

INTRODUCTION

According to the public health policy literature, walking is identified as the most amenable physical activity behavior for adults [1]. Thus, it is important to ensure effective walking for both healthy and impaired populations. Gait can be divided into two main phases: stance and swing. Each of the phases can also be divided into several sub-phases. Generally, the gait cycle begins from the time of initial contact with the floor by the heel (0% of gait cycle) and ends at the point of the next heel strike (100% of gait cycle) on the same foot (Figure 1).

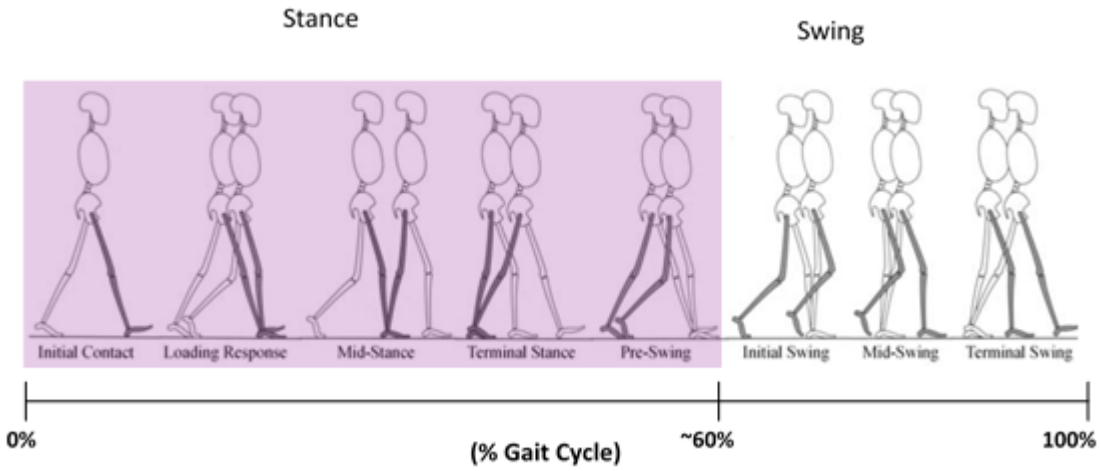

Figure 1 Gait of human walking (Borrowed from Prof. Hsiao-Wecksler's ME481 Lecture Notes).

The first sub-phase is called Initial Contact. This phase is followed by the Loading Response where the neutral alignment of the ankle is reached. In the sub-phase of Mid Stance, the foot becomes stationary and the tibia becomes the moving segment. At the end of stance (Terminal Stance and Pre-Swing), forward propulsion occurs when the plantarflexor muscles propel the body forward. After the stance phase, the swing begins and the foot is advanced for the next heel strike [2]. Swing phase can be divided

into Initial Swing, Mid-Swing and Terminal Swing. During the swing phase, the ankle joint generates approximately less than 0.2 Nm/kg torque in the dorsiflexion direction, while the plantarflexor muscle generates peak torques up to 1.2 Nm/kg body weight during the forward propulsion phase [3]. Moreover, a full walking cycle can be divided into single support phase (single foot in contact with the ground) and double support phase (both feet in contact with the ground) [4]. Gait analysis and knowledge of different phases of walking play important roles in determining healthy walking.

An ankle-foot orthosis (AFO) is an external device that can provide assistance to individuals with lower limb muscle impairments [5]. Numerous neurological disorders, muscular pathologies and injuries, including trauma, stroke, or multiple sclerosis can affect human gait. A large population in the United States (for example stroke (4.7M), polio (1M), multiple sclerosis (400K), spinal cord injury (200K), and cerebral palsy (100K)) can get benefit from the use of active lower limb orthoses [6].

Current commercial AFOs are generally passive, i.e., the device does not provide external power at the ankle joint during forward propulsion phase and swing phase, rather it just uses simple motion control by springs or mechanical switches [7]–[14]. Scientific studies on passive ankle foot orthoses mostly showed that these can prolong assisted standing and walking, however, there is a lack of information about their effect on functional walking [10]. Commercially available passive orthoses can replicate healthy ankle behavior at a satisfactory level in individuals capable of providing plantarflexor torque at low walking speeds. In contrast, an additional plantarflexor torque is necessary during forward propulsion at normal and fast walking speeds [15], [16]. In addition, Yamamoto et al. also showed that a passive AFO lacking plantarflexor assistance could not make a hemiplegic patient experience forward thrust of the knee joints [17]. Thus, passive AFOs can never help to move the body forward due to incapable of providing added power to the system. They can only help avoid unwanted motion like drop-foot by constraining motion. The absence of an energy source for plantarflexion results in gait deficiencies and a higher metabolic energy consumption for passive orthosis users [18].

Active and semi-active lower limb assistive devices have been developed over the last few decades to improve the locomotion of impaired populations [2]. A semi-active orthosis provides assistance using a real-time microcontroller by collecting information via sensors for determining gait phases [19], [20] and constrains motion when necessary. On the other hand, an active AFO has the ability to provide external torque at the ankle joint. From the review by Shorter et al. [7], we know that although assistive devices have been enhanced a lot during this time, researchers are facing difficulties to manufacture devices. The scope of studies for improving the current active ankle-foot orthosis have been mainly in advancing technology for increased magnitude, lighter weight, separation of power source from actuator and power transmission [6]. In research articles [21]–[44], different kinds of active and semi-active AFO and their controllers were described.

To overcome some of the limitations of current AFOs, we developed the portable pneumatically powered ankle-foot orthosis (PPAFO) in our Human Dynamics and Control Laboratory (HCDL). Our portable system separated the power source from the actuator to make a light weighted ankle-foot system. It is capable of providing both plantarflexor and dorsiflexor torque. Sensors are attached to the AFO to detect the gait events using a real-time microcontroller that also controls actuation. The description of our PPAFO is explained in section 1.1.

1.1 Description of Portable Powered Ankle-Foot Orthosis (PPAFO)

The PPAFO provides plantarflexor (toes up) or dorsiflexor (toes down) actuation using a pneumatic rotary actuator attached at the ankle joint (Figure 2). A dual-vane, bidirectional pneumatic actuator (PRN30D-90-45, Parker Hannifin, Cleveland, OH, USA) was used to build this PPAFO. This actuator has the ability to provide about 12 Nm of torque at 100 psig pressure. The actuations in two different directions are controlled by two solenoid valves (VUVG 5V; Festo Corp-US, Hauppauge, NY, USA). As a portable source of power, a compressed CO_2 bottle with embedded pressure regulator (JacPac J-6901-91, 20 oz capacity; Pipleline Inc., Waterloo, ON, Canada) can be attached to the subject's waist. This

allows our PPAFO to be used as untethered power system. However, in a laboratory experimental setup, the PPAFO can be connected to shop air as fuel instead of CO_2. We assume that these different power supplies and gases will have little impact on the control strategy. Since dorsiflexion requires less ankle torque, we used an additional pressure regulator (LRMA-QS-4; Festo Corp-US, Hauppauge, NY, USA) to reduce the pressure to 30 psig in the direction of dorsiflexion. This will avoid an overpowering torque in the direction of dorsiflexion. During swing, overpowering the dorsiflexion actuation will make the subject uncomfortable.

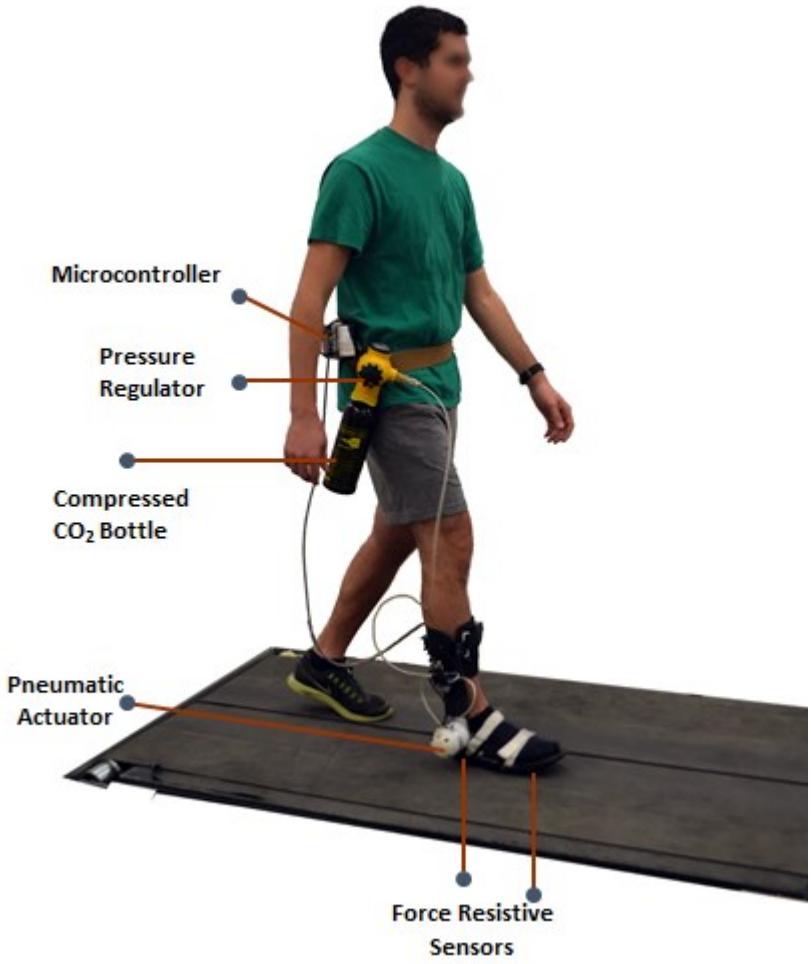

Figure 2 Walking with Portable Powered Ankle Foot Orthosis (PPAFO).

There are two types of control systems for the PPAFO. For the untethered system, an embedded microcontroller (MCU) (MSP430G2553, Texas Instruments, Dallas, USA) was used. On the other hand

for the tethered system, MATLAB Simulink software (v 7.13.0.564, the Mathworks, Waltham, MA, USA) interfaced with a data acquisition system (QUARC, Quanser Consulting Inc, Markham, ON, Canada) was used. The PPAFO uses three sensors: two force sensitive resistors (FSRs; 2”-square, SEN-09376 ROHS, SparkFun Electronics, Niwot, Colorado, USA) attached under the foot shell beneath the toes and heel, and a Hall effect angle sensor (KMA199E, NXP Semiconductors, San Jose, CA, USA) attached to the rotary actuator shaft to measure the ankle angle.

1.2 Literature review on controllers for orthotic and prosthetic devices

1.2.1 Controlling the actuation of orthotic and prosthetic devices

The behavior of the biological ankle-foot system is inherently nonlinear as the mechanical factors of the biological elements like skin, muscles, bones, tendons, ligaments, cartilage and connective tissues depend on different factors, such as deformation rate, position, and motion speed [45]. Moreover, different reactions of muscles for various electrical signals provided by the nervous system change the mechanical impedance of the ankle-foot system. Different subjects and different dysfunctional conditions have different effects on this behavior [46]. There is a wide range of ankle disabilities among patients. As a consequence, it is very challenging to design control in ankle-foot orthoses to mimic healthy walking for this nonlinear system. Jimenez-Fabian et al. mentioned different types of control strategies for active and semi-active ankle-foot orthoses, prostheses and exoskeletons in [18].

Despite many similarities, orthotic and prosthetic devices have distinct differences. The control of orthotic devices is more challenging compared to prosthetic devices, rehabilitation robots and other assistive devices. Though active orthoses, active prostheses, exoskeletons and rehabilitation robots are functionally alike from the mechatronic perspective, there is an enormous difference in control objectives and human interfaces in orthoses/prostheses compare to other devices [18]. Adaptation to different

working conditions, walking speeds, walking surfaces and user motion intent recognition are the main objectives for ankle-foot orthoses and prostheses [18]. The hardware configuration is the main difference between prosthetic and orthotic devices. Persons with an impaired limb wear orthotic devices, while persons with amputation wear prosthetic devices. Thus, the orthotic user must also bear the extra weight of the device in addition to the weight of their impaired limb while wearing orthoses. The weight of the device especially the weight of the actuator is one of the central issues of the orthotic devices from the point of designing. Moreover, the control system of active orthoses must address the possible lack of coordination between involuntary muscle reaction between the impaired limb and orthosis. The intrinsic limb dynamics must be dealt with by these orthotics devices [18]. Therefore, active orthotic devices need to address control and weight in different ways compared to prosthetic devices or rehabilitation robots.

Different sources of information are generally used as control signals for active orthoses and prostheses [18], [47]. The primary signals are: 1) foot switches, 2) ankle angle, 3) biomechanical signals, 4) electromyography (EMG) signals, 5) peripheral nervous system signals, 5) central nervous system signals, and 6) accelerometer or gyroscopic signals. However, mechanical signals like foot switches, ankle angles and EMG interfaces are very commonly found to be used in orthotic devices in the literature [18], [47].

One of the most common approaches to control a powered AFO to detect different gait events is to check whether each sensor measurement at any time goes above/below a predetermined threshold [5], [20], [22], [23], [28], [29], [42], [48]–[51]. Shorter et al. mentioned this controller that used sensors value directly for the PPAFO as a “Direct Event” controller [5], [49], [51]. In these works, the heel FSR and toe FSR signal were directly used to control the actuation of the PPAFO by detecting important gait events (Table 1). Heel strike was detected by identifying when heel FSR was only turned on, foot flat by onset of both sensors, heel off by off values of heel FSR and onset of toe FSR, and finally toe off by off values of both sensors.

Table 1 Direct Event (DE) controller decision scheme for the PPAFO (Adapted from [49]*).*

Gait Event	Heel Sensor		Toe Sensor		Torque Assist
	on	off	on	off	
Heel Strike	X			X	Dorsiflexor
Foot Flat	X		X		None
Heel Off		X			Plantarflexor
Toe Off		X		X	Dorsiflexor

Different approaches, similar to the Direct Event controller, have been used to control powered orthoses and prostheses in the literature. Researchers from Arizona State University detected zones or finite states using foot switches and ankle angular velocity, and used proportional-derivative (PD) structures for tracking a trajectory of a linear motor with a series elasticity element for controlling an active AFO [28], [29], [50]. Blaya et al. at MIT also proposed a finite state machine using sensor signals from capacitive force sensors and ankle angle directly and controlled the device by regulating the mechanical impedance of the orthosis [42], [52]. In a prosthetic system, Sup et al. at Vanderbilt University used a similar finite state machine by using sensor values from cylindrical force sensors, a load cell for axial load, and an ankle angle sensor directly in a tethered system with pneumatic actuators [53], [54]. Another group, Naito et al., compared shank angle and foot contact information with threshold values to determine three different phases: initial stance, mid-stance, and terminal stance/swing phases to control their semi-active AFO [21]. Some other approaches to detect gait events directly have utilized ground reaction force and moment at the ankle[22]; ankle angle [23]; as well as ankle angle and the direction of motion with accelerometer [25]. Moreno et al. also designed a leg orthosis that used signals from an inertial measurement unit (IMU) directly for control [55]. These approaches discussed Direct Event (DE) like controller. The DE controller has the disadvantage of detecting gait events when the relation between the gait events and sensor values do not have any direct relations. Moreover, application of the DE controller on impaired populations did not show satisfactory results due to different heel-toe gait patterns for walking disability [5]. Therefore, more robust and reliable approaches for controlling the actuation of powered AFOs are needed.

Electromyography (EMG) signal based controllers were other common approaches found to control powered AFOs [34], [36], [56]–[69]. Ferris et al. controlled their AFO with artificial pneumatic muscles using a proportional controller based on the amplitudes of the EMG signals of the tibialis anterior muscle for dorsiflexion and the soleus muscle for plantarflexion motion [34], [36]. Some groups proposed an artificial neural network approach and muscle model approach to control an ankle-foot prosthesis using the EMG signals from the amputee's residual limb [56]–[59]. Kawamoto et al. also used an EMG-based feedback controller for their HAL (Hybrid Assistive Leg) exoskeleton [60]. EMG signals were also utilized to control a leg exoskeleton by calculating required muscle forces [61]–[65]. Sawicki et al. proposed to use this type of AFO for rehabilitation of motor adaptation [68], [69]. However, user adaption to these types of systems is one of the challenges for the user. Kinnaird et al. found that, once adapted to walking with this AFO, soleus muscle activity reduced by 27% and medial gastrocnemius muscle activity reduced by 12% over time; and tibialis anterior activation during the first burst at heel strike reduced by 28% [66]. For this reason, subjects with EMG-controlled AFOs required an adaptation process. It was found to take 30-45 min of walking to adapt lower limb muscle activation patterns to control plantarflexion assistance [65]. Cain et al. compared the proportional EMG control with footswitch control and found that proportional myoelectric control reduced soleus muscle activity more than footswitch control alone [67]. Moreover, while working with impaired populations, collecting EMG signals is not necessarily an easy task to accomplish, especially in population with neuromuscular impairment. Therefore, we propose to estimate gait states, specifically as defined by percentage of the gait cycle (% GC) during walking, to control the PPAFO actuation.

Multiple advanced approaches for estimating different states are found in the literature. A *k*-nearest neighbor algorithm has been used to control orthoses and prostheses [5], [70]. This algorithm cannot achieve satisfactory control for AFOs due to susceptible to chattering and delays in classification process [5], [70]. Functional Electrical Stimulation (FES) based AFOs found in literature used both DE type controllers and advanced approaches (such as machine learning based algorithm and ankle angle

trajectory tracking by terminal sliding mode control) to control the AFO [71]–[75]. Researchers from University of California, Berkeley developed the Berkeley Lower Extremity Exoskeleton (BLEEX), which contained up to 14 degrees of freedom and the motion in sagittal plane was powered while other motion (abduction-adduction, ankle left-right rotations) were unpowered [76]–[79]. BLEEX used a multivariable nonlinear algorithm to robustly control its behavior. The control scheme needs no direct measurements from the user (i.e. force sensors from two foot plates), instead the controller estimates state based on measurements from the exoskeleton only [76]–[79]. However, a very accurate dynamic model of the system was necessary to control this exoskeleton [79]. Accurately modeling the ankle-foot system with powered AFO is very difficult for impaired populations. Our proposed algorithm scheme needs only training data which can be collected easily compared to going through deriving difficult mathematical models of the ankle-foot system.

Li et al. proposed a fractional time (FT) state estimation approach that depended only on the heel strike (HS) event for the PPAFO [20]. If subject speed changes, the FT estimator will wait for the next heel strike to begin adapting the speed change and will need another 4 to 5 strides to catch up with the new speed [5]. FT requires no training procedure because it assumed that every person walks in the same way. In real life, not all step or stride lengths or gait speeds are the same. FT cannot accommodate these problems during the cycle. Li et al. also proposed a cross-correlation (CC) based state estimation that used the cross-correlation between sensor signals and a gold-standard "true" gait cycle [5], [49]. Morris et al. compared the difference between CC state estimation based controllers with Direct Event [49]. According to that work, for a healthy subject, DE worked better than CC in terms of RMS [49]. Li et al. also mentioned that for healthy subjects, FT and CC performed comparably and also suggested that FT estimation performed well for healthy walking during comfortable walking speed [5]. However, for impaired populations, CC worked better compared to DE and FT estimation based controller. Moreover, for the impaired subject the magnitude of the FSR sensor was found inconsistent which lead to not

correctly identifying heel strikes sometimes. In these cases, the FT estimator failed to estimate effectively. The main equation for FT estimator is the following.

$$\hat{\lambda}_{FT} = 100\frac{(t - t_{hs})}{T} \quad (1)$$

Here, $\hat{\lambda}_{FT}$ represents the estimated percentage of gait cycle or gait state, t represents current time, t_{hs} represents time of the last heel strike event, and T represents period of the gait cycle.

In Study 1, we proposed two new estimators which addressed the limitations of addressing speed changes and reliance on only the heel strike event of the FT estimator. We hypothesized that our new estimators would be more reliable than the FT estimator for impaired populations.

1.2.2 Appropriate timing for plantarflexion actuation

Though powered AFOs have been proposed to assist walking (especially during propulsion or plantarflexion) for impaired populations, there have been few studies regarding the optimal timing of when to actuate the device for plantarflexion assistance [80], [81]. There is not much agreement among active AFO developers of when the AFO should be actuated for forward propulsion [80]. In the literature, it has been found that 50% of the positive muscle work (i.e., generation of mechanical energy) during walking is provided by the ankle joint [82]. High positive joint work is only required at the end of the ipsilateral leg's single stance phase during walking, when the heel of the leading (contralateral) leg strikes the ground [82]. While walking, the foot that needs torque in the ankle performs positive external work while the contralateral leg performs negative work (i.e., dissipation of mechanical energy) at heel strike [14]. Therefore, Kuo et al. used a simplified mathematical model to determine that effective and energy efficient ankle actuation should be when the contralateral leg undergoes heel contact on the ground [81]. It was predicted that four times more energy would be needed if actuation was given too early during the mid-stance phase instead of at the proper timing [81]. In practice, however, it is difficult to detect the contralateral leg's heel contact timing if an AFO is only worn on the ipsilateral leg.

Researchers explored different techniques to determine when to provide plantarflexor actuation to their powered AFOs. Malcolm et al. empirically tuned the optimal plantarflexor torque timing by examining metabolic cost during walking. According to this study, actuation timing at 37% ± 1% of gait cycle showed the highest reduction in metabolic cost (treadmill walking), and timing at 45% ± 2% GC was found to produce the highest performance index during walking (for ambulant exoskeletons) [80]. According the Malcolm et al. study, the onset of biological plantarflexor activation, which occurs around 15% GC, takes place much earlier than the optimal plantarflexion [80]. The reason for early biological activation might lie on the assumption that biological plantarflexor muscles might produce negative work by lengthening at the beginning of the stance phase [83]. Malcolm et al. [80] found that plantarflexion timing tuned purely on biological muscle activation was not ideal for reducing metabolic cost during steady state walking with plantarflexion assisting devices. Moreover, the study suggested that the most efficient timing for actuating a plantarflexion assistive devices was somewhere between 40% to 50% GC in different populations [80]. They found the lowest metabolic cost when the actuation started just before the contralateral leg's heel strike. In addition, Sawicki et al. conduct an experiment for patients with spinal cord injuries wearing a bilateral powered AFO, which was manually controlled by a therapist with pushbuttons. In that study, the average plantarflexor onset torque, for providing peak control signal activation or maximum air pressure to the pneumatic system ,was found to be at 43.5% ± 3.7% GC [69]. However, these study did not mention how ankle angles or biomechanics of the joints are different for different actuation timings. In addition to the energetics of the body system, we also need to see the effect on biomechanics of the joint while walking. Biomechanics data allow comparison of joint kinematics between how a person will walk relative to a healthy person. In Study 2, we proposed supervised learning classifier approach to determining the appropriate plantarflexor torque actuation timing during walking using the biomechanics data, instead of metabolic data.

1.2.3 Gait mode recognition while walking with a powered AFO

In everyday walking, one generally walks not only on the level ground but also up and down stairs and ramps. The gait behaviors for walking on the level ground, stair ascent/descent, ramp ascent/descent are different from each other. The gait mode is here defined by the individual's gait behavior while walking in one of these distinct environments. While helping impaired populations with powered AFOs, we need to address the issues of walking in various modes if the device is not constrained to operate only in a controlled level ground environment. Since ankle joint moment and ankle angle movements are different for different gait modes [84], the actuation scheme for powered AFO should be different. Therefore, it is essential to recognize the gait mode while walking with any powered AFO.

Several researchers have explored gait mode recognition; however, most of them were using prosthetic devices [18], [85]–[87]. For prosthetic devices, some of the researchers focused on knee joint prostheses. Koganezawa et al. claimed that lower limb amputees could ascend and descend stairs using their passive prosthesis after 1 hour of training [85]. However, no data with satisfactory results were mentioned in the article.

Some researchers used non-autonomous or manual switching schemes to deal with changing gait modes during walking. A user manually switches modes using Ottobock's C-Leg by tapping the heel [86]. However, this scheme is not autonomous. Au et al. proposed two finite state controllers to classify between level-ground and stair-descent mode using EMG signals measured from residual muscles in the amputated limb. The flexing of the gastrocnemius muscle was used to detect the transition from level-ground to stairs and the flexing of the tibialis anterior muscle was used to detect the transition back to level-ground mode [87]. For that study, three different variances of EMG signals were set as an input in a feed-forward artificial neural network to estimate the intended orientation of the foot orientation [87]. This algorithm was not automatically capable of switching state; rather the wearer used their residual limb muscles to express their intention. It also needed a higher number of sensor signals and could not detect stair ascent mode. Sometimes EMG signals are very weak for an impaired subject, especially one with

neuromuscular damage, and so EMG based gait mode recognition might not work well for certain impaired populations.

Multiple works were found to develop an autonomous system for detecting gait modes [54], [88]–[95]. Varol et al. [70] used a *k*-nearest neighbor algorithm to classify different gait modes for prostheses. The authors considered three different walking speeds as different gait modes [70]. The same group also used principle component analysis with Gaussian mixture models for gait mode recognition; this approach was capable of differentiating standing mode from walking mode for the Vanderbilt prostheses [88]–[90]. A supervisory intent classifier and mid-level controller based algorithm were used to switch modes [54]. However, these schemes were not capable of differentiating from walking on level ground to stair ascent/descent mode. Most of the previously developed autonomous methods had issues with one step delays, needing higher number of sensor inputs, or were impossible to use in real-time.

Another common approach for gait mode recognition involved using an inertial measurement unit (IMU) consisting of accelerometers and gyroscopes. Zhang et al. [91] developed an algorithm to predict upcoming terrain height during walking using a laser distance sensor attached to the waist or shank and four IMUs attached to the thigh, shank, foot. This algorithm needed a high number of sensors and heavy computation to deal with lots of data collected from the different sensors. Coley et al. [95] used a miniature gyroscope attached to the shank to detect the level ground and stair ascent modes during walking. Being a non-causal algorithm, this procedure could not be implemented in real-time. Furthermore, this algorithm was limited to detect stair ascent mode only. Li et al. proposed an algorithm that tracked the real-time 3D position of the foot using an IMU on the PPAFO [94]. However, there was a one-step delay in mode recognition [94]. There are currently no reliable and minimum number of sensors based gait mode recognition algorithms available which can detect all the modes without long delays. In Study 3, we proposed to also using an IMU to detect the gait mode but combine its signals with an artificial neural network.

1.3 Overview of studies

In this dissertation, three aspects of effective control for a powered AFO were proposed. In Study 1, improved methods for the estimation of the gait state (or percentage of gait cycle) during walking with the PPAFO was addressed. Two new methods were proposed: Modified Fractional Time (MFT) and artificial neural network (ANN). In Study 2, a multistep, supervised learning classification approach was developed to find the proper plantarflexor actuation timing during walking. A classifier algorithm, which was developed using a principal component and Fourier analysis on biomechanics data, was combined with a bisection search technique to quickly identify the optimal actuation timing. Finally in Study 3, controller schemes for recognizing different gait modes (walking on level ground, stair ascent/descent) were addressed. An artificial neural network based algorithm was proposed to detect different gait modes with less delay.

Chapter 2

Study 1: Estimating Gait State during Walking by Modified Fractional Time and Artificial Neural Networks

2.1 Abstract

Control of a powered ankle-foot orthosis (AFO) will be most effective, if we can successfully identify and actuate the AFO at specific times during the gait cycle, i.e., when to apply dorsiflexor or plantarflexor torque at the ankle. A simple approach to identifying gait events and controlling the AFO is by directly checking whether sensor signals go above or below a predetermined threshold (Direct Event control). An alternative approach is the use of pre-defined models to estimate the gait state, as represented by percentage of the gait cycle, from sensor signals and then use these estimated states to identify the gait events (State Estimation control). Previously a Fractional Time (FT) state estimator was developed that used only a heel contact sensor to define gait states. However, the FT estimator has a delayed response to changes in gait speed. Two estimators, Modified Fractional Time (MFT) and Artificial Neural Network (ANN), are introduced that use data from three sensors (heel contact, toe contact, and ankle angle). Three types of sub-studies were conducted to assess the effect of varying gait speed on accuracy of the estimators. In Sub-study A, the new algorithms were applied to simulated sensor signals that were artificially manipulated to examine the sensitivity of estimators on variations of speed change and input signal configuration. The simulated input signals were considered to represent the "true" gait states. In Sub-study B, experimental data were collected from five able-bodied subjects. Estimated state were determined from the three algorithms and compared to the "true" gait state defined by a motion capture system. Finally in Sub-study C, the AFO applied ankle torque during walking according to the estimated state as predicted for each algorithm. Experimental data were collected from one subject. "True" state from motion capture compared to estimated states from the three algorithms. The absolute mean error

(MAE) was computed using true and estimated state. From simulation Sub-study A, we found that MFT and ANN worked better when walking speed was not constant. It was also found that both MFT and ANN performed better when trained by varied signal, which suggested that subject specific training should be needed for these two new algorithms. According to Sub-study B, MFT and ANN performed similar to the previous FT algorithm during constant walking speed (mean error: < 6% GC). However, the performances of the new estimators were significantly better when walking with variable speeds (mean errors: 16% GC (FT), 7% GC (MFT), and 4% GC (ANN); $p < 0.05$). During application of controller (Sub-study C), MFT showed best result compared to controllers based on FT or ANN estimators.

2.2 Introduction

2.2.1 Motivation

An ankle foot orthosis (AFO) is an external device that can provide assistance to individuals with lower limb muscle impairment to correct gait deficiencies [7]. Healthy able-bodied gait generally begins from the time of initial contact of the heel with the floor, i.e., 0% gait cycle (% GC), and ends at the next heel strike of the same foot, 100% GC. Numerous neurological disorders, muscular pathologies and injuries, including trauma, stroke, or multiple sclerosis can affect gait [6].

Recently, powered AFOs and exoskeletons have been developed to explored robotic gait assistance[5], [7], [22], [23], [29], [42], [50], [51]. The portable pneumatically powered ankle foot orthosis (PPAFO) was recently developed and is capable of providing both plantarflexor and dorsiflexor torque at the ankle [51]. The PPAFO used force resistive sensors at the heel and ball of the foot and an ankle angle sensor.

One of the most common approaches to control a powered AFO to detect different gait events is to check whether each sensor measurement at any time goes above or below a predetermined threshold [22], [23], [28], [29], [42], [48]–[51]. Shorter et al. mentioned this controller that used sensors value directly for the PPAFO as a “Direct Event” controller [48], [51]. However, this approach will not work well when the sensor measurements have no direct relation to events of interest other than heel strike and toe off [5].

Moreover, the reliability of DE controllers can decrease when used under fatigue or impairment [5]. To overcome these difficulties, some researchers have proposed to characterize the gait cycle as multiple states and provide the actuation according to the states [5], [49], [96].

One way to define state is by correlating with percentage of gait cycle during walking [5], [96]. If percentage of gait cycle can be known, the actuation can be provided with higher accuracy while walking and it can be useful for controlling a powered AFO. In other words, a higher accuracy can be achieved by estimating the percentage of the gait cycle in the resolution of 1% to control a powered AFO. In this case, one full gait cycle would be divided into 101 states (from states *0* to *100* and correlates with 0% to 100% GC). Therefore, a 1% GC change refers to 1 state change. After estimating the state, the actuation of the powered AFO can be given accordingly.

Multiple advanced approaches for estimating different states are found in the literature (e.g. [5], [73], [76]). However, some of these algorithms either cannot achieve satisfactory control for AFOs due to susceptibility to chattering and delays in classification process [5], [70] or a very accurate dynamic model of the system was necessary to control the exoskeleton [79].

Our group previously developed the portable powered ankle foot orthosis (PPAFO) [7] which was used to explore the control strategy for powered AFO [5], [49] (Figure 3). The PPAFO has three sensors: force resistive sensors (FSR) under the heel and ball of foot to detect foot contact, and a Hall effect sensor to record ankle angle. The PPAFO with tethered control system was used in this study.

Li. et al. proposed a controller based on gait state estimation using the PPAFO [1]. They proposed a fractional time (FT) state estimation approach that depended only on data from the heel FSR sensor and specifically only the heel strike (HS) event [5]. If gait speed changes, the FT estimator will wait for the next heel strike to begin adapting the speed change and will need another 4 to 5 strides to catch up with the new speed [5]. FT assumed that every person walks in the same way, and so no training procedure was necessary for this estimation. In practice, stride lengths and gait speeds change during daily life

walking. FT cannot accommodate these problems between cycles. These variations were even more pronounced in impaired subjects, as observed during pilot PPAFO work with test participants who were post-stroke or had moderate-severe multiple sclerosis. Occasionally, heel strike pressure varied between steps (mainly with impaired users). In this case, detection scheme sometimes missed identifying a heel strike. This miss can make a controller vulnerable and perform a couple of misfires of incorrect actuation time, which in the worst case could result in a trip or fall. Therefore, we need to design estimators that are more robust and reliable than FT and have the ability to adjust multiple times during a gait cycle. The controller should not be vulnerable to speed changes during walking. In this study, we proposed to develop state estimation algorithms to estimate the percentage of gait cycle during walking with more accuracy.

Two new estimators (Modified Fractional Time (MFT) estimator, and Artificial Neural Network (ANN) estimators) were introduced in this study that used data collected from multiple sensors on the device to overcome the previous issues. On the PPAFO, the input signals were the time-varying heel force sensitive resistor (FSR), toe FSR, and the ankle angle sensor signals observed over a gait cycle. Unlike the FT estimator, MFT is proposed to update eight times during a full gait cycle using three sensor signals. ANN is capable of estimating continuously across the gait cycle by using a moving window of six previous sets of data points, while MFT only updates eight times during a cycle and estimates linearly other times using moving average of gait cycle period. Our hypothesis was that MFT and ANN would be more reliable and robust compared to FT estimators.

We examined the performance of these estimators through three sub-studies. The Sub-study A used simulated input signals that were generated from previously collected walking data for analyzing the sensitivity of the proposed algorithms. The Sub-study B validated the algorithms' estimation performance on experimental data collected during a variety of walking trials that examined changes in gait speed or period. The Sub-study C actually implemented the actuation control of the PPAFO based on predicted gait states of each estimator.

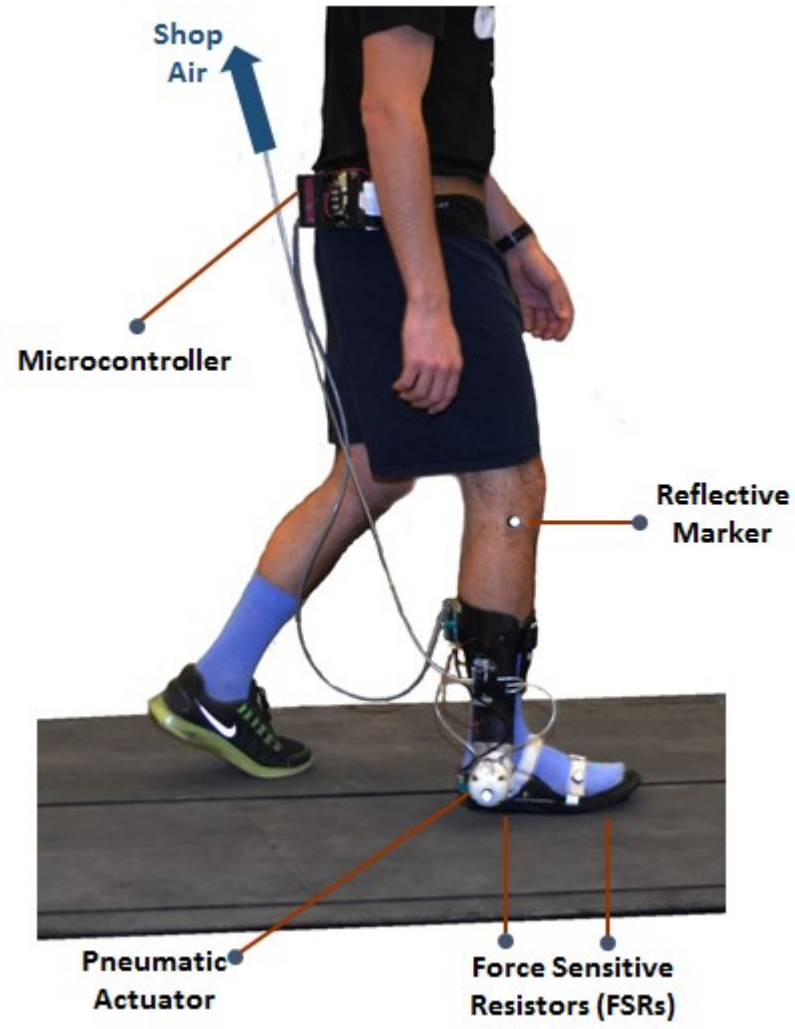

Figure 3 Subject walking with Portable Powered Ankle Foot Orthosis (PPAFO).

2.3 Methods

2.3.1 State estimation algorithms

2.3.1.1 Fractional Time (FT) state estimation

The Fractional Time (FT) estimator proposed by Li et al. [5] simply assumed that the gait states increased linearly from the start of the gait cycle, which was detected by heel strike. At any instance, the estimated state was determined by the FT estimator using the following equation.

$$\hat{\lambda}_{FT} = 100\frac{(t - t_{hs})}{T} \quad (2)$$

Here, $\hat{\lambda}_{FT}$ represents the estimated state (in %GC), t represents current time (in seconds), t_{hs} represents time of the last heel strike event, and T which is the moving average of the period at time t (in seconds) can be calculated via Equation (7).

2.3.1.2 Modified Fractional Time (MFT) state estimation

The MFT estimator used eight events during a gait cycle (Figure 6) and data from three sensors (heel force, toe force, ankle angle) to estimate the gait state (Figure 5). MFT was hypothesized to adapt faster than the FT estimator since the estimated states are updated eight times per cycles (at each event), rather than only once at heel strike. The MFT controller must be initially trained to an individual's gait pattern using the appropriate sensor signals gait data for an individual.

1. **Heel Strike (HS)**
2. **Middle of Initial Contact (MIC)**
3. **End of Loading Response (ELR)**
4. **Mid Stance (MS)**
5. **Terminal Stance (TS)**
6. **Pre Swing (PS)**
7. **Toe Off (TO)**
8. **Mid Swing (MSw)**

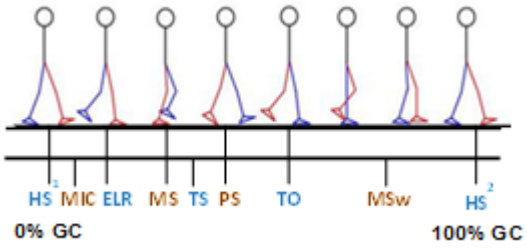

Figure 4 Definition of key events during a gait cycle. Odd numbered events (blue text) are detected from heel FSR and toe FSR sensors. Even numbered events (red text) are detected from all 3 sensors based on $\mu_{i,j}$ and $\sigma_{i,j}$ for each sensor.

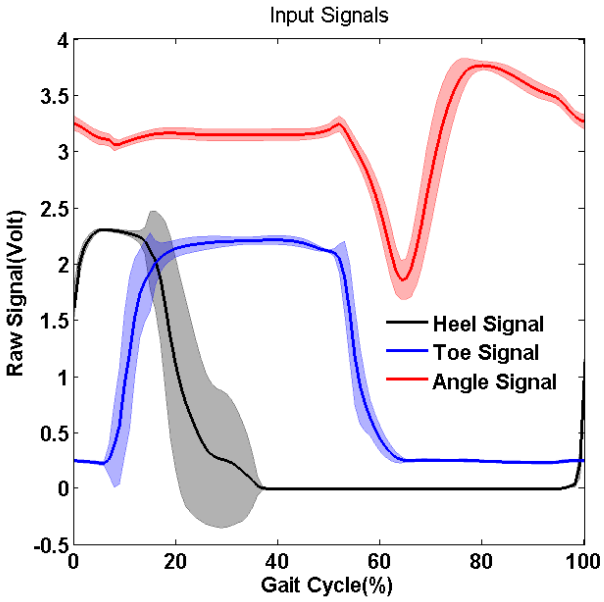

Figure 5 Mean values (solid line) and standard deviation (shaded areas) of input signals of a healthy walker over multiple gait cycles.

Sensor data were divided into gait cycles as defined by heel strike events. We assumed that the signals recorded by the sensors were in Gaussian distributions (Figure 5).

$$S_{H,j} \sim N(\mu_{H,j}, \sigma_{H,j}) \quad (3)$$

$$S_{T,j} \sim N(\mu_{T,j}, \sigma_{T,j}) \quad (4)$$

$$S_{A,j} \sim N(\mu_{A,j}, \sigma_{A,j}) \quad (5)$$

Here, $S_{H,j}, S_{T,j}, S_{A,j}$ are heel FSR sensor signal, toe FSR sensor signal, and ankle angle sensor signal, respectively. $N()$ represents the normal distribution, while μ and σ represent mean and standard deviation of corresponding signals, respectively. j represents the current gait state and ranges from *0* to *100* correlate with 0% to 100% GC (Figure 4 and Figure 6).

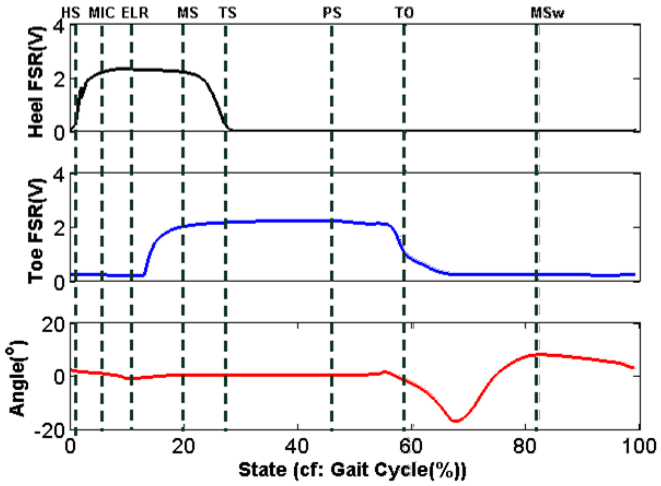

Figure 6 Sample gait events associated with specific states (% GC) as defined by the three sensor signals

MFT is based on dividing the gait cycle into eight events (Figure 4 and Figure 6).We assumed that the accuracy of detecting an event was high when the standard deviations of the sensors were low for a given state over multiple gait cycles. All the odd numbered events were detected by the values of heel FSR and toe FSR sensors only (blue text in Figure 4). The first event (HS^1) indicated the start of the gait cycle. It was triggered by heel strike, i.e., when the heel sensor signal was in a rising edge and toe sensor value is below a threshold value (Figure 6). End of Loading Response (ELR) was defined as the start of the loading response when the toe sensor signal was in a rising edge, and the heel sensor signal was above a threshold value. Terminal Stance (TS) indicated the end of the loading response and was detected when the heel sensor faced a falling edge and toe sensor was still above the threshold value. Toe Off (TO) event was detected by the falling edge of toe sensor and when heel sensor was below the threshold value. The even numbered events (red text in Figure 4), Middle of Initial Contact event (MIC), Mid Stance event (MS), Pre Swing phase event (PS), and Mid Swing event (MSw) were defined by the instances when there was minimum variation of the sensor signals between the respective odd numbered events. During subject-specific training of the estimator, we saved the corresponding state value (i.e., % GC) for each event in the vector $\boldsymbol{L}_e$, where e is from 1 to 8.

During walking, the saved values of $\boldsymbol{L_e}$ evaluated from the training data were used to estimate any state during a gait cycle. Between two event points, we assumed that the states increased linearly from the last detected event L_{LE} according to the average period of the gait cycle. Note that L_{LE} is a single scalar value within $\boldsymbol{L_e}$.Therefore, for any instance, the estimated state will be calculated by following equation.

$$\hat{\lambda}_{MFT} = L_{LE} + 100\frac{(t - t_{LE})}{T(t)} \quad (6)$$

Where

$$T(t) = 0.9\,T(t - \Delta t) + 0.1\,T_{current} \quad (7)$$

Here, $\hat{\lambda}_{MFT}$ is the state estimated by the MFT state estimator since the last detected event L_{LE} (in % GC), t represents the current time (in seconds), t_{LE} represents the time for the last detected event, and $T(t)$ is the moving average of the period at time t (in seconds). $T_{current}$ is the time between two consecutive occurrences of event L_{LE}, and Δt is is sampling time (here, for 120 Hz sampling rate, $\Delta t = 0.0083\ s$).

Due to noise in signals and unavoidable variation in walking, it might be possible that one or two events would not be detected during a gait cycle. In these cases, the algorithm will still follow Equation (5) and continue with a linear interpolation from the last detected event until the next detected event.

2.3.1.3 Artificial Neural Network (ANN) state estimation

A feed-forward Artificial Neural Network (ANN) [97] with one hidden layer was designed to estimate gait states during walking. Unlike MFT, which identified eight events and then estimated the intervening states via linear interpolation, the ANN estimator continuously estimated states across a gait cycle based on a moving window from the previous six data points. Using a log-sigmoid function as the hidden layer's activation function, a mathematical model was constructed from an artificial neural network that estimated the state during walking by using the three sensor signal values.

$$\hat{\lambda}_{ANN} = f(S_H, S_T, S_A) \quad (8)$$

where $\hat{\lambda}_{ANN}$ is the estimated state by the ANN state estimator, S_H = heel sensor values, S_T = toe sensor values, S_A = angle sensor values, and f is a function based on the three signals.

The artificial neural network was constructed using multiple layers with activation functions and represented the function f as a whole. The subject-specific parameters for constructing the ANN were calculated by minimizing a cost function (Equation (13)) from the training data. The construction of ANN and the procedure to find the parameters are discussed in following paragraphs.

The basic structure of the neural network used in this study consisted of three layers: an input layer, followed by a hidden layer, and an output layer (Figure 7). In the input layer, there was an input vector $\boldsymbol{x}$ which consisted of signals from the three sensors with six tap delays each, for a total of 18 elements. The hidden layer had ten neurons and used log-sigmoid activation functions. The output layer had a single neuron and used a linear activation function, which provided the estimated state value during walking $\hat{\lambda}_{ANN}$.

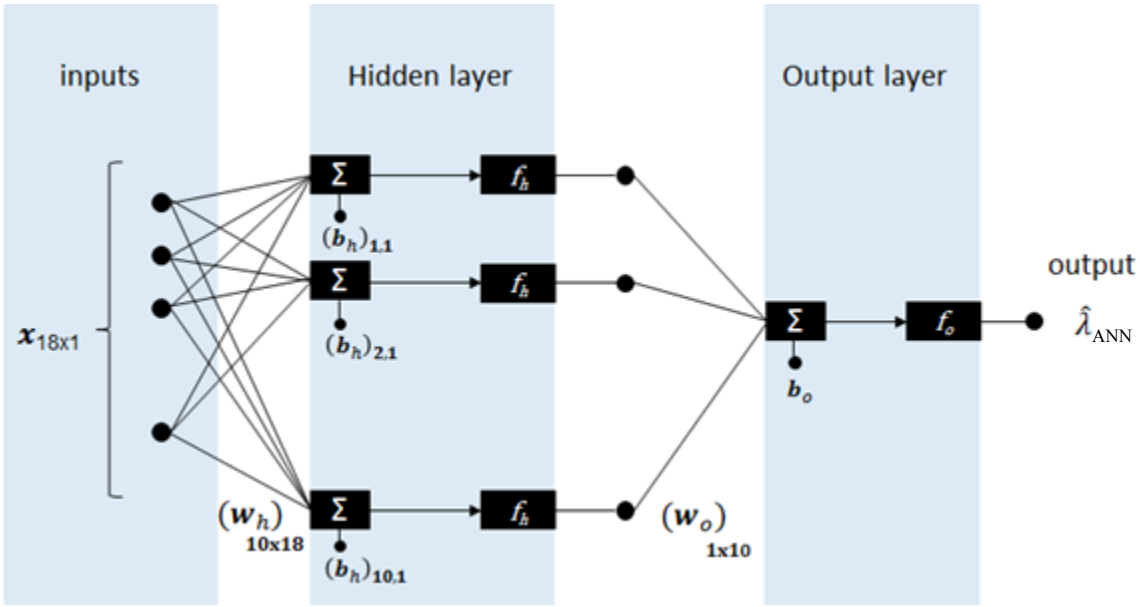

Figure 7 Artificial neural network structure for estimation of state for three input sensors.

Log-sigmoid functions were used as the activation function in the hidden layer. The output vector of the hidden layer, $\boldsymbol{a_h}$ can be found from the following equation:

$$\boldsymbol{a_h} = f_h(\boldsymbol{w}_h\boldsymbol{x} + \boldsymbol{b}_h) \quad (9)$$

Here, $\boldsymbol{x}$ is the input vector with 18 elements. $(\boldsymbol{w_h}, \boldsymbol{b_h})$ are called weights and biases of the hidden layer. $f_h(n)$ can be expressed as

$$f_h(n) = \frac{1}{e^{\boldsymbol{n}} + 1} \quad (10)$$

The result of the output layer, $\hat{\lambda}_{ANN}(t)$, can be found using output layer parameters $(\boldsymbol{w_o}, \boldsymbol{b_o})$.

$$\hat{\lambda}_{ANN}(t) = f_o(\boldsymbol{w}_o\boldsymbol{a}_h + \boldsymbol{b}_o) \quad (11)$$

Where, $(\boldsymbol{w_o}, \boldsymbol{b_o})$ are the weights and biases of the output layer. $f_o(n)$ is the output layer activation function and here it is used as linear activation function:

$$f_o(n) = n \quad (12)$$

The parameters $(\boldsymbol{w_h}, \boldsymbol{b_h})$ and $(\boldsymbol{w_o}, \boldsymbol{b_o})$ are necessary to find the output for any input $\boldsymbol{x}(t)$. Training is needed for finding these parameters.

For training purposes, we defined a cost function that will be minimized by a Gauss-Newton approximation to the Hessian matrix using the Levenberg-Marquardt algorithm [98], [99]. Hagan et al. described a Bayesian regularized training in [99]. The cost function *E* was defined as:

$$E = \alpha \sum (\tilde{t}_i - \hat{\lambda}_{i_{ANN}})^2 + \beta\, E_w \quad (13)$$

Where, $\tilde{t}_i$ is the target value or true state during walking (computed by following procedure described in section 2.3.3.2.1), $\hat{\lambda}_{i_{ANN}}$is the estimated state or output of the network at the ith data point, E_w is the sum of squares of the network weights, and α and β are objective function parameters. The update laws of Bayesian optimization of regularization parameters α and β , were described in [99].

2.3.1.4 Training of state estimators

The previous Fractional Time algorithm did not need a training period, whereas Modified Fractional Time and Artificial Neural Network state estimation algorithms required prior training. As FT state estimation only depended on heel strike, there was no reason to have training before each subject. However, MFT and ANN state estimation depend on the full profile of the sensor signals over a gait cycle. Therefore it was necessary to create a set of training data to define subject-specific estimation models for MFT and ANN. For each user, gait data must be collected prior to the training of the MFT and ANN estimators. Ideally 30 cycles of data are needed for better results. For training, a subject will walk at his/her comfortable speed, and data from the sensors will be collected.

2.3.2 Sub-study A: Sensitivity analysis

This study used a controlled data set to examine the sensitivity of the estimators on variations of speed change and input signal changes before collecting experimental data. This study examined the performance of the three state estimation algorithms (FT, MFT, and ANN) by using artificially modified heel FSR, toe FSR, and ankle angle sensor signal data to simulate different walking conditions over 120 strides. The sensitivity of the estimators to variations in timing or amplitude of the sensor signals was examined by varying the characteristic of one sensor signal, while holding the other signals the same. The sensitivity to variations in walking speed (or gait cycle period) was explored by varying gait cycle period over short transients of one step or longer transitions of ten steps. The effect of the structure of the training data was also investigated by using training data with or without variations in the sensor signals. The simulated data were created by adjusting experimental gait data collected during a previous study [100] or recent pilot work.

2.3.2.1 Simulated sensor values for a gait cycle from real data

Heel FSR, toe FSR, and ankle angle sensor data collected from five subjects for another study [100] and two additional subjects were used for creating the simulated data for this study. The data from the

five subjects involved 3 minutes of walking on a treadmill at the subject's comfortable walking speed while wearing the PPAFO on the right leg. The two additional subjects walked over-ground (not on treadmill) for 6 minutes while wearing the PPAFO on the right leg. All data were collected when the Direct Event controller was used.

There were two types of variations added to the actual real average signals. The first type was adding variation in the heel, toe and angle sensor signals. Another type was adding variation to gait cycle period. To understand how variation in a sensor signal affected each estimator's performance, average characteristics of each sensor were determined. The timing of heel sensor off; toe sensor on and off; offset, amplification and time of peak plantarflexion angle on angle sensor were quantified using the previous five subjects' data [100]. Heel off was defined by the time (in %GC) when the heel FSR signal went below a threshold value. Toe on and toe off were similarly defined but using the toe FSR signal. Angle offset was defined as the shift or drift in ankle angle from 0º (i.e., ankle angle neutral position) over multiple gait cycles (in degrees). Amplification of range angle was the ratio of ranges of motion from one stride to the next. Peak plantarflexion timing (% GC) was defined as when the peak plantarflexion angle value was found.

These average characteristics were then used to create simulated sensor signals to feed into the estimators' algorithms. For example, to create a simulated heel FSR signal with variation, the timing of when the heel sensor signal went low (or considered off) varied across the simulated data set such that the mean and standard error of the timing was at 21.6% ± 2.3% GC. For this case, the toe FSR and ankle angle sensor signals were created such that the respective timings, offset, and amplification values were set to be the same (i.e., mean value).

From the 6 min walk data from two subjects, the average gait cycle period was found to be 1.31 ± 0.12 sec (mean ± S.E.). Using these data, six walking conditions were each simulated with gait data of

120 strides, which was approximately 2 min worth of data (Table 3). The selected time periods were chosen as follows: t1 was the same as mean value of the gait cycle period (1.31 sec), t2 was one standard error below the mean value (i.e., 1.19 sec), and t3 was one standard error above the mean value (i.e., 1.43 sec).

We created simulated data by combining variation of one sensor signal and walking condition together. The Table 4 shows which sensor variations and walking conditions were used to compare the different estimators.

Table 2 Statistical data (mean ± S.E.) for different sensors from experimental data (treadmill walking).

Heel off (% GC)	Toe on (% GC)	Toe off (% GC)	Angle offset (degree)	Amplification of angle	Peak plantarflexion time (%GC)
21.6 ± 2.3	12.0 ± 3.1	60.3 ± 0.8	2.0 ± 0.6	1.00 ± 0.04	62.1 ± 0.7

Table 3 Different walking conditions of generated simulated data for sensitivity analysis.

Condition 0	Full random gait cycle period (such that had average of 1.31 ± 0.12 sec) for 120 strides
Condition 1	All strides have same gait cycle period (t1 = 1.31 sec) for 120 strides
Condition 2	Alternating 10 strides in t1 period and next 10 in t2 period (1.19 sec) for first 60 strides Alternating 10 strides in t1 period and next 10 in t3 period (1.43 sec) for last 60 strides
Condition 3a	Alternating 10 strides in t1 period and 1 stride in **faster** t2 period for 120 strides
Condition 3b	Alternating 10 strides in t1 period and 1 steps in **slower** t3 period for 120 strides
Condition 3	60 strides like Condition 3a and next 60 strides like Condition 3b

Table 4 Factors used for comparison of different estimators.

	No variations	Heel signal variation	Toe signal variation	Angle offset variation	Angle Amplification variation	Angle timing variation
Condition 0	x					
Condition 1		x	x	x	x	x
Condition 2	x	x	x	x	x	x
Condition 3a	x					
Condition 3b	x					
Condition 3		x	x	x	x	x

2.3.2.2 Training protocol of simulation study

Different sets of data were used to test the sensitivity of the MFT and ANN estimators to choice in training data. As stated earlier, the FT estimator did not need any training. For the MFT and ANN estimators, the training and test data had opposite variation characteristics for a given sensor signal test case. That is, for some cases, training was performed on unvaried average signals and tested with data that had variation in the given signal. In other cases, training was performed with variation in the given signal and tested on unvaried signals. It should be noted that for all the cases, training data and testing data were always different.

2.3.3 Sub-study B: Experimental study

The main purpose of this study is to evaluate of each estimators' performance experimentally. This study examined the performance of the three state estimation algorithms by using experimental data collected while the test participant walked on a treadmill wearing the PPAFO.

Five healthy adult male subjects (age 24.2 ± 3.6 years, height 1.72 ± 0.08 m, weight 76.9 ± 7.9 kg) participated in this study. None had any neurological, gait, or postural disorders. All gave informed consent and this study was approved by the university Institutional Review Board.

Each subject walked with the PPAFO on his right leg. There are two types of control system for the PPAFO : a) untethered system (using an embedded microcontroller: MSP430G2553, Texas Instruments, Dallas), & b) wired system (connected to computer and DAQ: QUARC, Quanser Consulting Inc, Markham, ON, Canada). Untethered systems were used in Sub-study B while wired system were used for Sub-study C. The subject walked on a force sensing treadmill (Instrumented Treadmill, TM07, Bertec Corp., Columbus, OH) to collect vertical ground reaction force data. Reflected markers were attached to the PPAFO over three anatomic landmarks: (lateral epicondyle of tibia, lateral malleolus of fibula, and first metatarsal head). Kinematic data for the reflective markers were collected by a three-camera motion capture system at 120 fps (Vicon, Oxford, UK Model 460) and data from force plates of the treadmill were collected at 1200 Hz. Ankle joint kinematics were calculated using a custom MATLAB program (v 8.1.0.604, the Mathworks Inc., Natick, MA, USA). A 4^{th} order Butterworth low pass filter with a cut-off frequency of 8 Hz was applied to the motion capture data for calculating the ankle angle. For actuation control consistency in the study, the PPAFO was actuated using the Direct Event control scheme [5]. The data collected were used to compare the estimated gait states from each estimator algorithm to the measured "true" gait states as defined by the motion capture and ground reaction force data.

2.3.3.1 Experimental protocol

Data for three testing conditions were collected for each subject in the following order.

Condition 1: Quiet stance data

The subject stood on the treadmill for 30 sec to collect quiet stance kinematic data to find the offset of the PPAFO angle sensor relative to the ankle angle measured from the motion marker positions.

Condition 2: Constant speed

The subject walked on the treadmill for 2 min at his comfortable speed. Two trials were performed and recorded. The average value for subject-specific comfortable speed across all five subjects was 0.9 ± 0.11 m/s.

Condition 3: Variable speeds

The subject started walking on the treadmill at 0.1 m/s slower than comfortable speed. After every 30 sec, the speed was increased 0.1 m/s until reaching the final speed of 0.2 m/s more than comfortable speed. Two trials were performed and recorded. The value of 0.1 m/s was found after rounding the one standard deviation value of walking speed got from the previously collected experimental data used in Sub-study A.

2.3.3.2 Data analysis

2.3.3.2.1 Calculation of true state

The true state was calculated via the gold standard movement data defined by the motion capture and force plate data following the method described at [5], [96]. A six dimensional (6-D) vector $\boldsymbol{p}(t)$, based on the ankle angle, bilateral GRFs and their derivatives, was used to define any position in a gait cycle at time, t. One gait cycle were divided into 101 states (between 0% to 100% GC). A linearly weighted regression model $\overline{\boldsymbol{p}}$ (consisting of six elements for each state of the 101 states) was built using the 6-D data sets across all gait cycles. Later this model was used to calculate the true state across all gait cycles after comparing the 6-D vector $\boldsymbol{p}(t)$ with the model for any time t (Equation 14) by nearest neighbor algorithm [5], [96].

$$\lambda(t) = \underset{\lambda^* \in [0,100)}{\arg} \; min \, \|\boldsymbol{p}(t) - \overline{\boldsymbol{p}}(\lambda^*)\|_2 \tag{14}$$

Where, $\lambda(t)$ is the true state, $\boldsymbol{p}(t)$ is the six dimensional vector at time *t,* $\overline{\boldsymbol{p}}(\lambda^*)$ is found from regression model, and λ^* is state or parameter for $\overline{\boldsymbol{p}}$ and has value from 0 to 99.

2.3.3.2.2 Estimation comparison metrics

Similar to the sensitivity analysis (Sub-study A), the sensor data from these two test walking conditions (Conditions 2 & 3) were used to estimate the states over the multiple gait cycles using the FT, MFT, and ANN algorithms.

To train the MFT and ANN estimators, the first 30 seconds of data from the first trial of Condition 2 were used as training data for both state estimation techniques. The parameters for the eight events, described in section 2.3.1.2, were calculated and later used for finding the gait states during walking for the MFT estimator. For ANN estimators, the weights and biases were measured from the training data as in section 2.3.1.3.

To test the estimators, data from Conditions 2 (comfortable speed) and 3 (variable speeds) were used. For Condition 2, the remaining 1.5 minutes of the first trial and the full 2 minutes of the second trial were used as testing data. For Condition 3, both 2 minute trials were used as testing data. Later, the Mean Absolute Error (MAE) for each estimator was calculated against the true state. The MAE (% GC) was defined by taking the average of the absolute value of error across all gait cycles for a given condition (Equation 15). The errors across these data were calculated by computing the difference between the estimated stated and the true state for any time.

$$MAE = \underset{t\in[0,n]}{\text{average}} \left|\hat{\lambda}(t) - \lambda(t)\right| \tag{15}$$

Where, $\lambda(t)$ represents the true state, $\hat{\lambda}(t)$ represents the estimated state based on FT, MFT, or ANN, t represents current time, and n represents 3.5 minutes of walking data for Condition 2 or 4 minutes of walking data for Condition 3.

Two-way repeated measures ANOVA (speed × estimators) was conducted with Bonferroni confidence interval adjustment and post hoc analysis using Tukey's HSD tests (SPSS Statistics 22; IBM, Armonk, NY, USA). P-values of less than 0.05 were considered significant.

Statistical analyses were also done separately on different gait phases (stance and swing) to see how estimator performance changed for the different phases. The main reason for using a state estimation technique is for controlling a powered AFO to actuate the device at desired times during a gait cycle, such as applying plantarflexor torque during late stance for propulsion; therefore, correct state estimation

during the stance phase is more important as actuation is needed at specific times (%GC) of this phase. This is the reason to analyze the data in terms of different phases.

2.3.4 Sub-study C: Application to controller

The primary purpose of this study was to see which estimator (FT, MFT and ANN) worked best when actuation was provided based on predicted estimated state. The FT, MFT or ANN state estimator was implemented and the actuation was provided to the PPAFO based on estimated states. The performance of the implementation of these three estimators was compared. One subject walked on the treadmill for conditions controlled by the FT, MFT or ANN estimators. During walking, states were calculated in real-time and using the state value, the PPAFO provided actuation at a suitable time. The walking speed varied for different trials, and later results were compared for different cases.

One healthy adult male subject (age 24 years, height 1.75 m, weight 71 kg) participated in this study. The subject gave informed consent and this study was approved by the university of Institutional Review Board.

The subject performed different testing conditions on the same treadmill mentioned in the previous section. Three reflected markers were attached and data for the markers were collected by the same motion capture system at 120 fps. Data from force plates of the treadmill were collected at 1200 Hz. Unlike Sub-study B, all dorsiflexor and plantarflexor torque actuation timings were performed based on the estimated state from a given algorithm according to [2] (Table 5).

Table 5 Actuation scheme for Sub-study C [2].

Estimated State	Actuation Scheme
0% to 7%	Dorsiflexor Torque
7 % to 48%	No Actuation
48% to 62%	Plantarflexor Torque
65% to 100%	Dorsiflexor Torque

2.3.4.1 Experimental protocol

Data for four testing conditions were collected for each subject in the following order.

Condition 1: Quiet stance data

Quiet stance data were collected same as Sub-study B (see section 2.3.3.1).

Condition 2: Collection of training data in comfortable speed

The subject walked on the treadmill for 1 min at his comfortable speed while the FT estimator was used to estimate the state and actuation was provided according to Table 5. The last 30 seconds of these data were used as training data for MFT and ANN estimators, following the methods described in sections 2.3.1.2 and 2.3.1.3, respectively.

Condition 3: Constant speed

The subject walked for 2 min at his comfortable speed while actuations were given according to estimated state using the FT, MFT or ANN estimator. Two trials for each estimator were performed and recorded.

Condition 4: Variable speeds

The subject started walking at 0.1 m/s slower than comfortable speed. After every 30 sec, the speed was increased until reaching the final speed of 0.2 m/s more than comfortable speed. Two trials for each estimator (FT, MFT, ANN) were performed and recorded, similar to Sub-study B.

2.3.4.2 Estimation comparison metrics

Similar to the Sub-study B, for each estimator application, the error of the estimator was defined by the difference between the true state and the estimated state for each % GC. The true states were calculated as described in 2.3.3.2.1. The estimated states for FT, MFT and ANN were calculated as described in 2, 2.3.1.2 and 2.3.1.3 in real time and actuation timings applied as per Table 5. The MAE was computed similar as Equation 15.

2.4 Results

2.4.1 Results for sensitivity analysis study (Sub-study A)

According to Sub-study A, ANN outperformed MFT and FT when gait speed was varied; however, FT performed best only when gait speed was kept constant (Table 6 and Table 7). ANN performed best and FT performed worst when variation was only added to stride period and no variation added to any of the input signals (Table 6). As FT only depends on heel strike, while variation was introduced to both stride periods and input signals, FT was found to have less impact on the variability of different sensors; however, its performance decreased for different conditions where stride periods were varied (Table 7). MAEs for both MFT and ANN were smaller when algorithms were trained by varied input signal compared to train by unvaried signals (Table 7). ANN was less sensitive when variations were added to gait stride periods.

Table 6 Mean Absolute Error (%GC) for different estimators when only gait stride period was varied.

Stride Period Variation	No Variation in Input Signals		
	FT*	**MFT**	**ANN**
Condition 0	13.6	8.8	1.4
Condition 2	11.5	7.4	1.7
Condition 3a	6.2	6.5	1.6
Condition 3b	5.9	7.6	1.0

* No training needed for FT estimator

Table 7 Mean Absolute Error (%GC) for different estimators using simulated input signals.

	Stride period Variation	Trained by Unvaried Input Signals			Trained by Varied Input Signal		
	Condition	**FT***	**MFT**	**ANN**	**FT***	**MFT**	**ANN**
Heel Sensor Variation	1	1.3	6.1	2.8	1.5	5.4	1.7
	2	14.8	8.9	2.2	14.8	8.8	2.6
	3	6.3	7.2	2.7	6.3	6.6	1.8
Toe Sensor variation	1	1.5	5.3	3.5	1.5	5.1	1.6
	2	14.5	8.4	3.1	14.5	8.6	3.0
	3	6.2	6.5	3.4	6.2	6.4	1.8
Angle Sensor Offset	1	1.5	7.0	6.0	1.5	6.1	1.6
	2	14.5	9.8	5.1	14.5	9.4	3.6
	3	6.2	8.9	7.0	6.2	8.8	2.0
Angle Sensor Magnification	1	1.5	5.4	3.4	1.5	5.3	1.6
	2	14.5	8.1	3.3	14.5	8.0	3.5
	3	6.2	7.3	3.4	6.2	6.3	1.9
Peak Plantarflexion Variation	1	1.5	5.6	3.2	1.5	6.5	1.6
	2	14.5	8.3	2.7	14.5	8.8	3.8
	3	6.2	7.1	2.9	6.2	7.5	2.0

* No training needed for FT estimator

2.4.2 Results from experimental data (Sub-study B)

MFT and ANN performed similar to the previous FT algorithm during constant walking speed (MAE: all less than 6% GC); however, the performances of the new estimators were statistically significantly better when walking with variable speeds (Table 8). Considering all the estimators, MAE of variable speed trials are non-statistically larger than that of constant speed trials (Table 9). MAE for the ANN estimator had the smallest value compared to the other two estimators for variable speed trials, while MAE for MFT estimator had smallest values for constant speed trials (Table 8). Statistically, the MAE of the FT estimator was significantly larger than that of MFT ($p<0.001$) and ANN ($p<0.001$). However, The MAE of MFT and ANN estimators were not significantly different. We found a non-statistically significant trend that ANN estimator had smaller and larger MAE than MFT in variable speed trials and in constant speed trials, respectively.

For stance and swing, it was found again that the overall MAE for comfortable speed trials was significantly smaller than that of variable speed trials across all estimators (both $p<0.001$).

During only stance for the comfortable speed condition, there were not any significance differences between the different estimators, though MFT had a non-statistical trend to have lower values than the other two estimators. For the variable speed condition during stance, the MAE for MFT and ANN were significantly smaller than that for FT estimators ($p < 0.014$ and $p<0.001$, respectively). MAE of ANN was also significantly smaller than that of MFT ($p<0.010$) during stance for variable speed trials. For FT and MFT during stance, the trials from the variable speed condition showed significantly larger MAE than trials for comfortable speed ($p<0.001$ and $p<0.001$, respectively). For MFT, MAE for comfortable speed and variables speeds were statistically the same for comfortable speed ($p = 0.85$).Overall without considering speed, during swing, MFT and ANN performed significantly better than FT ($p<0.001$ and $p < 0.001$ respectively) while the MAE of MFT and ANN were statistically same.

During only swing phase, MFT worked best in constant speed trials and ANN worked best in variable speed trials. The MAE for FT was significantly different from constant speed trials to variable speeds ($p< 0.001$); while for MFT and ANN, they were statistically similar. During swing for constant speed trials, FT had significantly larger MAE than MFT ($p<0.02$) and statistically similar to ANN ($p=0.07$). For variable speed trials during swing phase, both MFT and ANN performed significantly better than FT ($p<0.001$ and $p<0.001$ respectively), while MFT and ANN performed statistically similar to each other ($p = 0.63$). Overall consideration all estimators, the MAE for comfortable speed trials was also significantly smaller than that of variable speed trials ($p<0.001$).

Table 8 Mean Absolute Error (%GC) for different estimators, different types of speed, and different phases of gait.

		FT (11.2 ± 6.3)	MFT (5.1 ± 2.6)	ANN (4.4 ± 0.6)
Overall	Constant ST	6.2 ± 1.9	3.3 ± 0.7	4.3 ± 0.8
	Variable ST	16.2 ± 4.9	7.0 ± 2.4	4.5 ± 0.5
Stance Only	Constant ST	4.0 ± 1.3	3.1 ± 1.3	3.9 ± 1.4
	Variable ST	10.4 ± 2.9	7.4 ± 2.8	4.1 ± 0.6
Swing Only	Constant ST	9.7 ± 3.0	3.5 ± 1.0	4.9 ± 0.6
	Variable ST	15.7 ± 8.6	6.4 ± 3.1	5.1 ± 1.5

Table 9 Mean Absolute Error (%GC) for two types of speed condition across all three estimators.

MAE for Constant Speed Trails (Constant ST)	4.6 ± 1.7
MAE Variable Speed Trials (Variable ST)	9.2 ± 6.0

2.4.3 Results from application to controller (Sub-study C)

The MAE for ANN and MFT both had smaller values compare to FT while actuation was given based on the estimated sate (Table 10). MAE for constant speed trials had smaller value compared to MAE for variable speed trials (Table 11). According to result from Sub-study C, the MAE for MFT estimator was smaller than other two estimators (FT, ANN) for both constant and variable speed trials. During both

stance and swing, MFT had smallest value of MAE while ANN had smaller MAE value compared to FT estimators.

Table 10 Mean Absolute Error (%GC) for different estimator and different types of speed.

		FT (9.6 ± 4.4)	MFT (3.91 ± 1.4)	ANN (5.94 ± 1.7)
Overall	Constant ST	6.4 ± 0.3	2.9 ± 0.1	4.8 ± 0.7
	Variable ST	12.7 ± 4.3	4.9 ± 1.3	7.1 ± 0.4
Stance Only	Constant ST	4.4 ± 0.3	2.9 ± 0.2	3.7 ± 1.4
	Variable ST	9.4 ± 3.9	5.5 ± 1.6	6.5 ± 0.3
Swing Only	Constant ST	9.7 ± 1.3	2.9 ± 0.5	6.4 ± 0.3
	Variable ST	17.3 ± 3.7	3.9 ± 0.9	7.8 ± 0.2

Table 11 Mean Absolute Error (%GC) for two types of speed condition across all three estimators.

MAE for Constant Speed Trails (Constant ST)	4.70 ± 1.8
MAE Variable Speed Trials (Variable ST)	8.24 ± 4.0

2.5 Discussion

The main purpose of this study was to improve the control system of powered AFOs, which are assistive robotic devices for human walking. One approach (state estimation) is to estimate the percentage of gait cycle (% GC) or gait state during walking and provide actuation via the powered AFO at a desired state. Previously, Fractional Time (FT) state estimation [5] was developed to estimate the percentage of gait cycle during walking. The FT estimator has limitations when estimating during changes in gait speeds. Generally, cadence of a healthy able-bodied walker varies from step to step due to different stride length, turning, and gait speed change. Walking parameters may be even more inconsistent for impaired population. In this study, Modified Fractional Time (MFT) and Artificial Neural Network (ANN) state estimation techniques were developed to overcome these limitations.

To examine the sensitivity of the estimators to controlled variations of gait speed and input signals on both training and test data, the proposed algorithms were evaluated by using a simulated data set (Sub-

study A). Two types of variations were introduced into the simulated input signals: variation to input signals, variation to stride speed. When the variation was only applied to period of the stride, we found that ANN worked best compare to FT and MFT. According to this simulation study, the performance of ANN was similar when the stride period was varied which suggests that ANN is not sensitive to changes of walking speed and showed better results in all cases (Table 6). However, the performance of FT and MFT varied for different types of period changes. When both types of variations (input signals and speed changes) were introduced to simulated input signals, FT was found to be worst when the speed changed after 10 strides alternatively. Compared to FT, MFT was found to work better for the conditions when stride periods were the same, and when stride period were changed alternatively after 10 stride (Table 6). However, for the condition when only one stride period was varied after each ten strides, FT and MFT performed similarly in this sensitive analysis study. Moreover, training of MFT and ANN were also performed in two cases: training using 1) unvaried signals, and 2) varied signals. Both ANN and MFT showed better performance while trained using varied signals. These results suggest that, for MFT and ANN, we need to train for every subject separately. Overall, MFT and ANN performed better compared to FT according to this sub study.

In Sub-study B, Each estimator's performance was evaluated in terms of walking at the same or variable speeds using experimental data. According to this sub-study, ANN had the smallest MAE value compared to FT and MFT. The MFT estimator had the (non-statistically) best overall performance trend when walking at the same speed compared to other estimators. MFT and ANN had statistically smaller MAE than FT when walking at variable speed (mean errors: 16% GC (FT), 7% GC (MFT), and 4% GC (ANN); $p < 0.05$). Being able to update state once during one full gait period, FT has lower performance and reliability compared to others. Due to the simplicity of the estimator and associated controller, the FT estimator is a good choice when walking on a treadmill, but its performance may likely go down when walking in highly variable situations of daily life conditions. The ANN estimator estimated a gait state using six previous values of the input signal. Due to this continuous calculation, ANN should work best.

However, ANN needs higher computational cost and higher memory in the microcontroller. To implement ANN on the PPAFO, we would need to use an advanced microcontroller which may likely increase electrical consumption and lead to reduced runtime of the system. Decisions on cost of operation versus accuracy and robustness of state estimation need to be considered when selecting an estimation approach. Overall, MFT and ANN performed better during both same and variable speeds.

In Sub-study C, each estimator's performance was evaluated when the actuation of the PPAFO was provided based on predicted gait states from the given estimator. According to this study, controllers that used the MFT or ANN estimators were found to perform better during both constant speed and variable speed trials compared to FT (Table 8). Although the ANN controller showed better performance compared to the FT controller, the ANN controller performed worse than MFT controller (Table 8). According to Sub-study B, the performance of ANN worked similar for constant speed and variable speed, however Sub-study C showed differently. The Direct Event (DE) controller was used in Sub-study B, while the actuation in Sub-study C was given according to predicted estimated state and actuation timing following values given in Table 5. As Table 5 was showing only the generic behavior of normal walking behavior when not wearing any external devices, using the values for actuation timing might cause greater errors with the ANN controller. In essence, the performance of MFT was found best during both same and variable speeds.

Although promising results were found while using the proposed algorithms for controlling the PPAFO, there are several limitations. Firstly, data from only five subjects for Sub-Study B and only one subject for Sub-study C were collected. More data might help to interpret the performance of the estimators and controllers more accurately. Next, although three sensors (two force sensitive resistor and Hall effect angle sensor) were used in these studies, it was assumed that these same algorithms could work with signals from different sensors. Future studies should investigate state estimation accuracy when using other sensors, such as IMU sensors. Furthermore, as mentioned above, we used generic plantarflexor torque timing based on normative values for providing actuation in Sub-study C. Study 2 in

Chapter 3 seeks to improve performance by proposing an effective way for determining the appropriate plantarflexor timing for actuating the PPAFO using predicted estimated state. Finally, further studies should to implement these algorithms on impaired subject populations. The MFT algorithm was used in an over-ground, non-treadmill study on 16 people with moderate to severe multiple sclerosis [101] .

Each estimator's performance varied in terms of walking at the same or variable speeds. The MFT estimator had the (non-statistically) best overall performance trend when walking at the constant speed and when actuation was provided using the estimated state (Sub-studies B and C). MFT and ANN had statistically smaller errors from the true state than FT (according to Sub-study B). Without need for any training and being able to update state once during one full gait period, FT has lower performance and reliability compared to others. As the ANN estimator estimated a gait state continuously using six previous values of the input signals, ANN was hypothesized to work best. Experimental results showed that ANN worked significantly better than MFT only during stance for variable speed trials (Sub-study B). As powered AFO control mostly depends on the detectability of events during different stance positions, ANN should perform better for walking without a treadmill. If walking speed does not change considerably, MFT will also perform well. Since gait patterns of impaired subjects differ a lot from one step to another, it was speculated that ANN should work better on impaired subjects. However, according to Sub-study C, ANN was not found to perform better than the MFT. Overall considering all the sub studies, MFT was found to perform best during both same and variable speeds.

2.6 Conclusion

When developing powered orthotic devices or exoskeletons, properly timed control of powered assistance during walking is a crucial task to prevent tripping or fall risk. Estimation of the gait state during walking allows for tuning the actuation timing especially when direct measurement of the state fails. Two new techniques (Modified Fractional Time, Artificial Neural Network) were described here to estimate the percentage of gait cycle (or gait state) and were compared with a previously proposed FT

technique. Sub-study A concluded that FT showed good results only while walking at constant speed. Although, MFT and ANN need subject-specific training, they were found to perform better than FT when subjects walked at variable speeds. Experimentally, Sub-study B demonstrated that MFT and ANN performed similar to the previous FT algorithm during constant walking speed (MAE between true and estimated states: all less than 6% GC). However, the performances of the new estimators were significantly better when walking with variable speeds (mean errors: 16% GC (FT), 7% GC (MFT), and 4% GC (ANN); $p < 0.05$). Sub-study C demonstrated that MFT performed best when the actuation was given according to predicted estimated state. In essence, FT showed good results only while walking at constant speed. On the other hand, MFT and ANN performed better during both constant and variable speed tests. MFT was considered as best estimator among all estimators for having consistently small error for all the sub studies. MFT has recently been used in an over-ground, non-treadmill study on a population with impaired gait due to multiple sclerosis.

Chapter 3

Study 2: A classification algorithm for finding plantarflexor actuation timing during walking with a powered AFO

3.1 Abstract

The development of powered orthoses and exoskeletons for robotic gait assistance has led to new issues related to their control. Tuning for appropriate plantarflexor actuation timing is especially relevant for giving actuation to the ankle joint when a state estimation controller is used for identification of the state, or percent gait cycle, during walking with powered AFOs. A multistep supervised learning algorithm is proposed which determines the appropriate plantarflexor actuation timing based on ankle angle data. After training the classifier with collected gait data, the classifier algorithm can be used in combination with a bisection search method to quickly identify the appropriate actuation timing for a specific user. Gait data were collected from five subjects who walked on a treadmill while wearing a powered AFO. Accuracy of the classifier algorithm was evaluated by comparing the classifier's results against those determined from a cross-correlation of ankle angle data collected while just wearing shoes to those when the PPAFO was actuated at different timings. The effects of different training data sets on accuracy were also examined in this study. The classifier worked best when the algorithm was trained for each subject's own data (mean error 0.7% GC). The study also concluded that it is also possible to make a training data from different subjects (mean error 0.7%) when the interest is to find other subject's appropriate plantarflexor actuation timing. The proposed method can be applied quickly for finding appropriate actuation timing successfully.

3.2 Introduction

The development of powered orthoses and exoskeletons for robotic gait assistance has led to new issues related to their control [5]. For example, when providing powered assistance to the ankle during late stance and propulsion, it is crucial to detect the appropriate time in the gait cycle (GC) for providing plantarflexor actuation to aid with limb propulsion. Limited work has been published regarding appropriate plantarflexor actuation timing [5], [69], [80], [81]. It has been suggested through mathematical models that four times more energy is needed if actuation is given too early during the mid-stance phase instead of at the proper timing [81]. Experimentally, it has been found that 50% of the positive muscle work (i.e., generation of mechanical energy) during walking is provided by the ankle joint [82]. Researchers developing powered lower limb orthoses or prostheses have mainly commented on push-off timing or push-off work in terms of metabolic cost reduction during walking [80], [102]–[109]. Many of these groups provided plantarflexor actuation at 43% GC based on a study that found the greatest reduction in metabolic cost at that timing [80]. In the paper of this study by Malcolm et al., the authors suggested that actuation timing between 40% - 50% GC would be the most efficient for plantarflexion assisting devices [80]. Currently, no systematic approach is available to determine subject-specific timing and magnitude of assistance while using powered exoskeletons [110]. In this study, we focused on exploring changes in joint biomechanics of gait (ankle angle) due to different actuation timings and the possibility of finding a systematic approach for determining actuation timing.

The portable powered ankle-foot orthosis (PPAFO), developed in our group [51], is capable of providing both plantarflexor and dorsiflexor torque by using a pneumatic rotary actuator at the ankle [5], [7], [48], [49], [51], [100] (Figure 9). The PPAFO has three sensors: force resistive sensors (FSRs) under the heel and ball of foot to detect foot contact, and a Hall effect sensor to record ankle angle. The PPAFO with tethered control system was used in this study.

Joint biomechanics data (specifically ankle angle) can be observed to vary considerably when the plantarflexor torque actuation timing was varied by using the PPAFO (Figure 8). For example, sudden jumps toward the plantarflexion direction are observed when the PPAFO provided plantarflexor torque earlier than necessary (30% and 40% GC, dotted blue and dotted red lines, Figure 8). When actuation was given late, the maximum amplitude and timing in the plantarflexion direction were inconsistent (55% and 60% GC, solid green and maroon lines, Figure 8). The plantarflexion maximum range of motion was diminished and a discontinuity in the motion was observed due to delayed assistance from the PPAFO. The plantarflexor actuation timing for this subject that created the smoothest ankle angle profile was found to be 49% GC (solid black line). At this timing, these early and late artifacts were minimized.

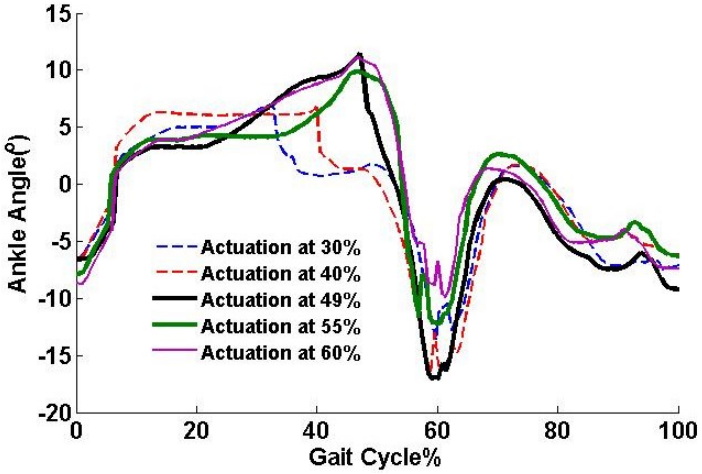

Figure 8 Ankle angle at different actuation timings of the PPAFO. Positive values indicate dorsiflexion.

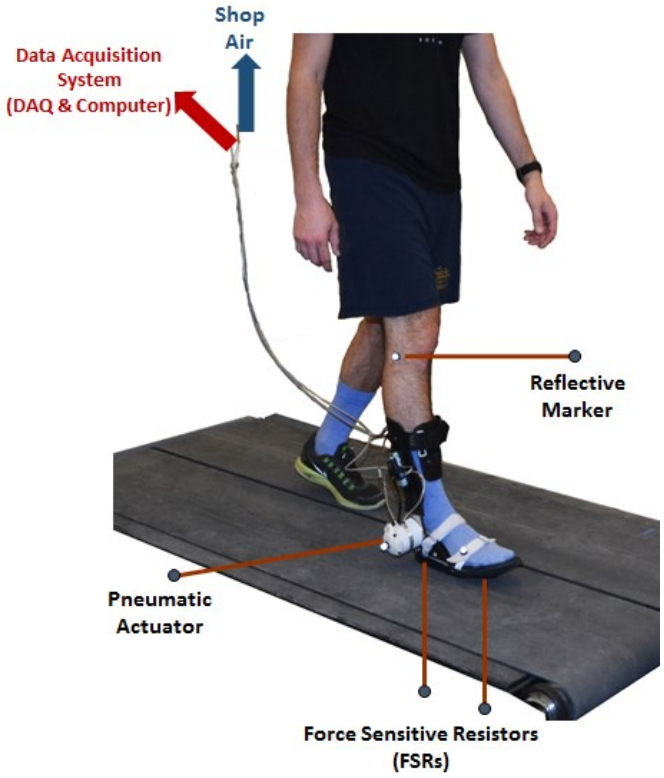

Figure 9 Subject walking with PPAFO.

By estimation of a walker's instantaneous state of the limb during a single stride, as represented by a specific percentage of the gait cycle, it is possible detect and control for various gait events. Early state estimation controlled PPAFO studies ([5], [49]) used dorsiflexor and plantarflexor actuation timings based on established normative event timings for healthy able-bodied adult gait [2], [5], [49]. However, it was observed that using these generic normative timings, especially for plantarflexor actuation, could produce either early or late joint biomechanics profiles [111]. Thus, plantarflexor actuation timings were often further fine-tuned for a given subject by using a trial and error method. A systematic technique to determine appropriate actuation timing using biomechanics data would eliminate the need for trial and error tuning.

In the current study, we proposed a supervised learning classification approach to identify plantarflexor actuation as either early actuation or late actuation using biomechanics data (ankle angle)

collected during walking. The following describes the classification algorithm, integration of the algorithm with a bisection search approach for quickly identifying appropriate actuation timing, and assessments to validate the method and evaluate the effect on classification accuracy due to changes in the training of the classifier.

3.3 Methodology

A multistep, supervised learning classification approach was developed. This approach used a reduced-dimension feature map that was derived from a principal component analysis related to the coefficients of a Fourier transformation of a training data set of ankle angle signals. Probability density functions based on these feature maps were used to determine whether to classify an actuation timing as being too early or too late. After training, the classifier algorithm was combined with a bisection search technique to quickly identify the appropriate actuation timing. Gait data were collected on five healthy young adults. Accuracy of the classifier algorithm was evaluated by comparing the classifier's results against those determined from a cross-correlation of ankle angle data collected while just wearing shoes to those when the PPAFO was actuated at different timings. The effects of the dimension size of the feature map on classification accuracy were examined. The effects of different training data sets on accuracy were also assessed by creating training sets based on one or more test subjects.

3.3.1 Approach to finding appropriate actuation timing

3.3.1.1 Classification algorithm

Walking data (sagittal plane ankle angle position) while wearing the PPAFO were used for training the classifier. Seven conditions were collected, where plantarflexor actuation timings were set to start at 30%, 35%, 40%, 45%, 50%, 55% or 60% GC. For each condition, the last 20 strides of data were extracted from 30 seconds of collected data. After collection of the training data, ankle angle profiles were visually inspected and categorized so that each condition was defined as being either early or late using an approach similar to that used when describing the results presented in Figure 8.

Next, a multistep approach was used to train the classifier. First, the ankle angle data were described as Fourier coefficients by using a discrete Fourier transformation. These coefficients were then organized into a training matrix representing early and late cases. Using principal component analysis, a linear map (or feature matrix) was derived from this Fourier coefficient training matrix. The dimension of the feature matrix was further reduced by including only the top principal components or features. Probability density functions, based on the Fourier coefficients of the training data projected onto this reduced dimension feature subspace, were developed. These probability functions can then be used to separate new gait data (individual or multiple strides for a given actuation timing condition) into early or late classifications. See the appendix in chapter 6 for full derivation of this algorithm.

3.3.1.2 Bisection search method using the classifier

After training the classifier (i.e., deriving the probability density functions), the classifier algorithm was used in combination with a bisection search [112] to quickly find the appropriate plantarflexor actuation timing for a specific user. The bisection method proceeded as follows. Assume an upper and lower range of plantarflexor actuation timing, i.e., 60% to 30% gait cycle. As the first test trial, the actuation timing would be provided at the middle of this range; i.e., 45%. After 30 s of walking, the classification algorithm would be applied to the ankle angle data of the last 20 strides. Each of these 20 strides would be individually classified as either early or late. The classification of the majority of these 20 strides was used to define whether the given actuation timing would be considered early or late. If the timing was classified as early actuation, then the second trial will have a timing set to be the mid-point (rounded up to the nearest integer) between the upper range and middle value; thus bisecting the available range. In this example, the value would be set to 52%. (A similar bisection process would be applied if the actuation was classified as late.) Then the classification algorithm would be applied to the newly collected gait data to determine if the timing value was early or late. This process would be repeated until convergence to a single % GC timing (rounded up to the integer value). At most, six iterations would be needed to find the proper timing using this technique.

3.3.2 Experimental study

3.3.2.1 Subjects

Five healthy adult males (26.4 ± 5.0 years, height 1.8 ± 4.7 m, weight 80.7 ± 5.8 kg), without any neurological, gait, or postural disorders, participated in the study. All subjects gave informed consent, and this study was approved by the university's Institutional Review Board.

3.3.2.2 Experimental protocol

Each subject participated in two sessions of experiments in the same day with a break of up to 10 min. There were two footwear conditions per session (shoes only, and PPAFO on the right leg). In session-01, the training data for the classifier were collected. In session-02, the combined classifier and bisection search technique was applied to collect data and determine the appropriate actuation timing for each subject. During the break between sessions, the classifier was trained with session-01 data.

During both sessions, gait data were collected. For the first trial in each session, the subject wore his own running shoes. The subject walked on a powered treadmill (Instrumented Treadmill, Bertec Corp., Columbus, OH) for 30 seconds at his own self-selected speed. This same walking speed was also used for all PPAFO trials for a given subject. Reflective markers were placed on the right leg over three anatomic landmarks: lateral epicondyle of tibia, lateral malleolus of fibula, and first metatarsal head. Movement of the motion markers were recorded using a three-camera motion system (Vicon, Oxford, UK Model 460), which was sampled at 120 fps. Ankle joint kinematics were calculated using a custom MATLAB program (v 8.1.0.604, the Mathworks Inc., Natick, MA, USA). A 4^{th} order Butterworth low pass filter with a cut-off frequency of 8 Hz was applied to the motion capture data for calculating the ankle angle. For PPAFO trials, the ankle angle data were recorded from the Hall effect angle sensor on the device. The PPAFO used a fractional time state estimation controller [5] to implement the plantarflexor actuation timing. During session-01, plantarflexor actuation timing started at 30% GC and increased to 60% GC by increments of 5% GC for each trial, for a total of seven trials. After completing these trials, the ankle data

were visually inspected and the 5% GC interval which contained the transition between early and late actuation was identified. Four additional trials at 1% GC increments were then collected to fill this interval. The expectation was to find the appropriate actuation timing at a resolution of 1% GC within this interval. During session-02, the bisection search was used to find the appropriate actuation timing (see section 3.3.1.2). Finally, additional trials at 1% GC resolution were collected to compare with actuation timings used in session-01.

3.3.3 Data analysis

3.3.3.1 Cross-correlation analysis to define true state

In this study, it was assumed that replicating joint biomechanics (sagittal plane ankle angle behavior) of a healthy walker, especially during late stance and propulsion, was the goal of the controller of the powered AFO. Therefore, a plantarflexor actuation timing that resulted in an ankle angle profile that most closely reproduced the ankle profile during shoe only walking was considered to be the appropriate actuation timing (or true state) (Figure 10). Since our test subjects were healthy and able-bodied, a cross-correlation analysis of a subject's own ankle angle data collected while wearing shoes to those when the PPAFO was actuated at different timings was used to identify the true state. The actuation timing (% GC) that was associated with the maximum cross-correlation value was considered to be the true state actuation timing. For each subject, the true state timing was found by taking the average of the timings for both session-01 and session-02

To check the accuracy of the classification algorithm, the plantarflexor actuation timing from the classifier was compared with the timing obtained from the cross-correlation analysis. The error was defined by the absolute value of the difference between timings (in % GC).

$$Error = abs|\ timing\ by\ classifier - true\ state\ timing\ by\ cross\text{-}correlation\ | \quad (16)$$

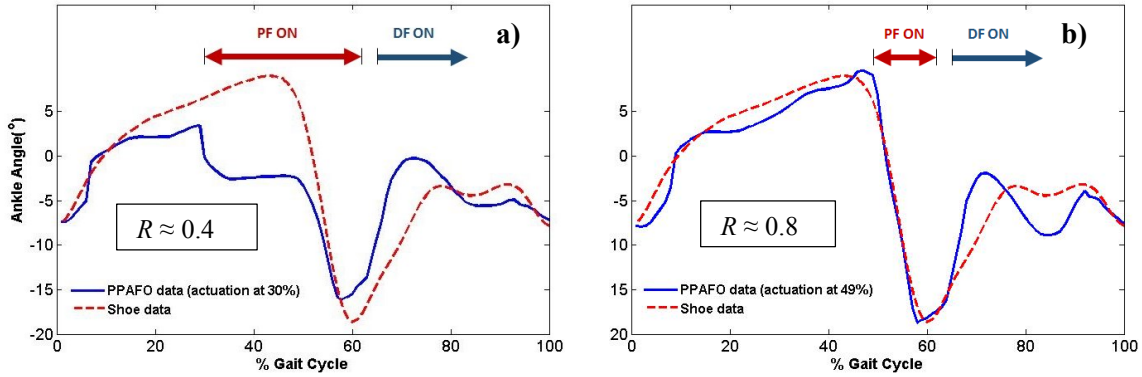

Figure 10 Example of cross-correlation values(R) for two cases from Sub 01. (a) when actuation timing started at 30% GC, (b) when actuation timing started at 49% GC, which was found to be the true appropriate timing.

**PF = Plangarflexor actuation; DF = Dorsiflexor actuation*

3.3.3.2 Examining effect of modifications to classifier training

During post-processing, the effects of changes in the classifier training on the accuracy of the classifier were analyzed. During session-02, appropriate timing was determined in real-time when the algorithm was trained by each subject's own data. Post-process analyses of actuation timings were evaluated for different values of reduced dimension, *d,* and different types of training data. These are discussed in following sections:

3.3.3.2.1 Effect of feature matrix dimension size

Training data defined the feature matrix, which defined the probability density functions, which in turn were used to classify whether actuation timing was early or late. The dimension of the feature matrix *d* can be reduced to include top principal components or features. During session-02, real-time data were collected and classified when the value of *d* was *20*. This value was chosen from a pilot study prior to this study, which found best results for this value, (however, larger error for smaller and larger value of *d* presumably for smaller feature extraction and over training, respectively). To examine the effect of feature matrix dimension on classifier accuracy, we examined a variety of values for *d* (10, 15, 20, and 25), which can be thought of as representing the first 10 to 25 principal components.

3.3.3.2.2 Effect of training by different single or multiple subjects

The effects on classifier accuracy were analyzed when training was done by using other subject's data to assess whether the classifier algorithm will still be successful at identifying the appropriate actuation timing of new users for whom personal training data are not available. The first analysis examined the effect on prediction accuracy for each subject when the classifier algorithm was trained by data from a single different subject. We then ranked the accuracy of these classifiers. The rank from training with a given subject's data was based on the mean of the errors across all five subjects. Finally, the accuracy of the classifier was assessed when the classifier was trained by the best two, three, four or all five subjects' data.

3.4 Results

3.4.1 Finding "true" plantarflexor timing from cross-correlation analysis

A cross-correlation analysis was used to find the appropriate (or true) actuation timing, as discussed in section 3.3.3.1. For each subject, the cross-correlation values increased with actuation time and after reaching a peak, the values started to decrease (Figure 11). The maximum peak value was considered as the appropriate actuation timing for that specific subject. The appropriate actuation timing, for each subject, was found by averaging peak values from session-01 and session-02 (TABLE 12). For each subject, the peak was found at different actuation timings.

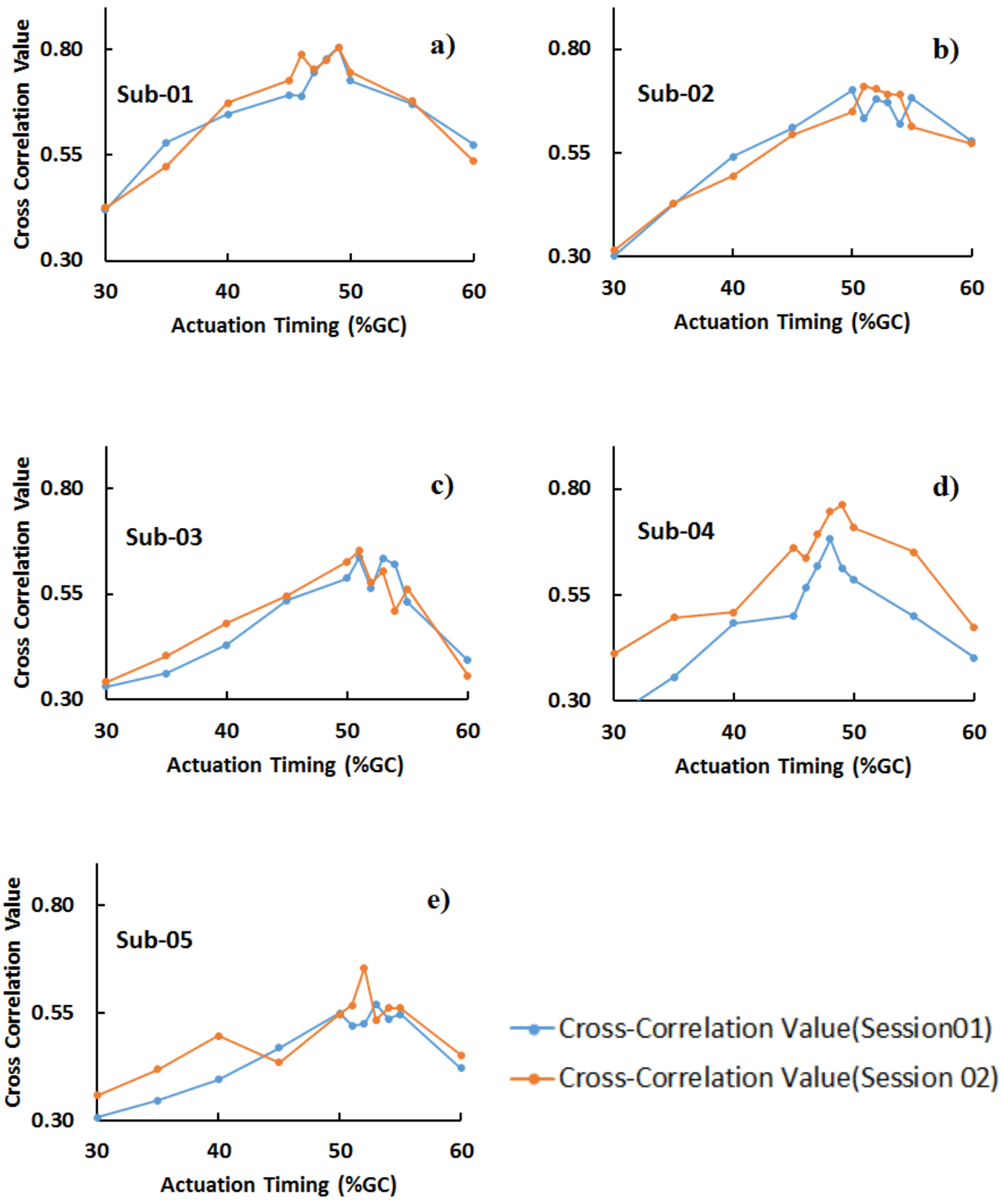

Figure 11 Cross-correlation values for each subject.

TABLE 12 Actuation Timing found by Cross-Correlation and Classifier Method (When Trained by Own Data).

Trained by own	Timing by Cross Correlation (% GC)	Timing By Classifier Method (% GC)			
		d=10	d=15	d=20	d=25
Sub 01	49.0	49	49	49	49
Sub 02	50.5	52	52	51	52
Sub 03	51.0	50	50	50	50
Sub 04	48.5	48	48	48	48
Sub 05	52.5	52	52	51	52

3.4.2 Effect of feature matrix dimension size

When the algorithm was trained by the subject's own data, the appropriate actuation timing for each subject was calculated using any value of *d* from *10*, *15*, *20* and *25* (TABLE 12). For all values of *d*, the accuracies of the classifier when trained by one's own data were found to be quite satisfactory, such that the error between the predicted timing from the classifier and the true timing from the cross-correlation analysis ranged from 0.0% to 1.5% GC and average error of *0.70% GC* across all five subjects. No particular value of *d* seemed to affect the accuracy of the classifier when the algorithm was trained with one's own data. The classifier however failed to converge when the dimension was reduced too much (*d* = *10* or *15*) and other subjects' data were used for training, as will be presented below.

3.4.3 Effect of training by different single or multiple subjects

The appropriate actuation timings and errors were calculated using the proposed algorithm when the classifier was trained by different subjects. When the classifier was trained by a different single subject, the error ranged from 0.5% to 6.5% GC (TABLE 13). It was found that for *d=10* and *d=15*, there were multiple times when the algorithm could not reach a solution. For d=*20* and *25*, the algorithm always converge to a value, except the case when the classifier was trained by subject -05 (TABLE 13). For *d* = *20*, the mean average error from sub-01 to sub-05 were 1.10%, 2.50%, 1.90%, 1.10% and 2.70% GC, respectively. For *d= 25*, these values were 1.10%, 1.50%, 1.50%, 1.30% and 2.50% GC, respectively.

For these reason, the value *20* and *25* for *d* were considered to use in the analysis of training with data from multiple subjects.

Based on these mean of error values when *d* was 20 or 25, the rank for training with a specific subject's data from best to worst accuracy were: subjects 01, 04, 03, 02 and 05, respectively. This ranking was used to select the training data from the best two, three, four and all five subjects.

TABLE 13 Actuation Timing found by Cross-Correlation and Classifier Method (When Trained by Specific Subject's Data).

	Subject No.	Timing by Cross Correlation (% GC)	Timing By Classifier Method (% GC)			
			d=10	d=15	d=20	d=25
Trained by Sub01	Sub 01	49.0	49	49	49	49
	Sub 02	50.5	x	x	52	50
	Sub 03	51.0	52	52	52	52
	Sub 04	48.5	48	49	49	50
	Sub 05	52.5	x	51	50	50
Trained by Sub02	Sub 01	49.0	55	55	50	50
	Sub 02	50.5	52	52	51	52
	Sub 03	51.0	55	54	54	54
	Sub 04	48.5	51	55	51	55
	Sub 05	52.5	52	52	52	52
Trained by Sub03	Sub 01	49.0	47	47	48	48
	Sub 02	50.5	48	49	48	48
	Sub 03	51.0	50	50	50	50
	Sub 04	48.5	47	47	48	48
	Sub 05	52.5	49	48	50	48
Trained by Sub04	Sub 01	49.0	48	48	48	49
	Sub 02	50.5	52	51	50	50
	Sub 03	51.0	52	50	50	50
	Sub 04	48.5	48	48	48	48
	Sub 05	52.5	49	49	49	49
Trained by Sub05	Sub 01	49.0	x	50	50	50
	Sub 02	50.5	x	x	x	55
	Sub 03	51.0	52	53	52	52
	Sub 04	48.5	x	55	55	55
	Sub 05	52.5	52	52	51	52

Symbol 'x' indicates cases when the proposed algorithm could not converge to a solution.

The classifier was trained by data from two, three, four or five subjects. When the training data were derived from the best two subjects (Sub-01 and 04), the error ranged from 0.0% to 2.5% GC and the average error was 0.9% GC for both *d=20* and *d=25*. (TABLE 14). When training data were derived from three subjects (Sub 01,03,04), the error ranged from 0.0% to 3.5% GC and the average error was 1.1% GC (for both *d= 20* and *25*). When the training data were derived from four subjects (Sub 01, 02, 03, 04), the error ranged from 0.0% to 4.5% GC and the average errors were 1.1% GC (for *d=20*) and 1.30% GC (for *d =25*). When data from all five subjects were used to train the classifier, the error was from 0.0% to 1.5% GC and the average errors were 0.7% GC (for *d=20*) and 0.9% GC (for *d =25*).The predicted actuation timings from the classifier method for Sub-05 were always smaller than the true actuation timing determined from the cross-correlation analysis. The error value was also always the largest for Sub-05 compared to any other subject, when the classifier was trained by any subject(s) other than Sub-05. However, when training data were collected from all five subjects, the error was found low even for Sub-05.

TABLE 14 Actuation Timing found by Cross-Correlation and Classifier Method (Trained by Multiple Subjects' Data).

	Subject No.	Timing by Cross Correlation (% GC)	Timing By Classifier Method (% GC)	
			d=20	d=25
Trained by Sub 01 & 04	Sub 01	49.0	49	49
	Sub 02	50.5	50	50
	Sub 03	51.0	50	50
	Sub 04	48.5	48	48
	Sub 05	52.5	50	50
Trained by Sub 01, 03, 04	Sub 01	49.0	49	49
	Sub 02	50.5	50	50
	Sub 03	51.0	50	50
	Sub 04	48.5	49	49
	Sub 05	52.5	49	49
Trained by Sub 01, 02, 03, 04	Sub 01	49.0	49	49
	Sub 02	50.5	50	50
	Sub 03	51.0	50	50
	Sub 04	48.5	49	49
	Sub 05	52.5	49	48
Trained by all Sub	Sub 01	49.0	49	50
	Sub 02	50.5	50	50
	Sub 03	51.0	50	50
	Sub 04	48.5	48	49
	Sub 05	52.5	51	51

3.5 Discussion

For gait improvement using a powered AFO, the knowledge of actuation timing for plantarflexion motion of a subject is very important. If the plantarflexor actuation by the PPAFO was early, the subject would feel constraint in the direction of the dorsiflexion side of his foot due to the desired downward motion of the PPAFO. In contrast, if the plantarflexor actuation timing was too late, the maximum range of motion in the plantarflexion direction could be diminished due to delayed assistance from the PPAFO and also there was an unwanted motion during the movement in the plantarflexion direction due to asynchronous relation between plantarflexor actuation by the PPAFO and human ankle-foot system. Our

proposed classifier algorithm successfully found the appropriate plantarflexor actuation timing during walking using the biomechanics data of a subject (i.e., sagittal plane ankle angle).

The results found from the classifier method were compared with the "true" appropriate actuation timing found from the cross-correlation analysis. For all the cases, the error (absolute difference between results and true value) were found quite small (mean error = 1.3 % GC considering all the conditions). This promising result demonstrated that the proposed algorithm can successfully find the appropriate torque timing with high accuracy.

The classifier worked best when the algorithm was trained by a subject's own data. The result from the proposed algorithm was compared with the values found from cross-correlation analysis. Specifically, for sub-01, the algorithm showed best performance while sub-04 showed the second best result. Error values for different subjects were similar for all values of *d*. These results suggest that, when training data were collected from each subject separately, the reduced dimension of the feature matrix can be as low as 10, which would be computationally least expensive among other values of *d*. Moreover, the proposed algorithm could be used to find appropriate plantarflexor actuation timing successfully with mean error values of 0.7% when each subject uses his/her own training data. However, it is neither efficient nor realistic to do two data collection sessions per new user. Rather, it would be more effective to be able to determine appropriate actuation timing for a new user by using an already trained classifier algorithm based on data from other users.

The data were therefore also analyzed when different subjects' data were used as training data. When training from a single different subject, the best result was found for *d=20*. The error for *d = 10 and 15* could be quite large up to 6.5% GC and in some cases the classifier could not converge to identifying an actuation time (TABLE 13). This result suggests that the feature matrix's dimension was reduced too much when *d* was set to values of *10* and *15*. When the values of *d* was *20*, the algorithm worked best (mean error = 1.5% GC) compared to other values. In most of the cases, the errors are same for *d = 20* and *d=25*. However, the mean error for *d=25* increased while training data collected from Sub 03 and 05.

Overall, training with data from only sub-01 worked best, and training with data from sub-05 was the worst.

The effectiveness of training data, when the algorithm was trained by the data from more than one subjects, was also evaluated in this study. Before using more than one subject's data as training data, a rank list of training data was made according to mean error. Training with data from sub-01 was found to have the best result, and sub-04, sub-03 and sub-02 were found as 2^{nd}, 3^{rd} and 4^{th} best training data. Unfortunately, training data from sub-05 had the highest error.

Using the rank of training data, the algorithm was trained by more than one subjects' data and training using data from all subjects was found to be most effective. The mean errors for five subjects were found 1.10% (for both $d= 20$) when training data were used from all subjects. So, for new users, we can use training data from all five subjects to find the appropriate actuation timing.

The proposed algorithm can be implemented to find plantarflexor timing for a new subject by just using training parameters calculated from the data of all subjects in this study. On the other hand, the cross-correlation analysis, which was conducted to validate the proposed algorithms, needs the ankle angle profile to compare with PPAFO ankle data for any new subject. However, it is not always feasible to collect subject specific ankle angle using expensive motion capture systems in non-laboratory environment. In this case, the proposed classifier method, which can use the previous training data, has a tremendous advantage over cross-correlation analysis for determining the appropriate plantarflexor timing.

One of the limitations of this study was that data from only five subjects were collected. More data will help to interpret performance of the algorithm more accurately. There is a scope to study the proposed algorithm to compare with the study where energetic data (metabolic cost) were used to find appropriate plantarflexor actuation timing. Moreover, implementing the proposed algorithm to impaired subject is another scope of this study.

The proposed classifier method was applied to find appropriate plantarflexor actuation timing in this study. This biomechanics based method could be used as an alternative approach compared to the method that used metabolic cost for finding actuation timing. Moreover, the proposed method can be applied quickly for finding appropriate actuation timing; whereas optimization methods using metabolic data can be time consuming (few strides vs. 10s of minutes).

3.6 Conclusion

Primary purpose of this study was to develop a systematic approach to find the plantarflexor actuation timing using biomechanics data during human walking using a powered AFO. For gait improvement using powered AFO, the actuation timing of plantarflexion motion is crucial. Most of these prior studies were based on metabolic data rather than biomechanics data (e.g., joint kinematics) [5], [69], [80], [81]. The proposed classifier algorithm needs training data prior to applying to experiment to find the appropriate actuation timing. Gait data for five subjects were collected to find the performance of the proposed method. The results were compared with the value found from another technique that used cross-correlation analysis on gait data. When the algorithm was trained each time for each subject, the performance of the algorithm was found best (mean error 0.7% GC). In addition to this, the study also concluded that it is also possible to make a training data from different subjects when the interest is to find other subject's appropriate plantarflexor actuation timing. Promising results were found when the training data were collected from all subjects. In this study, we took a biomechanics approach and used replication of ankle angle kinematics to mimic healthy able-bodied gait as the optimization criteria. This approach was able to identify appropriate actuation timing quickly within a few strides (less than 10 minutes).

Chapter 4

Study 3: Detection of gait modes using artificial neural network during walking with a powered ankle-foot orthosis

4.1 Abstract

This paper presents an algorithm, for use with a powered ankle-foot orthosis (i.e., PPAFO) that can automatically detect changes in gait modes (level ground, ascent and descent of stairs or ramps); thus allowing for appropriate ankle actuation control during swing phase. An artificial neural network (ANN) algorithm used input signals from an inertial measurement unit and foot switches, i.e., vertical velocity and segment angle of the foot. Output from the ANN were filtered and adjusted to generate a final data set used to classify different gait modes. Five healthy male subjects walked with the PPAFO on the right leg for two test scenarios (walking over level ground and up and down stairs or a ramp; three trials per scenario). Success rate was quantified by the number of correctly classified steps with respect to the total number of steps. The results indicated that the proposed algorithm's success rate was high (99.3%, 100%, and 98.3% for level, ascent and descent modes in the stairs scenario, respectively; 98.9%, 97.8%, and 100% for ramp). The proposed algorithm continuously detected each step's gait mode with faster timing and higher accuracy compared to a previous algorithm.

4.2 Introduction

Everyday walking is generally not only limited to level, over-ground walking but also involves ascending and descending stairs and ramps. Lower limb joint kinematics and kinetics change with different types of walking environments, or gait modes [84]. Therefore, the ability to recognize and

control for different gait modes when using powered lower limb prostheses or orthoses must be addressed if the devices are to be used beyond treadmill walking or walking around a clinic or laboratory.

Several studies have explored gait mode recognition [18], [54], [70], [84]–[93], [95], [114]–[116]. Most were for prosthetic devices [18], [47], [85]–[90], [114]. Some used manual switching schemes to deal with changing gait modes during walking. Bock et al. [86] demonstrated an approach where a user manually switches modes using Ottobock's C-Leg by tapping the heel. Au et al. proposed two finite state controllers to classify between level-ground and stair-descent mode using electromyography signals measured from intentionally activated residual muscles in the amputated limb [87]. This approach also needed a large number of sensor signals and could not detect stair-ascent mode. These algorithms were not autonomous and needed user's input [86], [87].

Other studies have used autonomous systems for detecting gait modes. A number of methods (using socket interface forces, ankle angle and knee angle as input signals) were studied by the group at Vanderbilt University for use with their lower limb prosthesis [70], [88]–[90], [114]. A *k*-nearest neighbor algorithm to classify different gait modes was used; however, in that study, three different walking speeds were considered the different gait modes and not changes in walking environment [70]. In a separate study, principle component analysis with Gaussian mixture models was used for gait mode recognition; two modes (standing and walking mode) were considered as gait modes [88]–[90]. A supervisory intent classifier combined with a mid-level controller based algorithm to switch modes was also examined [54]. These schemes were capable of detecting different modes only during level ground walking (Mode 1: stance flexion/extension; Mode 2: pre-swing; Mode 3: swing flexion, Mode 4: swing extension). Another common approach for gait mode recognition involved using inertial measurement units (IMU) or other sensors [91]–[93], [115]. Zhang et al. [91] developed an algorithm to predict upcoming terrain height using a large number of sensors (laser sensor and four IMUs). This algorithm needed heavy computation to deal with lots of data collected from the different sensors. Coley et al. [95]

used a miniature gyroscope attached to the shank to detect level ground and stair ascent modes. Being a non-causal algorithm, this procedure could not be implemented in real-time and had to be implemented during post-processing of the data since future input is needed for the algorithm. Jang et al. [116] measured hip joint angles of both legs and signals from IMUs at the moment of foot contact to recognize level ground, stair ascent, or stair descent by using a hip exoskeleton. This algorithm had a one-step delay, such that the first step transitioning into a new mode was always unrecognized.

Li and Hsiao-Wecksler [115] proposed an algorithm to recognize gait modes by using the Portable Powered Ankle-Foot Orthosis (PPAFO). The PPAFO can provide powered dorsiflexor or plantarflexor torque assistance to the ankle joint using a pneumatic system and waist-worn tank of compressed carbon dioxide (Figure 12). The algorithm used the real-time vertical position and orientation of the foot using an IMU on the PPAFO and also foot-ground contact information from force sensitive resistor (FSR) sensors under the heel and toe. This algorithm used training data to calculate optimal threshold values for different stair heights; then during test cases, the algorithm checked the height between two consecutive strides and foot orientation to detect changes in gait mode. Limitations of this algorithm were dependence on trained stair heights and a one-step delay in mode recognition.

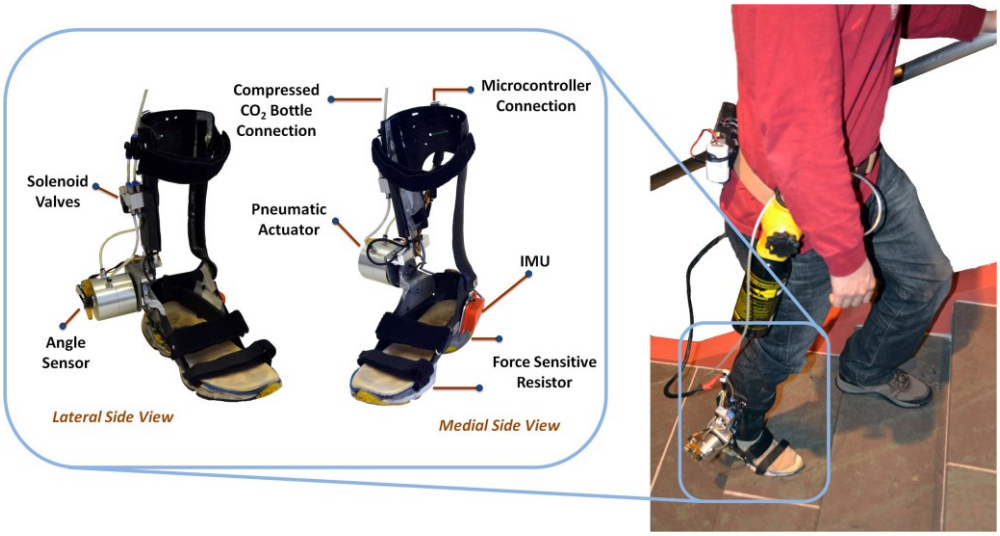

Figure 12 The Pneumatic Portable Powered Ankle-Foot Orthosis (PPAFO).

In summary, existing gait mode recognition schemes have shortcomings of not being autonomous [86], [87], one-step delay [94], [116], difficulty of implementation in real-time [70], [88]–[90], dependency on trained stair heights [115], or need for a large number of sensors [91]–[93]. There are currently no reliable and minimum number of sensors based gait mode recognition algorithms available which can detect all the modes without long delays. In this study, we proposed an artificial neural network (ANN) based algorithm to detect gait modes automatically. We hypothesized that this approach would detect different gait modes (level ground, ascent of stairs or ramps, and descent of stairs or ramps) with higher accuracy and less delay than the previous autonomous algorithm that was proposed in Li and Hsiao-Wecksler [115].

4.3 Method

4.3.1 Proposed approach

A supervised learning recognition approach was developed using an artificial neural network (ANN) for detecting the gait modes. This approach used a multi-layer feedforward ANN of one hidden layer with 10 neurons. Vertical foot velocity and foot segment angle were used as the inputs. Training was done to

determine model parameters, then the approach was applied to gait data collected on five healthy young adults. Success rate of the proposed algorithm was evaluated and compared with the previously developed algorithm by Li and Hsiao-Wecksler [115].

4.3.1.1 Design of artificial neural network

A feed-forward, multi-layer, artificial neural network [97] was used to perform gait mode recognition (Figure 13). In the input layer, there was an input vector which consisted of two sensor signals (foot velocity and segment angle) with six tap delays each, for a total of 12 elements. The hidden layer had 10 neurons and used log-sigmoid activation functions. The output layer had three neurons and used a linear activation function, which provided a vector with three elements.

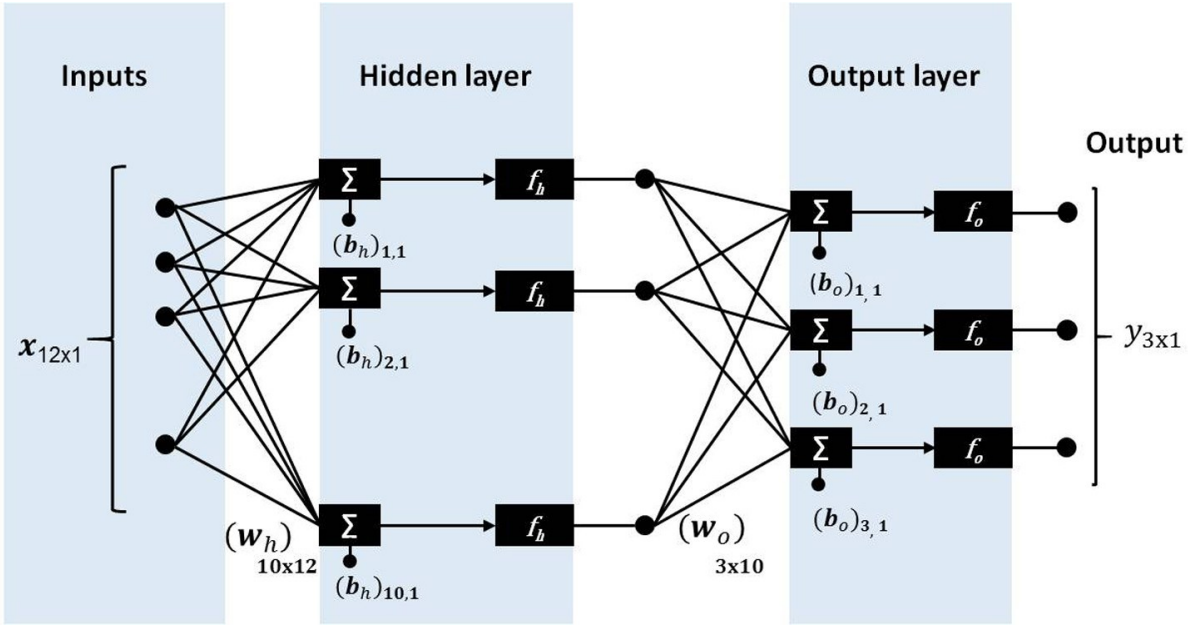

Figure 13 Artificial neural network structure for gait mode recognition.

Log-sigmoid functions were used as the activation function in the hidden layer. So the output of the hidden layer, $\boldsymbol{a_h}$, can found from the following Equation (17).

$$\boldsymbol{a}_h = f_h(\boldsymbol{w}_h \boldsymbol{x} + \boldsymbol{b}_h) \tag{17}$$

Here, $\boldsymbol{x}$ is the vector of inputs, and $(\boldsymbol{w_h}, \boldsymbol{b_h})$ are called weights and biases of the hidden layers. $f_h(n)$ can be expressed as Equation (18).

$$f_h(n) = \frac{1}{e^{\boldsymbol{n}} + 1} \tag{18}$$

The output layer provided the vector $\boldsymbol{y}(t)$ which can be found using Equation (19).

$$\boldsymbol{y}(t) = f_o(\boldsymbol{w}_o \boldsymbol{a}_h + \boldsymbol{b}_o) \tag{19}$$

Where, $(\boldsymbol{w_o}, \boldsymbol{b_o})$ are the weights and biases of the output layer. $f_o(n)$ is the output layer activation function, which was defined as a linear activation function:

$$f_o(n) = n \tag{20}$$

The parameters $(\boldsymbol{w_h}, \boldsymbol{b_h})$ and $(\boldsymbol{w_o}, \boldsymbol{b_o})$ will be estimated for finding the output of the multi-layer neural network for any input $\boldsymbol{x}(t)$ and training is needed to evaluate these parameters. The gait modes, observed during the collection of training data, were used as the target values $(\boldsymbol{t}_i)$ for training the ANN. During the training, we minimized the cost function E (Equation (21)) by using Lavenberg-Marquardt algorithm with Bayesian regularization described by Hagan et al. [117], [118].

$$E = \alpha \sum |\boldsymbol{t}_i - \boldsymbol{y}_i|^2 + \beta \, E_w \tag{21}$$

Here, $\boldsymbol{y}_i$ is the output of the network at the i^{th} data point, $\boldsymbol{t}_i$ is the target output of the i^{th} data point and has the same structure as $\boldsymbol{y}_i$, E_w is the sum of squares of all the network weights and biases (i.e. $\boldsymbol{w_h}, \boldsymbol{b_h}, \boldsymbol{w_o}, \boldsymbol{b_o}$), and α and β are cost function parameters. The update laws of Bayesian optimization of regularization parameters α and β, were described in [118]. Target output vector, $\boldsymbol{t}_i$, has three elements. The values of this vector represent the gait mode of walking. TABLE 15 illustrates the meaning of the possible structures of the $\boldsymbol{t}_i$ vectors.

TABLE 15 Three element representation of target vector for different gait modes.

$\boldsymbol{t^A} = \begin{bmatrix}1\\0\\0\end{bmatrix} \xrightarrow{\text{represents}}$ Ascent mode	$\boldsymbol{t^L} = \begin{bmatrix}0\\1\\0\end{bmatrix} \xrightarrow{\text{represents}}$ Level ground mode
$\boldsymbol{t^D} = \begin{bmatrix}0\\0\\1\end{bmatrix} \xrightarrow{\text{represents}}$ Descent mode	$\boldsymbol{t^X} = \begin{bmatrix}0\\0\\0\end{bmatrix} \xrightarrow{\text{represents}}$ Undetermined mode

4.3.1.2 Collection of ANN input

Detecting the input signals plays an important role for developing an algorithm for any task. In this study, our task was to recognize a change in gait mode. It has been observed that the sagittal plane rotation of the shank is different for level ground walking and stair walking [95]. From pilot data, we also found similar differences in foot segment rotation due to these different gait modes. Moreover, the vertical component of the velocity of the foot is also observed to be different for level ground, stair ascent and descent modes [119]. For these reasons, we used the vertical velocity and segment angle of the foot shell of the PPAFO as input signals to an artificial neural network.

The vertical component of velocity and foot segment angle were calculated using an IMU sensor. Before any calculation, the readings of the IMU were converted from IMU coordinates to earth coordinates for estimating the orientation of the IMU (see [115] for detailed procedure). For finding velocity, the obvious approach was to directly integrate the acceleration in the z direction. However, this approach became erroneous because of long term drifts. This long term drift can be avoided by recalibrating the velocity reading at every zero-acceleration instance [94], [119]. Usually, the vertical component of the acceleration reading should be g (g = 9.81 m/s2) when the foot segment is at rest during mid-stance phase. However, because of error in orientation of the signal and the input noise, we assumed that the zero-acceleration instance was achieved when Eq. (22) holds.

$$\|a_z - g\| < \varepsilon_g \tag{22}$$

Here, a_z is the vertical component of acceleration in the world coordinate system collected from the IMU accelerometer, ε_g is the threshold value found from statistical data so that the zero-acceleration instance

will only occur during mid-stance during walking when the foot is in a stationary position. However, due to noise during data collection, if this zero instance cannot be achieved via equation (22) for any step, the heel FSR and toe FSR can be used to detect this event. That is, generally, during the zero-acceleration-instance, both the heel and toe FSRs should be turned on since they are in contact with the ground. For calculating the foot pitch angle (foot segment angle), data were collected in a quaternion based coordinate. Using the equation found from the data sheet of the IMU (XSens MTi-28A53G35), the foot segment angle was calculated. Thus the input signals, vertical component of velocity and foot segment angle (Figure 14), were derived.

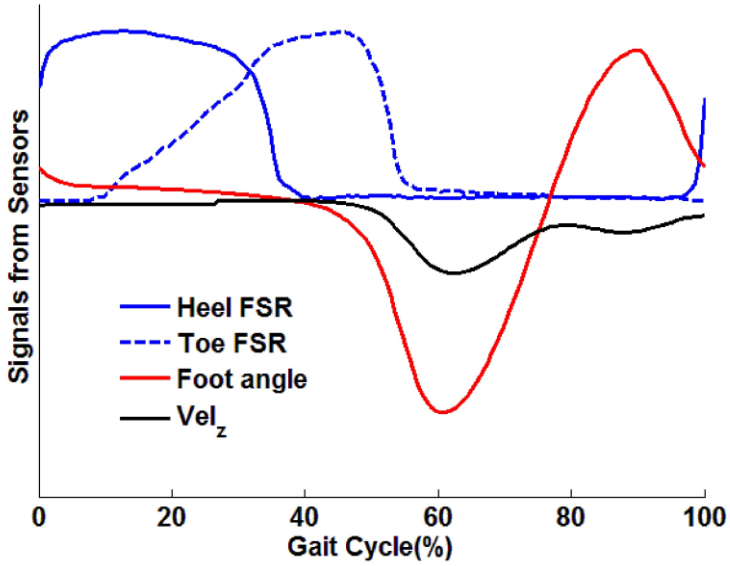

Figure 14 Different sensor signals during walking

4.3.1.3 Conditioning of ANN output

4.3.1.3.1 Filtering the output of the network

The output from the network $\boldsymbol{y}(t)$ was filtered to attenuate unwanted noise (Figure 15). $\boldsymbol{y}$ was passed through a first order filter with time constant ϵ to obtain a new output variable $\overline{\boldsymbol{y}}$. For this study, the time

constant for the filter, ϵ is chosen as 0.02 sec. The equation for the first order filter was described in Equation (23).

$$\epsilon\,\dot{\overline{\boldsymbol{y}}} + \overline{\boldsymbol{y}} = \boldsymbol{y}\ , \quad \overline{\boldsymbol{y}}(0) = \boldsymbol{y}(0) \tag{23}$$

4.3.1.3.2 Conversion to binary values

The filtered output $\overline{\boldsymbol{y}}$ was used to detect gait modes. The values of each of the three elements of the output vector $\boldsymbol{y}$ are non-integer; thus, the elements of the filtered output $\overline{\boldsymbol{y}}$ are also non-integer values (Figure 15). Each element was converted to either "0" or "1" (integer binary value) using after establishing a threshold value. From the training data, the thresholding value for each element was calculated by minimizing the risk using a loss matrix as described below [113].

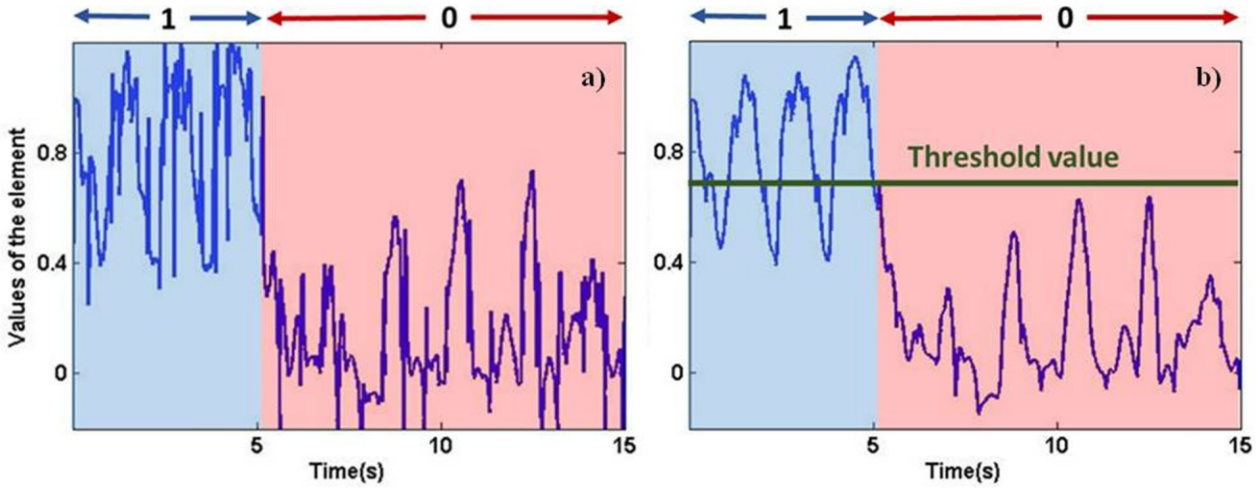

Figure 15 Example of the values of an element of vector $\boldsymbol{y}$ and $\overline{\boldsymbol{y}}$. (a) Output of ANN before filtering($\boldsymbol{y}$), (b) output after filtering ($\overline{\boldsymbol{y}}$).

Let us assume, there were two classes ($w_1$and w_2) for each element of the filtered output vector. w_1 represents the class when the value of the element should be 0 and w_2 represents the class when the value of the element should be 1. Assume that z is the non-integer value of the element. λ_{ij} is a penalty term which is known as the loss that depends on the wrong decision. The loss matrix [113] L is defined by following equation:

$$L = \begin{bmatrix} \lambda_{11} & \lambda_{12} \\ \lambda_{21} & \lambda_{22} \end{bmatrix}$$

Here λ_{ij} means the value of risk if an element of class i is classified as class j. As $\lambda_{11}$and λ_{22} represent the risk of classified correctly, these two values should be 0. We assumed that the element misclassifying class-1 has higher risk compare to misclassifying class-2 to be on the conservative side for detecting a gait mode. We chose the value of risk of misclassifying class-1 (λ_{12}) is twice as that of misclassification of class-2 (λ_{21}). That means we chose

$$\lambda_{12} = 2\,\lambda_{21}$$

So, we chose our loss matrix as below:

$$L = \begin{bmatrix} 0 & 1.0 \\ 0.5 & 0 \end{bmatrix}$$

We assumed that these two classes with the single element value z have Gaussian probability density functions.

$$p(z|w_1) = \frac{1}{2\,\sigma_1\sqrt{\pi}}\, e^{-\frac{(z-\mu_1)^2}{2\,{\sigma_1}^2}} \tag{24}$$

$$p(z|w_2) = \frac{1}{2\,\sigma_2\sqrt{\pi}}\, e^{-\frac{(z-\mu_2)^2}{2\,{\sigma_2}^2}} \tag{25}$$

Here, (μ_1, σ_1) and (μ_2, σ_2) are means and standard deviations of probability density functions, $p(z|w_1)$ and $p(z|w_2)$, respectively. According to [113], the threshold value z_o in this study can be found by solving following equation:

$$z_o: \qquad \lambda_{12}\, p(z|w_1) = \lambda_{21}\, p(z|w_2) \tag{26}$$

For this study, (μ_1, σ_1) and (μ_2, σ_2) for each element of the output vector can be found from the training data. Using these threshold values, each of the three elements of the vector ($\overline{\boldsymbol{y}}$) was converted to either "0" or "1" and, thus, $\overline{\boldsymbol{y}}$ will be converted to $\hat{\boldsymbol{y}}$, which is a binary version of $\overline{\boldsymbol{y}}$.

4.3.1.4 Classification of different modes

The proposed approach to detect the gait modes was implemented on the testing data by using the parameters determined from the training data. Assume, $\boldsymbol{x}'$was the input vector for any instance. Using the network parameters ($\boldsymbol{w_h}, \boldsymbol{b_h}, \boldsymbol{w_o}, \boldsymbol{b_o}$, determined during training), the output $\boldsymbol{y}'$ was calculated by Equation (17) – (20). Each of the elements of vector was first filtered (Equation (23)) and later converted to binary value to determine the vector $\widehat{\boldsymbol{y}}'$ (by using three thresholding values found from the training data). Thus using the final output vector, $\widehat{\boldsymbol{y}}'$, the current gait mode was determined using the values for each element as given in Table 1.

$$\boldsymbol{Current\ gait\ mode} \Longrightarrow \begin{cases} \text{if } \widehat{\boldsymbol{y}}' = \boldsymbol{t^A}, & \text{Ascend mode} \\ \text{if } \widehat{\boldsymbol{y}}' = \boldsymbol{t^D}, & \text{Descend mode} \\ \text{if } \widehat{\boldsymbol{y}}' = \boldsymbol{t^L}, & \text{Level ground mode} \end{cases} \tag{27}$$

4.3.2 Experimental data collection

Data collected in the previous study [115] were used to evaluate the proposed ANN based algorithm. In that study, five healthy male subjects (average age: 23.4 y, average weight: 82.0 kg, height 178.6 cm) participated and gave informed consent. The study was approved by University of Illinois Institutional Review Board. The subjects wore the PPAFO on the right leg.

The detailed hardware description of the PPAFO can be found in [115]. The PPAFO used a dual-vane bidirectional pneumatic rotary actuator (PRN30D-90-45, Parker Hannifin, Cleveland, OH, USA) to provide plantarflexor and dorsiflexor torque at the ankle joint using a small portable compressed carbon dioxide tank (JacPac J-6901-91, 20 oz capacity; Pipeline Inc., Waterloo, ON, Canada) (Figure 12). The PPAFO generated about 12 Nm of plantarflexor torque at 100 psig pressure, and the dorsiflexor torque could be down regulated such that weight of the subject's relaxed foot was supported in a neutral (90°) position when seated [51]. In the current study, analyzed data were generated when the PPAFO was operated in passive mode with no ankle torque assistance. An embedded micro-controller

(TMS320F28335, CPU:150 MHz, Texas Instruments, Dallas, TX, USA) controlled the actuator by using solenoid valves and collected input signals from two force sensitive resistors (FSR), a rotary potentiometer for ankle angle, and an inertial measurement unit (IMU). The FSRs (#403, 2" square; Interlink Electronics Inc., Camarillo, CA, USA) were attached under the heel and ball of the foot between the foot shell and sole. The IMU (XSens MTi-28A53G35; XSens Technologies; Enschede, The Netherlands) was attached to the foot shell. It measured 3-DOF acceleration, angular rate and magnetic field. All signals were sampled at 200 Hz. Signals collected from the FSRs and IMU were used for gait mode recognition.

During a testing session, the subject walked with the PPAFO for two test scenarios and three trials per scenario. Two test scenarios were collected: walking on level ground and outdoor stairs, and walking on level ground and an indoor ramp. The total height after traversing two steps was 28 cm (i.e., 14 cm per step rise). The ramp had a 6 degree grade. Specifically, for the stair scenario, subjects walked uninterrupted in the following order: 1) 3 to 4 steps on level ground, 2) 6 steps ascending stairs, 3) 3 to 4 steps on level ground, 4) turn back, 5) 3 to 4 steps on level ground, 6) 6 steps descending stairs, and 7) 3 to 4 steps on level ground. For the ramp scenario, the following order was used: 1) 3 to 4 steps on level ground, 2) 8 to 10 steps ascending the ramp, 3) turn back, 4) 8 to 10 step in descending the ramp, and 5) 3 to 4 steps on level ground. For each scenario, the first trial was used to train the algorithm, and the other two trials were used to evaluate the performance of the proposed algorithm.

4.3.3 Data Analysis

IMU and FSR data from the experimental trials were processed using the classification algorithm proposed above (in section 4.3.1) and using the previous algorithm [115]. Figure 16 illustrates an example of filtered output of the artificial neural network. The red line represented the first element ($\bar{\boldsymbol{y}}'[\mathbf{1}]$) of the vector, $\bar{\boldsymbol{y}}'$, which indicated ascent mode. Similarly green (indication of level mode) and blue (indication of descent mode) represented the second ($\bar{\boldsymbol{y}}'[\mathbf{2}]$ and third ($\bar{\boldsymbol{y}}'[\mathbf{3}]$) elements of the filtered

output vector of the network, respectively (Figure 16). High values for an element signal were used to classify each step.

To understand how quickly each algorithm could detect a new gait mode, this time was computed from the start of the swing phase of the transition step and measured as a function of percentage of gait cycle (% GC) from the start of swing. One gait cycle was defined by consecutive heel strikes of the same limb and normalized into 0 – 100% GC.

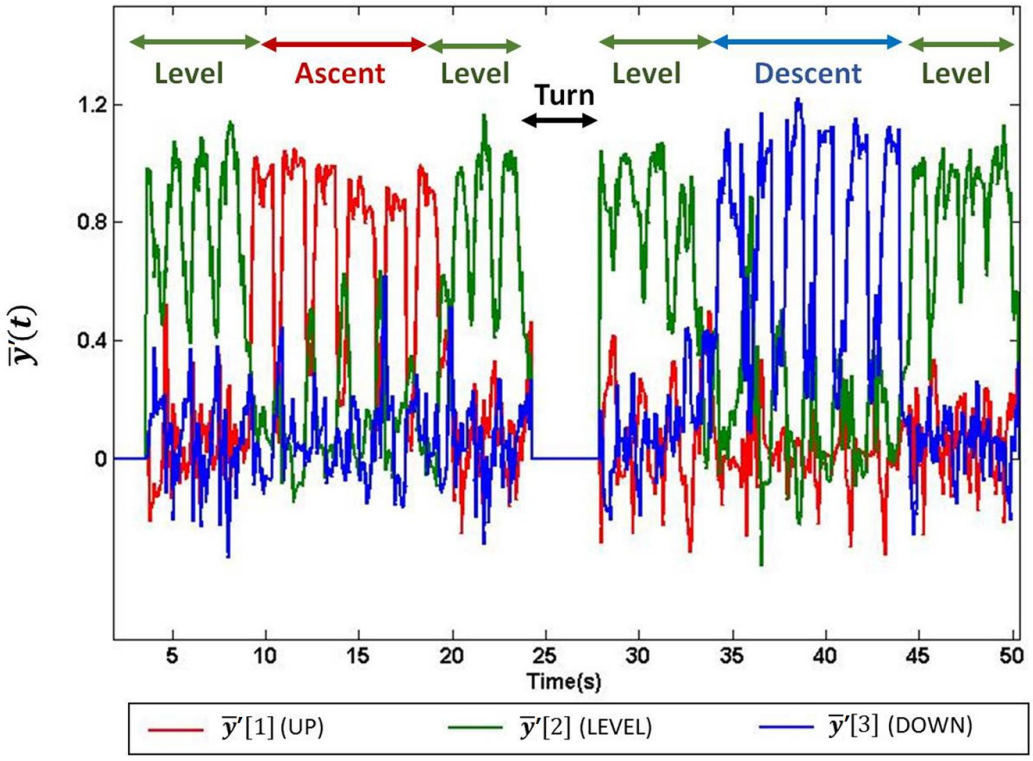

Figure 16 Output of the artificial neural networks for different mode of walking.

Success rate was used to evaluate the performance of the algorithm for correctly identifying the gait mode of each step. Success rate was defined by Equation (28) [115]:

$$Success\ Rate = \frac{Number\ of\ Correctly\ Recognized\ Steps}{Number\ of\ Total\ Steps} \times 100\% \quad (28)$$

The results of the newly proposed algorithm were compared with that of the algorithm described in [115].

4.4 Results

After applying this approach, it was found that the estimator can detect each mode more effectively compared to the previously developed algorithm [115] (Figure 17). The previous method had more incorrect step classifications. The previous algorithm was also not able to recognize the new mode until partway into the next step after the transition; thus resulting in a one-step delay. The new algorithm was able to recognize the new mode during the swing phase of the step during the transition. The proposed algorithm was able to detect a new gait mode within 28% GC, on average, after the start of the swing phase during the stair scenario (16% GC for ramp); whereas with the previous algorithm, the new gait mode was detected 77% GC after swing for the stair scenario (73% GC for ramp), which put this time into the next step.

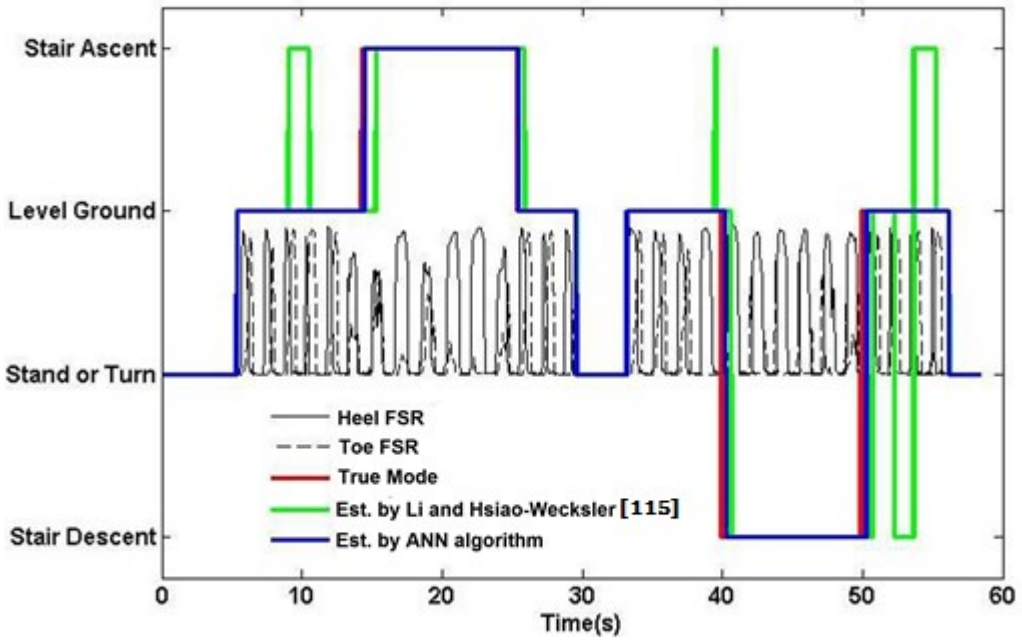

Figure 17 Comparison between True Mode and mode estimated by the original Li and Hsiao-Wecksler [115] and ANN algorithms.

Success rates for the proposed algorithm while walking during the stair scenario (TABLE 17) and ramp scenario (TABLE 17) were found to be larger compared to the results from the previous algorithm. Sub01 showed the best result for both algorithms (100%). However, success rate of other subjects had different values when compared between two algorithms. Sub03 and Sub04 also had 100% success rate when the proposed algorithm was used. Overall, while subjects were walking during the stair scenario, success rate to detect level ground, ascent mode and descent mode were 99.3%, 100.0% and 98.3%, respectively. On the other hand, using the previous algorithm, these values were 93.4%, 98.3% and 93.3%. Similar results were found when subjects walked during the ramp scenario.

TABLE 16 Success rate during stair scenario.

	ANN Algorithm Success Rate (%)			Algorithm by Li and Hsiao-Wecksler [115] Success Rate (%)		
	Level Mode	Ascent Mode	Descent Mode	Level Mode	Ascent Mode	Descent Mode
Sub01	*100.0*	*100.0*	*100.0*	*100.0*	*100.0*	*100.0*
Sub02	*96.9*	*100.0*	*100.0*	*81.3*	*100.0*	*91.7*
Sub03	*100.0*	*100.0*	*100.0*	*100.0*	*100.0*	*91.7*
Sub04	*100.0*	*100.0*	*100.0*	*93.3*	*91.7*	*91.7*
Sub05	*100.0*	*100.0*	*91.7*	*93.3*	*100.0*	*91.7*
Overall	*99.3*	*100.0*	*98.3*	*93.4*	*98.3*	*93.3*

TABLE 17 Success rate during ramp scenario.

	ANN Algorithm Success Rate (%)			Algorithm by Li and Hsiao-Wecksler [115] Success Rate (%)		
	Level Mode	Ascent Mode	Descent Mode	Level Mode	Ascent Mode	Descent Mode
Sub01	*95.0*	*100.0*	*100.0*	*90.0*	*100.0*	*94.7*
Sub02	*100.0*	*100.0*	*100.0*	*94.4*	*94.1*	*93.8*
Sub03	*100.0*	*90.0*	*100.0*	*94.4*	*90.0*	*95.0*
Sub04	*100.0*	*100.0*	*100.0*	*93.3*	*100.0*	*94.1*
Sub05	*100.0*	*100.0*	*100.0*	*87.5*	*100.0*	*93.8*
Overall	*98.9*	*97.8*	*100.0*	*92.0*	*96.7*	*94.3*

4.5 Discussion

4.5.1 Experimental observation

The primary purpose of this study was to develop an algorithm to automatically distinguish different gait modes (level ground, ascent and descent of stairs or ramps), as controller schemes for powered devices vary for different gait modes. When walking on level ground and ascending stairs or ramps, the

ankle should be dorsiflexed and the toes held up to prevent tripping. When descending, the ankle is plantarflexed and the toes point downward in preparation for contacting the lower surface. The proposed gait mode recognition algorithm, using an artificial neural network, successfully classified gait mode with high accuracy and without the previous one-step delay limitation. For both stair and ramp scenarios, the proposed algorithm demonstrated better performance compared to algorithm developed by Li and Hsiao-Wecksler [115] (TABLE 17 and TABLE 17).

For the stair scenario, the proposed algorithm worked very good in ascent mode condition with an average success rate of 100%, while the previous vertical position tracking algorithm had an average success rate of 98.3% [115]. In level ground walking, the overall success rate was 99.3%, while previously it was 93.4%. The proposed algorithm had also shown better performance in descent mode in the stair scenario. Most of the time, except Sub-02 for level ground mode and Sub05 for descent mode, the proposed algorithm's success rate was 100%. As a whole, when walking on stairs, the new algorithm performed better than the previous method based on success rate.

For the ramp scenario, the proposed algorithm had 98.9%, 97.8% and 100% average success rate at level ground walking, ascent mode, and descent mode, respectively. All of these values are better than the corresponding values when the previous algorithm was used. For ramp descent mode, the proposed algorithm had the best result having 100% of success rate for all subjects. In the level ground mode, the proposed algorithm also had a 100% success rate, except for Sub-01. Similarly, except for Sub-03, the proposed algorithm had a 100% success rate. Overall, the new algorithm showed promising results while walking on the ramp.

The proposed algorithm used an artificial neural network where the inputs were a six sample size window from the input signals: vertical velocity and foot segment angle. This algorithm was able to detect modes continuously, i.e., soon after the new step was started. The average delay to detect a new gait mode was 28% GC and 16% GC after start of swing phase for stair and ramp scenarios, respectively.

The previous algorithm depended on the height of the stair size or the grade of the ramp, i.e., the algorithm required new training to calculate thresholds for vertical position for stairs with different heights and ramps with different grades. On the other hand, the new proposed algorithm should recognize the gait mode after subject-specific training regardless of stair height and it will be faster at detecting the gait mode as the calculations are done continuously.

4.5.2 Limitations and future recommendations

Though the proposed algorithm showed promising results, there are some limitations of this study. One limitation of the proposed algorithm was that we used subject-specific training. Ideally, a best approach should not depend on subject and will work for all subjects using the same training data. Making training data from multiple subjects or using input from multiple IMUs (e.g., one IMU on foot and another IMU on shank) might help to overcome this limitation. Furthermore, we used the success rate as the measurement of the performance of the algorithms. As mentioned in [115], it is not clear what should be the acceptable value of success rate [90], [91], [95], [120], [121].

There are several aspects of this study which open prospects for new studies. The current algorithm was developed and applied on previously collected data. Implementation of the current algorithm to detect the gait mode and change the actuation accordingly should be addressed in the future. It was hypothesized that the proposed algorithm should not depend on stair height and the grade of the slope. A new study should check the claim. Overall, the current study demonstrated that an artificial neural network can be used to detect gait modes with higher accuracy and opened new opportunities for exploring the area of recognizing gait modes.

4.6 Conclusion

Portability of powered orthotic or prosthetic devices opened new challenges to detect gait modes (level ground, ascent and descent during walking on stairs or ramps). The actuation of these kinds of powered assistive devices should be changed accordingly based on the gait modes. Manually switching for a new gait mode is the most common approach. In this study, a novel algorithm based on an artificial neural network was proposed which continuously analyzed the input signals for automatically detecting the gait mode using an inertial measurement unit. This algorithm recognized new gait modes faster and with higher accuracy than a previous method used with the PPAFO.

CHAPTER 5

Conclusion and Future Work

This dissertation was focused on improving human gait using a powered Ankle-Foot Orthosis (AFO). An AFO can provide assistance to individuals with lower limb muscle impairments [7]. The knowledge of gait plays an important role for assisting an individual by powered AFO during walking. Generally, the gait cycle begins from the time of initial contact of the heel with the floor (0% of gait cycle) and ends at the point of the next heel strike (100% of gait cycle) of the same foot. If gait state, which can be represented by the percentage of gait cycle (% GC), can be estimated successfully, the control of a powered AFO can be more effective. Active lower limb assistive devices (prosthetic and orthotic devices) have been developed over the last few years to improve the locomotion of impaired populations [2]. However, powered AFOs, described in different literature [7], [21]–[44], had limitation in terms of controls. To explore the control strategy, we developed the portable powered ankle foot orthosis (PPAFO) in our Human Dynamics and Control Laboratory (HCDL). Three aspects of effective control for a powered AFO were proposed in this dissertation. In Study-01, improved methods for the estimation of the gait state during walking with the PPAFO were addressed. Two new methods were proposed in this study: Modified Fractional Time (MFT) and Artificial Neural Network (ANN). In Study 2, a machine learning based algorithm was proposed to find the proper plantarflexor actuation timing during walking with the PPAFO. Finally in Study 3, recognition of different gait modes (level ground, ascent, and descent) was addressed. An artificial neural network based algorithm was proposed to detect different gait modes.

5.1 Gait State Estimation (Study-01)

The main purpose of this study was to improve the estimation of percentage of gait while walking with a powered AFOs. One approach (state estimation approach) is to estimate the gait state during

walking and provide actuation via a powered AFO at a desired state value. Previously, Fractional Time (FT) state estimation [5] was developed; however, FT has limitations when gait speed changes. Generally, cadence of a healthy able-bodied walker varies from step to step due to different stride length, turning, and gait speed changes. Walking parameters may be even more inconsistent for impaired populations. In this study, Modified Fractional Time (MFT) and Artificial Neural Network (ANN) state estimation techniques were developed to overcome the limitations of FT.

Sub-Study A used simulated gait data and demonstrated that FT showed good results only while walking at constant speed. However, MFT and ANN were more robust and worked better when speed changed, which would be the case in real-world walking situations. Similarly, Sub-Study B used experimentally-collected gait data and also demonstrated that MFT and ANN performed similar to the previous FT algorithm during constant walking speed. However, the performances of the new estimators were significantly better when walking with variable speeds. Sub-Study C demonstrated experimentally that a controller, which used the MFT state estimator, performed best when the actuation was given according to predicted estimated state. In essence, these studies found that FT showed good results, but only while walking at constant speed. On the other hand, MFT and ANN performed better during both same and variable speeds. MFT was considered as best estimator among all estimators for having consistently small error for all the sub studies. MFT has recently been used in an over-ground, non-treadmill study on a population with impaired gait due to multiple sclerosis.

5.2 Finding Plantarflexor Torque Timing (Study 02)

The primary purpose of this study was to develop a systematic approach to find the plantarflexor actuation timing using biomechanics data (joint kinematics) during walking while using a powered AFO. For gait improvement using powered AFOs, the implementation of appropriate actuation timing for plantarflexion motion is very important [111]. If the plantarflexor torque by the PPAFO was early, the subject would feel constraint in the direction of the dorsiflexion side of his foot due to the desired

downward motion of the PPAFO. In contrast, if the plantarflexor actuation timing was too late, the maximum range of motion in the plantarflexion direction would be diminished due to delayed assistance from PPAFO and also there was an unwanted noisy motion during the movement in the plantarflexion direction due to asynchronous relation between plantarflexor torque by PPAFO and human ankle-foot system.

In this study, a multistep supervised learning algorithm was proposed which determined the appropriate plantarflexor actuation timing based on ankle angle data. After training the classifier with collected gait data, the classifier algorithm was used in combination with a bisection search method to quickly identify the appropriate actuation timing for a specific user.

Our proposed algorithm successfully found the appropriate plantarflexor torque timing during walking using the biomechanics data of healthy able-bodied subjects (i.e., sagittal plane ankle angle). The proposed algorithm needs training data prior to applying the algorithm to general use of the device. When the algorithm was trained with a subject's own personal data, the performance of the algorithm was found to be the best. However, it may not be possible to collect training data for a particular user or use of training data collected on an impaired population is not appropriate, since the goal is to replicate normal healthy gait biomechanics. Therefore, we examined the effect of using training data from one or more different subjects on the accuracy of predicting appropriate plantarflexor actuation timing. We found that using training data from more able-bodied subjects improved prediction accuracy.

Other research groups have followed a functional approach and used minimization of metabolic cost during walking with a powered orthotic or prosthetic as the optimization criteria for detecting appropriate plantarflexor actuation timing [80], [102]–[109]. However, optimizing timing using metabolic data can be time consuming (10s of minutes of walking). In this study, we took a biomechanics approach and used replication of ankle angle kinematics to mimic healthy able-bodied gait as the optimization criteria. This approach was able to identify appropriate actuation timing quickly within a few strides (less than 10 minutes).

5.3 Gait Mode Recognition (Study 03)

The primary purpose of this study was to distinguish different gait modes (level ground, ascent, and descent) automatically as the controller schemes for powered AFO are different for different gait modes. Portability of powered orthotic or prosthetic devices opened new challenges to detect gait modes. The actuation of these kinds of powered assistive device should be changed accordingly based on the gait modes. Manually switching for different gait modes are most common [86], [87]; however, some researchers are also working on detecting gait modes automatically [54], [70], [88]–[90], [114].

In this study, a novel algorithm based on artificial neural network was proposed that continuously analyzed the input signals for detecting the gait mode using an inertial measurement unit (IMU) with faster time and higher accuracy. The vertical velocity and foot segment angle of the foot shell of the PPAFO were used as input signals to the artificial neural network. The output from the ANN were filtered and adjusted to generate a final data set used to classify different gait modes.

The proposed gait mode recognition approach successfully classified gait mode with very good accuracy. For both stair and ramp scenarios, the proposed algorithm showed better performance compared to algorithm developed by Li and Hsiao-Wecksler [115]. The experimental results showed promising result (Success rate: 99.3%, 100%, 98% for level, ascent and descent mode in stairs, respectively; 98.9%, 97.8%, 100% for level, ascent and descent mode in ramps) detecting the gait modes.

5.4 Limitation and Future Recommendation

Three studies conducted in this dissertation opened opportunities to explore new studies. The primary purpose of all studies presented in this dissertation was to improve the gait of an individual while walking

with a powered AFO. Though the results found from the studies were very promising, there are some limitations.

The following are some limitations and future recommendations based on study-01 where two new methods were proposed to estimate the gait state. Firstly, data from only five subjects for Sub-Study B and only one subject for Sub-Study C were collected. More data might help to interpret the performance of the controller more accurately. Next, although three sensors (two force sensitive resistor and one Hall effect angle sensor) were used in this study, it is assumed that the same algorithm could work for different types of signals from different sensors. Future studies should investigate state estimation accuracy when using other sensors, such as IMU sensors. Furthermore, we used generic plantarflexor torque timing based on average normal able-bodied walking data [122] for providing the actuation timings in Sub-Study C; however, from Study 2 of this dissertation, we know that subject-specific actuation timings will improve gait biomechanics. Finally, further studies should to implement these algorithms on impaired subject populations. The MFT algorithm was used in an over-ground, non-treadmill study on 16 people with moderate to severe multiple sclerosis [101] .

There are also a few limitations in study -02, where the primary purpose was to develop a systematic approach to find the plantarflexor actuation timing using biomechanics data during human walking using a powered AFO. Similar to study-01, data from only five subjects were collected. Data from more able-bodied subjects will help to interpret the performance more accurately. Future studies could be done to compare results using the proposed algorithm with results where energetic data (metabolic cost) were used to find the appropriate plantarflexor torque timing. Implementing the proposed algorithm to different group impaired population is another possible future study.

Like the other two studies, there are also few limitations in study -03, where the primary purpose was to distinguish different gait modes automatically. The previous algorithm by Li and Hsiao-Wecksler had a limitation of a one-step delay. Although the newly proposed algorithm was faster at detecting a new gait mode, there was still a delay in detecting the gait mode. The algorithm detected the gait mode during the

swing phase before the next step. The average delay to detect the gait mode was 28% GC and 17% GC after starting of the swing phase for stair and ramp scenarios. Moreover, subject-specific training is needed for the proposed algorithm. If the parameter calculated from the data from one subject was used to test the algorithm for different subject, the result was not found satisfactory. Furthermore, we used the success rate as the measurement of the performance of the algorithms. As mentioned in [115], there is not enough study about the acceptable value of success rate [90], [91], [95], [120], [121]. Implementation of the current algorithm to detect the gait mode and change the actuation accordingly could be a good opportunity to look at. It is hypothesized that the proposed algorithm should not depend on stair height and the grade of the slope. A future study can be proposed to check the claim.

The main purpose of this dissertation was to improve the control system of powered AFOs. Primarily, two new estimators were introduced to find the gait state with higher accuracy (Study 01). Later, a systematic approach was presented to find the appropriate timing for plantarflexor actuation of powered AFOs (Study 02). Finally, a classifier was proposed to detect the different gait modes (level ground, ascent and descent of stairs or ramps) (Study 3). Overall, the dissertation focused on assisting an individual wearing powered AFOs in walking in different situations. The proposed approaches and algorithms introduced in this dissertation showed very promising results that proved that these methods can successfully improve the control system of powered AFOs.

Appendix

A.1 Approach for early/late actuation timing classifier

This classifier approach separates powered ankle-foot orthosis gait data as either early or late plantarflexor actuation timing. Flexion-extension ankle angle data of multiple gait cycles (or strides) collected at different plantarflexor actuation timings were used as training data for the classifier. In this study, subjects walked on a treadmill for 30 seconds during seven plantarflexor actuation timing conditions ($Q = 7$): 30%, 35%, 40%, 45%, 50%, 55% and 60% GC. For each condition, the last 20 gait cycles ($\alpha = 20$) for the limb with the orthosis were used for the training data. Visual inspection of the ankle angle profiles was used to categorize a condition was as being either early or late.

Let, $\boldsymbol{x}^{(q,i)}$ be a vector consisting of ankle angle data for a single gait cycle i that was collected when plantarflexor actuation was set to timing condition q. We can represent these data in terms of a Fourier series by using a discrete Fourier transformation:

$$\boldsymbol{x}^{(q,i)} = a_0^{(q,i)} + \sum_{n=1}^{N-1} \left(a_n^{(q,i)} \, cos(n\omega_o) + b_n^{(q,i)} \, sin(n\omega_o) \right) \tag{29}$$

$$\text{where, } q = 1 \; to \; Q \, ,$$

$$i = 1 \; to \; \alpha$$

Here, N represents the number of data points in a gait cycle, and the frequency, $\omega_o = 2\pi/N$. N is 100, as one gait cycle goes from 0% to 99% GC. $\boldsymbol{x}^{(q,i)}$ is defined such that $\boldsymbol{x}^{(q,i)} \in \mathbb{R}^N$

Rearranging Equation (29), we can find the following:

$$\boldsymbol{x}^{(q,i)} = a_0^{(q,i)} + [cos\,\omega_o \quad cos\,2\omega_o \quad \dots \quad cos\,(N-1)\omega_o] \begin{bmatrix} a_1^{(q,i)} \\ a_2^{(q,i)} \\ a_3^{(q,i)} \\ \vdots \\ a_{N-1}^{(q,i)} \end{bmatrix}$$

$$+ [sin\omega_o \quad sin2\omega_o \quad \dots \quad sin\,(N-1)\omega_o] \begin{bmatrix} b_1^{(q,i)} \\ b_2^{(q,i)} \\ b_3^{(q,i)} \\ \vdots \\ b_{N-1}^{(q,i)} \end{bmatrix} \tag{30}$$

Due to symmetry of these coefficients, we can represent $\boldsymbol{x}^{(q,i)}$ with a reduced number of coefficients. We define this vector of required coefficients as $\boldsymbol{c}^{(q,i)}$ such that $\boldsymbol{c}^{(q,i)} \in \mathbb{R}^{(N+1)}$. Therefore we can now represent $\boldsymbol{x}^{(q,i)}$ as $\boldsymbol{c}^{(q,i)}$.

$$\boldsymbol{x}^{(q,i)} \xRightarrow{represented\ by} \begin{bmatrix} a_0^{(q,i)} \\ a_1^{(q,i)} \\ a_2^{(q,i)} \\ a_3^{(q,i)} \\ \vdots \\ a_{N-1}^{(q,i)} \\ b_1^{(q,i)} \\ b_2^{(q,i)} \\ b_3^{(q,i)} \\ \vdots \\ b_{N-1}^{(q,i)} \end{bmatrix} \xRightarrow{represented\ by} \begin{bmatrix} a_0^{(q,i)} \\ a_1^{(q,i)} \\ a_2^{(q,i)} \\ a_3^{(q,i)} \\ \vdots \\ a_{\frac{N}{2}}^{(q,i)} \\ b_1^{(q,i)} \\ b_2^{(q,i)} \\ b_3^{(q,i)} \\ \vdots \\ b_{\frac{N}{2}}^{(q,i)} \end{bmatrix} \triangleq \boldsymbol{c}^{(q,i)} \tag{31}$$

Next, we will separate these coefficients to represent two cases. The first case involves all strides collected when the timing condition was classified as early. The second involves all strides collected when the condition was classified as late. In other words, Q number of conditions can be now divided into Q_E early cases (indices from 1 to Q_E) and Q_L late cases (indices from $Q_E + 1$ to $Q_E + Q_L$). The $\boldsymbol{c^q}$ matrix, which is in $\mathbb{R}^{(N+1)\times\alpha}$ space, is now defined by all 20 strides for the q^{th} condition (Equation (32)).

$$\boldsymbol{c^q} = [\boldsymbol{c^{q,1}} \quad \boldsymbol{c^{q,2}} \quad \dots \quad \boldsymbol{c^{q,\alpha}}] \tag{32}$$

Let that the matrices of these Fourier coefficients for all strides of all conditions classified as early and late timing cases be given as $\boldsymbol{C_E}$ and $\boldsymbol{C_L}$, respectively (Equation (33) and Equation (34)). Here, $\boldsymbol{C_E} \in \mathbb{R}^{(N+1)\times(\alpha Q_1)}$ and $\boldsymbol{C_L} \in \mathbb{R}^{(N+1)\times(\alpha Q_2)}$.

$$\boldsymbol{C_E} = [\boldsymbol{c^1} \quad \boldsymbol{c^2} \quad \dots \quad \boldsymbol{c^{Q_E}}] \tag{33}$$

$$\boldsymbol{C_L} = [\boldsymbol{c^{Q_E+1}} \quad \boldsymbol{c^{Q_L+2}} \quad \dots \quad \boldsymbol{c^{Q_E+Q_L}}] \tag{34}$$

where,

$$Q_E \triangleq number\ of\ early\ cases$$

$$Q_L \triangleq number\ of\ late\ cases$$

$$Q = total\ number\ of actuation\ timing\ conditions = Q_E + Q_L$$

$$i = 1\ to\ \alpha$$

Therefore, the full training matrix $\boldsymbol{C}$, where $\boldsymbol{C} \in \mathbb{R}^{(N+1)\times(\alpha Q)}$, can be described as:

$$\boldsymbol{C} = [\boldsymbol{C}_E \quad \boldsymbol{C}_L] \tag{35}$$

Rather than using this large matrix in the classification process, we will use principle component analysis (PCA) [113] to identify important features of the training data and formulate a reduced dimension matrix for the classifier. First, we adjust for matrix $\boldsymbol{C}$ to have a zero-mean to fulfill the requirement of PCA. Then, we calculate the covariance matrix $Cov(\boldsymbol{C})$ from the zero-mean adjusted training matrix $\boldsymbol{C}$.

Next, we find the eigenvalues and eigenvectors of $Cov(\boldsymbol{C})$.

$$Cov\,(C) \;\Big\}\; \begin{cases} \xrightarrow{sorted\ eigenvalues\ (descended)} & [\lambda_1 \quad \lambda_2 \quad \lambda_3 \quad \dots \quad \lambda_{N+1}] \\ \xrightarrow{corresponding\ eigenvectors} & [v_1 \quad v_2 \quad v_3 \quad \dots \quad v_{N+1}] \end{cases}$$

For PCA, we are interested in finding a reduced number of important features *d* that are still able to capture the essence of the training matrix. In this study, we examined a variety of values for *d* (10, 15, 20, and 25), which can be thought of as representing the first 10 to 25 principal components. So, the reduced eigenvalue matrix ($\boldsymbol{V_r} \in \mathbb{R}^{d\times d}$) and reduced eigenvector matrix ($\boldsymbol{\Lambda_r} \in \mathbb{R}^{(N+1)\times d}$) are:

$$\boldsymbol{\Lambda_r} = \begin{bmatrix} \lambda_1 & 0 & 0 & 0 \\ 0 & \lambda_2 & 0 & 0 \\ 0 & 0 & \ddots & \vdots \\ 0 & 0 & \dots & \lambda_d \end{bmatrix} \tag{36}$$

and

$$\boldsymbol{V_r} = [\boldsymbol{v}_1 \quad \boldsymbol{v}_2 \quad \cdots \quad \boldsymbol{v}_d] \tag{37}$$

Using these two matrices, we find the linear map or the feature matrix $\boldsymbol{W}$ (such that, $\boldsymbol{W} \in \mathbb{R}^{d\times(N+1)}$) for reducing the dimension.

$$\boldsymbol{W} = \left[(\boldsymbol{\Lambda}_r)^{-\frac{1}{2}} \times \boldsymbol{V}_r{}^T\right] \tag{38}$$

Previously, we characterized $\boldsymbol{x}^{(q,i)}$by $\boldsymbol{c}^{(q,i)}$. Now, using the feature matrix, we can represent $\boldsymbol{c}^{(q,i)}$ as $\boldsymbol{z}^{(q,i)}$ by reducing the dimension from $\mathbb{R}^{(N+1)}$ to $\mathbb{R}^d$. Here, $\boldsymbol{z}^{(q,i)} \in \mathbb{R}^d$.

$$\boldsymbol{z}^{(q,i)} = \boldsymbol{W} \times \boldsymbol{c}^{(q,i)} \tag{39}$$

$$\boldsymbol{x}^{(q,i)} \xrightarrow{represted\ by} \begin{bmatrix} a_0^{(q,i)} \\ a_1^{(q,i)} \\ a_2^{(q,i)} \\ a_3^{(q,i)} \\ \vdots \\ a_{\frac{N}{2}}^{(q,i)} \\ b_1^{(q,i)} \\ b_2^{(q,i)} \\ b_3^{(q,i)} \\ \vdots \\ b_{\frac{N}{2}}^{(q,i)} \end{bmatrix} \triangleq \boldsymbol{c}^{(q,i)} \xrightarrow{represted\ by} \left[\boldsymbol{z}^{(q,i)}\right] \tag{40}$$

Now, we find the projection of the early cases matrix and late cases matrix on the reduced dimensional subspace. The matrices $\boldsymbol{Z_E} \in \mathbb{R}^{(d)\times(\alpha Q_1)}$ and $\boldsymbol{Z_L} \in \mathbb{R}^{(d)\times(\alpha Q_2)}$.

$$\boldsymbol{Z}_E = \boldsymbol{W} \times \boldsymbol{C}_E \tag{41}$$

$$\boldsymbol{Z}_L = \boldsymbol{W} \times \boldsymbol{C}_L \tag{42}$$

By taking the mean and covariance matrices of each column of $\boldsymbol{Z}_E$ and $\boldsymbol{Z}_L$, we find $\boldsymbol{\mu}_E$, $\boldsymbol{\sigma}_E$, $\boldsymbol{\mu}_E$ and $\boldsymbol{\sigma}_E$ (where, $\boldsymbol{\mu}_E \in \mathbb{R}^d$, $\boldsymbol{\sigma}_E \in \mathbb{R}^{d\times d}$, $\boldsymbol{\mu}_E \in \mathbb{R}^d$, and $\boldsymbol{\sigma}_E \in \mathbb{R}^{d\times d}$). These combined mean and covariance matrices represent the probability density functions for the parameters for early actuation and late actuation. Note that these probability density functions are multi-variable due to the use of matrices for the mean and covariance terms.

With these probability density functions defined from the training data, we can now classify any new set of actuated ankle angle data. Specifically, we use these probability functions to classify whether each stride for a given actuation timing condition is too early or late.

Let, the ankle angle values of the k^{th} stride be represented by the vector x'_k**.** This stride can described as a Fourier series vector c'_k vector using the same procedure described above. Using the feature matrix

derived from the training data, we can evaluate the reduced dimension vector z_k' for the new set of ankle angle data.

$$\boldsymbol{z}_k' = \boldsymbol{W} \times \boldsymbol{c}_k' \tag{43}$$

Using the mean and covariance matrix computed from the training data, we find the probability of the stride represented by z_k' as being early or late from the following equations.

$$\boldsymbol{p}_{z_k'|E} = \boldsymbol{N}(z_k', \boldsymbol{\mu}_E, \boldsymbol{\sigma}_E) \tag{44}$$

$$\boldsymbol{p}_{z_k'|L} = \boldsymbol{N}(z_k', \boldsymbol{\mu}_L, \boldsymbol{\sigma}_L) \tag{45}$$

If $\boldsymbol{p}_{z_k'|early}$ is greater than $\boldsymbol{p}_{z_k'|late}$, we say that the current stride's behavior appeared similar to the training actuation timings that were considered early. On the other hand, if $\boldsymbol{p}_{z_k'|late}$ is greater than $\boldsymbol{p}_{z_k'|early}$, the stride's behavior is similar to late actuation timing.

$$\begin{cases} \text{if } \boldsymbol{p}_{z_k'|E} > \boldsymbol{p}_{z_k'|L}\,, & \text{actuation is too early} \\ \text{if } \boldsymbol{p}_{z_k'|E} < \boldsymbol{p}_{z_k'|L}\,, & \text{actuation is too late} \end{cases} \tag{46}$$

Figure 18 provides a representation of a single variable probability density function (when *z* is a scalar) to illustrate early and late cases. In this figure, the dots represent the probably of stride *k*. In this case, the stride would be classified as late.

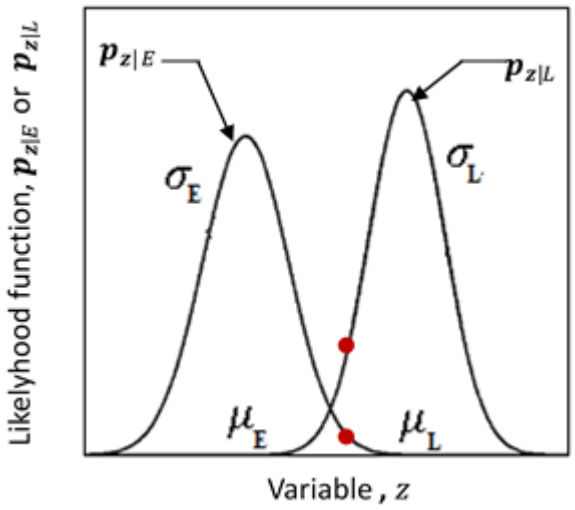

Figure 18 Example of a single variable probability density functions for early (E) and late (L) cases

Finally, to access whether a given actuation timing condition was considered to be too early or late, the classification of the majority of all assessed strides was used. For example, for an actuation timing of 55% GC, if 17 of 20 strides were classified as late, then the plantarflexor actuation timing condition of 55% GC was considered to be late.

A.2 Notation

Table 18 Notations.

$\boldsymbol{x}^{(q,i)}$	A vector consisting of ankle angle data for a single gait cycle i that was collected when plantarflexor actuation was set to timing condition q.
$\boldsymbol{C_E}$	The matrices of Fourier coefficients for all strides of early actuation conditions.
$\boldsymbol{C_L}$	The matrices of Fourier coefficients for all strides of late actuation conditions.
$\boldsymbol{W}$	feature matrix for performing PCA
$\boldsymbol{p}_{z_k'\|E}$	The probability of the stride represented by z_k' as being early.
$\boldsymbol{p}_{z_k'\|L}$	The probability of the stride represented by z_k' as being early.
Q	Total number of actuation timing conditions
Q_E	Number of early actuation cases
Q_L	Number of late actuation cases
α	Total number of gait cycles in one condition

References

[1] N. Owen, N. Humpel, E. Leslie, A. Bauman, and J. F. Sallis, "Understanding environmental influences on walking; Review and research agenda.," *Am. J. Prev. Med.*, vol. 27, no. 1, pp. 67–76, Jul. 2004.

[2] J. Perry and J. Burnfield, *Gait Analysis: Normal and Pathological Function*, 1st Editio. New Jersey: SLACK Incorporated, 1992.

[3] D. Winter, "Human balance and posture control during standing and walking," *Gait Posture*, vol. 3, no. 4, pp. 193–214, Dec. 1995.

[4] Q. Huang, K. Yokoi, S. Kajita, K. Kaneko, H. Arai, N. Koyachi, and K. Tanie, "Planning walking patterns for a biped robot," *Robot. Autom. IEEE Trans.*, vol. 17, no. 3, pp. 280–289, 2001.

[5] D. Y. Li, A. Becker, K. A. Shorter, T. Bretl, and E. T. Hsiao-Wecksler, "Estimating System State During Human Walking With a Powered Ankle-Foot Orthosis," *IEEE/ASME Trans. Mechatronics*, vol. 16, no. 5, pp. 835–844, Oct. 2011.

[6] A. M. Dollar and H. Herr, "Lower Extremity Exoskeletons and Active Orthoses: Challenges and State-of-the-Art," *IEEE Trans. Robot.*, vol. 24, no. 1, pp. 144–158, Feb. 2008.

[7] K. A. Shorter, J. Xia, E. T. Hsiao-Wecksler, W. K. Durfee, and G. F. Kogler, "Technologies for Powered Ankle-Foot Orthotic Systems: Possibilities and Challenges," *IEEE/ASME Trans. Mechatronics*, vol. 18, no. 1, pp. 337–347, Feb. 2013.

[8] G. K. Rose, "The principles and practice of hip guidance articulations," *Prosthet. Orthot. Int.*, vol. 3, no. 1, pp. 37–43, 1979.

[9] J. B. Redford, "Principles of orthotic devices," *Orthot. Etcetera, Williams Wilkins, Balt.*, pp. 1–20, 1986.

[10] J. P. Bakker, I. J. de Groot, H. Beckerman, B. A. de Jong, and G. J. Lankhorst, "The effects of knee-ankle-foot orthoses in the treatment of Duchenne muscular dystrophy: review of the literature.," *Clin. Rehabil.*, vol. 14, no. 4, pp. 343–59, Aug. 2000.

[11] C. E. Buckon, S. S. Thomas, S. Jakobson-Huston, M. Moor, M. Sussman, and M. Aiona, "Comparison of three ankle--foot orthosis configurations for children with spastic diplegia," *Dev. Med. Child Neurol.*, vol. 46, no. 09, pp. 590–598, 2004.

[12] H. B. Kitaoka, X. M. Crevoisier, K. Harbst, D. Hansen, B. Kotajarvi, and K. Kaufman, "The effect of custom-made braces for the ankle and hindfoot on ankle and foot kinematics and ground reaction forces," *Arch. Phys. Med. Rehabil.*, vol. 87, no. 1, pp. 130–135, 2006.

[13] G. K. Rose, "Orthotics: Principles and Practice. 1986." London: Williams Heinemann.

[14] J. C. Patzkowski, R. V Blanck, J. G. Owens, J. M. Wilken, K. L. Kirk, J. C. Wenke, J. R. Hsu, S. T. R. Consortium, and others, "Comparative effect of orthosis design on functional performance," *J. Bone Jt. Surg.*, vol. 94, no. 6, pp. 507–515, 2012.

[15] L. R. Palmer, "Sagittal plane characterization of normal human ankle function across a range of walking gait speeds," MIT, 2002.

[16] D. H. Gates, "Characterizing ankle function during stair ascent, descent, and level walking for ankle prosthesis and orthosis design," University of Virginia, 2004.

[17] S. Yamamoto, M. Ebina, S. Miyazaki, H. Kawai, and T. Kubota, "Development of a New Ankle-Foot Orthosis with Dorsiflexion Assist, Part 1: Desirable Characteristics of Ankle-Foot Orthoses for Hemiplegic Patients.," *JPO J. Prosthetics Orthot.*, vol. 9, no. 4, pp. 174–179, 1997.

[18] R. Jimenez-Fabian and O. Verlinden, "Review of control algorithms for robotic ankle systems in lower-limb orthoses, prostheses, and exoskeletons," *Med. Eng. Phys.*, vol. 34, no. 4, pp. 397–408, 2012.

[19] K. A. Shorter, Y. Li, T. Bretl, and E. T. Hsiao-Wecksler, “Modeling, control, and analysis of a robotic assist device,” *Mechatronics*, vol. 22, no. 8, pp. 1067–1077, Dec. 2012.

[20] Y. Li, K. A. Shorter, E. T. Hsiao-Wecksler, and T. Bretl, “Simulation and Experimental Analysis of a Portable Powered Ankle-Foot Orthosis Control,” in *ASME 2011 Dynamic Systems and Control Conference and Bath/ASME Symposium on Fluid Power and Motion Control, Volume 1*, 2011, pp. 77–84.

[21] H. Naito, Y. Akazawa, K. Tagaya, T. Matsumoto, and M. Tanaka, “An ankle-foot orthosis with a variable-resistance ankle joint using a magnetorheological-fluid rotary damper,” *J. Biomech. Sci. Eng.*, vol. 4, no. 2, pp. 182–191, 2009.

[22] J. Furusho, T. Kikuchi, M. Tokuda, T. Kakehashi, K. Ikeda, S. Morimoto, Y. Hashimoto, H. Tomiyama, A. Nakagawa, and Y. Akazawa, “Development of shear type compact MR brake for the intelligent ankle-foot orthosis and its control; research and development in NEDO for practical application of human support robot,” in *Rehabilitation Robotics, 2007. ICORR 2007. IEEE 10th International Conference on*, 2007, pp. 89–94.

[23] W. Svensson and U. Holmberg, “Ankle-foot-orthosis control in inclinations and stairs,” in *Robotics, Automation and Mechatronics, 2008 IEEE Conference on*, 2008, pp. 301–306.

[24] R. J. Farris, H. A. Quintero, T. J. Withrow, and M. Goldfarb, “Design and simulation of a joint-coupled orthosis for regulating FES-aided gait,” in *Robotics and Automation, 2009. ICRA’09. IEEE International Conference on*, 2009, pp. 1916–1922.

[25] T. Kikuchi, S. Tanida, K. Otsuki, T. Yasuda, and J. Furusho, “Development of third-generation intelligently controllable ankle-foot orthosis with compact MR fluid brake,” in *Robotics and Automation (ICRA), 2010 IEEE International Conference on*, 2010, pp. 2209–2214.

[26] S. Yamamoto, A. Hagiwara, T. Mizobe, O. Yokoyama, and T. Yasui, “Development of an ankle--

foot orthosis with an oil damper," *Prosthet. Orthot. Int.*, vol. 29, no. 3, pp. 209–219, 2005.

[27] K. W. Hollander and T. G. Sugar, "A robust control concept for robotic ankle gait assistance," in *Rehabilitation Robotics, 2007. ICORR 2007. IEEE 10th International Conference on*, 2007, pp. 119–123.

[28] A. W. Boehler, K. W. Hollander, T. G. Sugar, and D. Shin, "Design, implementation and test results of a robust control method for a powered ankle foot orthosis (AFO)," in *Robotics and Automation, 2008. ICRA 2008. IEEE International Conference on*, 2008, pp. 2025–2030.

[29] K. W. Hollander, R. Ilg, T. G. Sugar, and D. Herring, "An efficient robotic tendon for gait assistance," *J. Biomech. Eng.*, vol. 128, no. 5, pp. 788–791, 2006.

[30] S. K. Au, P. Dilworth, and H. Herr, "An ankle-foot emulation system for the study of human walking biomechanics," in *Robotics and Automation, 2006. ICRA 2006. Proceedings 2006 IEEE International Conference on*, 2006, pp. 2939–2945.

[31] A. M. Oymagil, J. K. Hitt, T. Sugar, and J. Fleeger, "Control of a regenerative braking powered ankle foot orthosis," in *Rehabilitation Robotics, 2007. ICORR 2007. IEEE 10th International Conference on*, 2007, pp. 28–34.

[32] J. Pratt, B. Krupp, and C. Morse, "Series elastic actuators for high fidelity force control," *Ind. Robot An Int. J.*, vol. 29, no. 3, pp. 234–241, 2002.

[33] J. B. Andersen and T. Sinkjær, "An actuator system for investigating electrophysiological and biomechanical features around the human ankle joint during gait," *Rehabil. Eng. IEEE Trans.*, vol. 3, no. 4, pp. 299–306, 1995.

[34] D. P. Ferris, J. M. Czerniecki, B. Hannaford, U. of Washington, and V. A. P. S. H. System, "An ankle-foot orthosis powered by artificial pneumatic muscles," *J. Appl. Biomech.*, vol. 21, no. 2, p. 189, 2005.

[35] D. P. Ferris, K. E. Gordon, G. S. Sawicki, and A. Peethambaran, “An improved powered ankle--foot orthosis using proportional myoelectric control,” *Gait Posture*, vol. 23, no. 4, pp. 425–428, 2006.

[36] D. P. Ferris and C. L. Lewis, “Robotic lower limb exoskeletons using proportional myoelectric control,” in *Engineering in Medicine and Biology Society, 2009. EMBC 2009. Annual International Conference of the IEEE*, 2009, pp. 2119–2124.

[37] S. Davis, J. Canderle, P. Artrit, N. Tsagarakis, and D. G. Caldwell, “Enhanced dynamic performance in pneumatic muscle actuators,” in *Robotics and Automation, 2002. Proceedings. ICRA’02. IEEE International Conference on*, 2002, vol. 3, pp. 2836–2841.

[38] K. E. Gordon, G. S. Sawicki, and D. P. Ferris, “Mechanical performance of artificial pneumatic muscles to power an ankle--foot orthosis,” *J. Biomech.*, vol. 39, no. 10, pp. 1832–1841, 2006.

[39] A. Roy, H. I. Krebs, S. L. Patterson, T. N. Judkins, I. Khanna, L. W. Forrester, R. M. Macko, and N. Hogan, “Measurement of human ankle stiffness using the anklebot,” in *Rehabilitation Robotics, 2007. ICORR 2007. IEEE 10th International Conference on*, 2007, pp. 356–363.

[40] C. Bulley, J. Shiels, K. Wilkie, and L. Salisbury, “User experiences, preferences and choices relating to functional electrical stimulation and ankle foot orthoses for foot-drop after stroke,” *Physiotherapy*, vol. 97, no. 3, pp. 226–233, 2011.

[41] F. Bethoux, H. L. Rogers, K. J. Nolan, G. M. Abrams, T. Annaswamy, M. Brandstater, B. Browne, J. M. Burnfield, W. Feng, M. J. Freed, C. Geis, J. Greenberg, M. Gudesblatt, F. Ikramuddin, A. Jayaraman, S. A. Kautz, H. L. Lutsep, S. Madhavan, J. Meilahn, W. S. Pease, N. Rao, S. Seetharama, P. Sethi, M. A. Turk, R. A. Wallis, and C. Kufta, “Long-Term Follow-up to a Randomized Controlled Trial Comparing Peroneal Nerve Functional Electrical Stimulation to an Ankle Foot Orthosis for Patients With Chronic Stroke.,” *Neurorehabil. Neural Repair*, p. 1545968315570325–, Feb. 2015.

[42] J. A. Blaya and H. Herr, “Adaptive control of a variable-impedance ankle-foot orthosis to assist drop-foot gait,” *Neural Syst. Rehabil. Eng. IEEE Trans.*, vol. 12, no. 1, pp. 24–31, 2004.

[43] S. Yamamoto, M. Ebina, M. Iwasaki, S. Kubo, H. Kawai, and T. Hayashi, “Comparative Study of Mechanical Characteristics of Plastic AFOs.,” *JPO J. Prosthetics Orthot.*, vol. 5, no. 2, p. 59, 1993.

[44] G. A. Pratt and M. M. Williamson, “Series elastic actuators,” in *Intelligent Robots and Systems 95.’Human Robot Interaction and Cooperative Robots', Proceedings. 1995 IEEE/RSJ International Conference on*, 1995, vol. 1, pp. 399–406.

[45] B. L. Riemann, R. G. DeMont, K. Ryu, and S. M. Lephart, “The effects of sex, joint angle, and the gastrocnemius muscle on passive ankle joint complex stiffness,” *J. Athl. Train.*, vol. 36, no. 4, p. 369, 2001.

[46] M. Mirbagheri, H. Barbeau, M. Ladouceur, and R. Kearney, “Intrinsic and reflex stiffness in normal and spastic, spinal cord injured subjects,” *Exp. brain Res.*, vol. 141, no. 4, pp. 446–459, 2001.

[47] H. A. Varol and M. Goldfarb, “Decomposition-based control for a powered knee and ankle transfemoral prosthesis,” in *Rehabilitation Robotics, 2007. ICORR 2007. IEEE 10th International Conference on*, 2007, pp. 783–789.

[48] K. A. Shorter, Y. Li, E. A. Morris, G. F. Kogler, and E. T. Hsiao-Wecksler, “Experimental evaluation of a portable powered ankle-foot orthosis.,” *Conf. Proc. ... Annu. Int. Conf. IEEE Eng. Med. Biol. Soc. IEEE Eng. Med. Biol. Soc. Annu. Conf.*, vol. 2011, pp. 624–7, Jan. 2011.

[49] E. A. Morris, K. A. Shorter, Y. Li, E. T. Hsiao-Wecksler, G. F. Kogler, T. Bretl, and W. K. Durfee, “Actuation Timing Strategies for a Portable Powered Ankle Foot Orthosis,” in *ASME 2011 Dynamic Systems and Control Conference and Bath/ASME Symposium on Fluid Power and*

Motion Control, Volume 2, 2011, pp. 807–814.

[50] J. Hitt, A. M. Oymagil, T. Sugar, K. Hollander, A. Boehler, and J. Fleeger, "Dynamically controlled ankle-foot orthosis (DCO) with regenerative kinetics: incrementally attaining user portability," in *Robotics and Automation, 2007 IEEE International Conference on*, 2007, pp. 1541–1546.

[51] K. A. Shorter, G. F. Kogler, E. Loth, W. K. Durfee, and E. T. Hsiao-Wecksler, "A portable powered ankle-foot orthosis for rehabilitation," *J. Rehabil. Res. Dev.*, vol. 48, pp. 459–472, 2011.

[52] J. A. Blaya, "Force-controllable ankle foot orthosis (AFO) to assist drop foot gait," Massachusetts Institute of Technology, 2002.

[53] F. Sup, H. A. Varol, J. Mitchell, T. Withrow, and M. Goldfarb, "Design and control of an active electrical knee and ankle prosthesis," in *Biomedical Robotics and Biomechatronics, 2008. BioRob 2008. 2nd IEEE RAS & EMBS International Conference on*, 2008, pp. 523–528.

[54] F. Sup, A. Bohara, and M. Goldfarb, "Design and control of a powered transfemoral prosthesis," *Int. J. Rob. Res.*, vol. 27, no. 2, pp. 263–273, 2008.

[55] J. C. Moreno, E. R. de Lima, A. F. Ruíz, F. J. Brunetti, and J. L. Pons, "Design and implementation of an inertial measurement unit for control of artificial limbs: application on leg orthoses," *Sensors Actuators B Chem.*, vol. 118, no. 1, pp. 333–337, 2006.

[56] S. K. Au, P. Bonato, and H. Herr, "An EMG-position controlled system for an active ankle-foot prosthesis: an initial experimental study," in *Rehabilitation Robotics, 2005. ICORR 2005. 9th International Conference on*, 2005, pp. 375–379.

[57] K. A. Farry, I. D. Walker, and R. G. Baraniuk, "Myoelectric teleoperation of a complex robotic hand," *Robot. Autom. IEEE Trans.*, vol. 12, no. 5, pp. 775–788, 1996.

[58] H.-P. Huang and C.-Y. Chen, "Development of a myoelectric discrimination system for a multi-

degree prosthetic hand," in *Robotics and Automation, 1999. Proceedings. 1999 IEEE International Conference on*, 1999, vol. 3, pp. 2392–2397.

[59] O. Fukuda, T. Tsuji, M. Kaneko, and A. Otsuka, "A human-assisting manipulator teleoperated by EMG signals and arm motions," *Robot. Autom. IEEE Trans.*, vol. 19, no. 2, pp. 210–222, 2003.

[60] H. Kawamoto, S. Lee, S. Kanbe, and Y. Sankai, "Power assist method for HAL-3 using EMG-based feedback controller," in *Systems, Man and Cybernetics, 2003. IEEE International Conference on*, 2003, vol. 2, pp. 1648–1653.

[61] C. Fleischer, C. Reinicke, and G. Hommel, "Predicting the intended motion with emg signals for an exoskeleton orthosis controller," in *Intelligent Robots and Systems, 2005.(IROS 2005). 2005 IEEE/RSJ International Conference on*, 2005, pp. 2029–2034.

[62] C. Fleischer and G. Hommel, "EMG-driven human model for orthosis control," in *Human Interaction with Machines*, Springer, 2006, pp. 69–76.

[63] C. Fleischer and G. Hommel, "Embedded control system for a powered leg exoskeleton," in *Embedded Systems--Modeling, Technology, and Applications*, Springer, 2006, pp. 177–185.

[64] C. Fleischer, K. Kondak, A. Wege, and I. Kossyk, "Research on Exoskeletons at the TU Berlin," in *Advances in Robotics Research*, Springer, 2009, pp. 335–346.

[65] K. E. Gordon and D. P. Ferris, "Learning to walk with a robotic ankle exoskeleton," *J. Biomech.*, vol. 40, no. 12, pp. 2636–2644, 2007.

[66] C. R. Kinnaird and D. P. Ferris, "Medial gastrocnemius myoelectric control of a robotic ankle exoskeleton," *Neural Syst. Rehabil. Eng. IEEE Trans.*, vol. 17, no. 1, pp. 31–37, 2009.

[67] S. M. Cain, K. E. Gordon, and D. P. Ferris, "Locomotor adaptation to a powered ankle-foot orthosis depends on control method," *J. Neuroeng. Rehabil.*, vol. 4, no. 1, pp. 1–13, 2007.

[68] G. S. Sawicki, K. E. Gordon, and D. P. Ferris, “Powered lower limb orthoses: applications in motor adaptation and rehabilitation,” in *Rehabilitation Robotics, 2005. ICORR 2005. 9th International Conference on*, 2005, pp. 206–211.

[69] G. S. Sawicki, A. Domingo, and D. P. Ferris, “The effects of powered ankle-foot orthoses on joint kinematics and muscle activation during walking in individuals with incomplete spinal cord injury.,” *J. Neuroeng. Rehabil.*, vol. 3, p. 3, 2005.

[70] H. A. Varol and M. Goldfarb, “Real-time intent recognition for a powered knee and ankle transfemoral prosthesis,” in *Rehabilitation Robotics, 2007. ICORR 2007. IEEE 10th International Conference on*, 2007, pp. 16–23.

[71] D. Popovic, “Externally powered and controlled orthotics and prosthetics,” *Biomed. Eng. HandBook. Boca Rat. CRC Press LLC*, 2000.

[72] D. Popovic and T. Sinkjær, “Improved control for functional electrical stimulation to restore walking,” *Hong Kong Physiother. J.*, vol. 18, no. 1, pp. 12–20, 2000.

[73] V. Nekoukar and A. Erfanian, “Adaptive terminal sliding mode control of ankle movement using functional electrical stimulation of agonist-antagonist muscles,” in *32nd Annual International Conference of the IEEE EMBS, Buenos Aires, Argentina*, 2010, pp. 5448–5451.

[74] B. W. Heller, P. H. Veltink, N. J. M. Rijkhoff, W. L. C. Rutten, and B. J. Andrews, “Reconstructing muscle activation during normal walking: a comparison of symbolic and connectionist machine learning techniques,” *Biol. Cybern.*, vol. 69, no. 4, pp. 327–335, 1993.

[75] A. Kostov, B. J. Andrews, D. B. Popovic, R. B. Stein, and W. W. Armstrong, “Machine learning in control of functional electrical stimulation systems for locomotion,” *Biomed. Eng. IEEE Trans.*, vol. 42, no. 6, pp. 541–551, 1995.

[76] H. Kazerooni, “The berkeley lower extremity exoskeleton project,” in *Experimental Robotics IX*,

Springer, 2006, pp. 291–301.

[77] H. Kazerooni, J.-L. Racine, L. Huang, and R. Steger, “On the control of the berkeley lower extremity exoskeleton (BLEEX),” in *Robotics and Automation, 2005. ICRA 2005. Proceedings of the 2005 IEEE International Conference on*, 2005, pp. 4353–4360.

[78] H. Kazerooni and R. Steger, “The Berkeley lower extremity exoskeleton,” *J. Dyn. Syst. Meas. Control*, vol. 128, no. 1, pp. 14–25, 2006.

[79] J. Ghan, R. Steger, and H. Kazerooni, “Control and system identification for the Berkeley lower extremity exoskeleton (BLEEX),” *Adv. Robot.*, vol. 20, no. 9, pp. 989–1014, 2006.

[80] P. Malcolm, W. Derave, S. Galle, and D. De Clercq, “A simple exoskeleton that assists plantarflexion can reduce the metabolic cost of human walking,” *PLoS One*, vol. 8, no. 2, p. e56137, 2013.

[81] A. D. Kuo, “Energetics of actively powered locomotion using the simplest walking model,” *J. Biomech. Eng.*, vol. 124, no. 1, pp. 113–120, 2002.

[82] D. A. WINTER, “Energy generation and absorption at the ankle and knee during fast, natural, and slow cadences.,” *Clin. Orthop. Relat. Res.*, vol. 175, pp. 147–154, 1983.

[83] M. Ishikawa, P. V Komi, M. J. Grey, V. Lepola, and G.-P. Bruggemann, “Muscle-tendon interaction and elastic energy usage in human walking,” *J. Appl. Physiol.*, vol. 99, no. 2, pp. 603–608, 2005.

[84] R. Riener, M. Rabuffetti, and C. Frigo, “Stair ascent and descent at different inclinations,” *Gait Posture*, vol. 15, no. 1, pp. 32–44, 2002.

[85] K. Koganezawa, H. Fujimoto, and I. Kato, “Multifunctional above-knee prosthesis for stairs’ walking,” *Prosthet. Orthot. Int.*, vol. 11, no. 3, pp. 139–145, 1987.

[86] O. Bock, “The Electronic C-Leg® Knee Joint System, Instructions for Use.” Published, 2002.

[87] S. Au, M. Berniker, and H. Herr, “Powered ankle-foot prosthesis to assist level-ground and stair-descent gaits,” *Neural Networks*, vol. 21, no. 4, pp. 654–666, 2008.

[88] H. A. Varol, F. Sup, and M. Goldfarb, “Real-time gait mode intent recognition of a powered knee and ankle prosthesis for standing and walking,” in *Biomedical Robotics and Biomechatronics, 2008. BioRob 2008. 2nd IEEE RAS & EMBS International Conference on*, 2008, pp. 66–72.

[89] H. A. Varol, F. Sup, and M. Goldfarb, “Powered sit-to-stand and assistive stand-to-sit framework for a powered transfemoral prosthesis,” in *Rehabilitation Robotics, 2009. ICORR 2009. IEEE International Conference on*, 2009, pp. 645–651.

[90] H. A. Varol, F. Sup, and M. Goldfarb, “Multiclass real-time intent recognition of a powered lower limb prosthesis,” *Biomed. Eng. IEEE Trans.*, vol. 57, no. 3, pp. 542–551, 2010.

[91] F. Zhang, Z. Fang, M. Liu, and H. Huang, “Preliminary design of a terrain recognition system,” in *Engineering in Medicine and Biology Society, EMBC, 2011 Annual International Conference of the IEEE*, 2011, pp. 5452–5455.

[92] K. Yuan, Q. Wang, J. Zhu, and L. Wang, “Motion control of a robotic transtibial prosthesis during transitions between level ground and stairs,” in *Control Conference (ECC), 2014 European*, 2014, pp. 2040–2045.

[93] K. Yuan, S. Sun, Z. Wang, Q. Wang, and L. Wang, “A fuzzy logic based terrain identification approach to prosthesis control using multi-sensor fusion,” in *Robotics and Automation (ICRA), 2013 IEEE International Conference on*, 2013, pp. 3376–3381.

[94] Y. David Li and E. T. Hsiao-Wecksler, “Gait mode recognition and control for a portable-powered ankle-foot orthosis.,” *IEEE Int. Conf. Rehabil. Robot.*, vol. 2013, p. 6650373, Jun. 2013.

[95] B. Coley, B. Najafi, A. Paraschiv-Ionescu, and K. Aminian, “Stair climbing detection during daily

physical activity using a miniature gyroscope," *Gait Posture*, vol. 22, no. 4, pp. 287–294, 2005.

[96] A. Forner-Cordero, H. Koopman, and F. C. T. Van Der Helm, "Describing gait as a sequence of states," *J. Biomech.*, vol. 39, no. 5, pp. 948–957, 2006.

[97] M. T. Hagan and others, *Neural network design*. .

[98] M. T. Hagan and M. B. Menhaj, "Training feedforward networks with the Marquardt algorithm.," *IEEE Trans. Neural Netw.*, vol. 5, no. 6, pp. 989–93, Jan. 1994.

[99] F. Dan Foresee and M. T. Hagan, "Gauss-Newton approximation to Bayesian learning," in *Proceedings of International Conference on Neural Networks (ICNN'97)*, 1997, vol. 3, pp. 1930–1935.

[100] M. K. Boes, M. Islam, Y. D. Li, and E. T. Hsiao-Wecksler, "Fuel Efficiency of a Portable Powered Ankle-Foot Orthosis," in *Rehabilitation Robotics (ICORR), 2013 IEEE International Conference on*, 2013, pp. 1–6.

[101] M. K. Boes, R. E. Klaren, R. M. Kesler, M. Islam, Y. Learmonth, M. N. Petrucci, R. W. Motl, and E. T. Hsiao-Wecksler, "Spatiotemporal and Metabolic Impacts on Gait of a Powered Ankle Exoskeleton in Persons with Multiple Sclerosis," in *Proceedings of the 39th Annual Meeting of the American Society of Biomechanics, Columbus, OH, USA*, 2015.

[102] S. Galle, P. Malcolm, W. Derave, and D. De Clercq, "Adaptation to walking with an exoskeleton that assists ankle extension.," *Gait Posture*, vol. 38, no. 3, pp. 495–9, Jul. 2013.

[103] P. Malcolm, R. E. Quesada, J. M. Caputo, and S. H. Collins, "The influence of push-off timing in a robotic ankle-foot prosthesis on the energetics and mechanics of walking," *J. Neuroeng. Rehabil.*, vol. 12, no. 1, 2015.

[104] J. M. Caputo and S. H. Collins, "Prosthetic ankle push-off work reduces metabolic rate but not collision work in non-amputee walking," *Sci. Rep.*, vol. 4, 2014.

[105] L. M. Mooney, E. J. Rouse, and H. M. Herr, “Autonomous exoskeleton reduces metabolic cost of human walking,” *J. Neuroeng. Rehabil.*, vol. 11, no. 1, p. 151, 2014.

[106] P. Malcolm, R. Quesada, J. Caputo, D. De Clercq, and S. Collins, “Effect of push-off timing on metabolic cost during walking with a universal ankle-foot prosthesis emulator,” in *Dynamic Walking 2014*, 2014.

[107] S. H. Collins, M. B. Wiggin, and G. S. Sawicki, “Reducing the energy cost of human walking using an unpowered exoskeleton,” *Nature*, 2015.

[108] P. H. Tzu-wei, K. A. Shorter, P. G. Adamczyk, and A. D. Kuo, “Mechanical and energetic consequences of reduced ankle plantar-flexion in human walking,” *J. Exp. Biol.*, vol. 218, no. 22, pp. 3541–3550, 2015.

[109] L. M. Mooney, E. J. Rouse, and H. M. Herr, “Autonomous exoskeleton reduces metabolic cost of human walking during load carriage,” *J. Neuroeng. Rehabil*, vol. 11, no. 5, p. 80, 2014.

[110] K. Z. Takahashi, M. D. Lewek, and G. S. Sawicki, “A neuromechanics-based powered ankle exoskeleton to assist walking post-stroke: a feasibility study,” *J. Neuroeng. Rehabil.*, vol. 12, no. 1, p. 23, 2015.

[111] M. K. Boes, M. Islam, K. Neville, and E. T. Hsiao-Wecksler, “Differences in ankle angle during gait due to variations in assistive torque timing,” in *7th World Congress of Biomechanics, Boston, MA*, 2014, pp. 1–6.

[112] R. L. Burden, J. D. Faires, and A. C. Reynolds, “Numerical Analysis: Prindle, Weber &.” and Schmidt Publishers, Boston, MA, 1985.

[113] S. Theodoridis and K. Koutroumbas, “Pattern recognition--Fourth edition, 2009.” Academic Press, pp. 14–409, 2009.

[114] B. Lawson, H. A. Varol, A. Huff, E. Erdemir, and M. Goldfarb, “Control of stair ascent and

descent with a powered transfemoral prosthesis," *Neural Syst. Rehabil. Eng. IEEE Trans.*, vol. 21, no. 3, pp. 466–473, 2013.

[115] Y. D. Li and E. T. Hsiao-Wecksler, "Gait mode recognition and control for a portable-powered ankle-foot orthosis," in *Rehabilitation robotics (ICORR), 2013 IEEE international conference on*, 2013, pp. 1–8.

[116] J. Jang, K. Kim, J. Lee, B. Lim, and Y. Shim, "Online gait task recognition algorithm for hip exoskeleton," in *Intelligent Robots and Systems (IROS), 2015 IEEE/RSJ International Conference on*, 2015, pp. 5327–5332.

[117] M. T. Hagan and M. B. Menhaj, "Training feedforward networks with the Marquardt algorithm," *Neural Networks, IEEE Trans.*, vol. 5, no. 6, pp. 989–993, 1994.

[118] F. D. Foresee and M. T. Hagan, "Gauss-Newton approximation to Bayesian learning," in *Proceedings of the 1997 international joint conference on neural networks*, 1997, vol. 3, pp. 1930–1935.

[119] X. Yun, E. R. Bachmann, H. Moore, and J. Calusdian, "Self-contained position tracking of human movement using small inertial/magnetic sensor modules," in *Robotics and Automation, 2007 IEEE International Conference on*, 2007, pp. 2526–2533.

[120] B. E. Lawson, H. A. Varol, F. Sup, and M. Goldfarb, "Stumble detection and classification for an intelligent transfemoral prosthesis," in *Engineering in medicine and biology society (EMBC), 2010 annual international conference of the IEEE*, 2010, pp. 511–514.

[121] F. Sup, H. A. Varol, and M. Goldfarb, "Upslope walking with a powered knee and ankle prosthesis: initial results with an amputee subject," *Neural Syst. Rehabil. Eng. IEEE Trans.*, vol. 19, no. 1, pp. 71–78, 2011.

[122] J. Perry, J. D. Fontaine, and S. Mulroy, "Findings in post-poliomyelitis syndrome," *J Bone Jt.*

Surg A, vol. 77, pp. 1148–1153, 1995.